COMPUTER APPLICATIONS IN THE EARTH SCIENCES:

COLLOQUIUM ON SIMULATION

Edited by

DANIEL F. MERRIAM

and

NAN CARNAHAN COCKE

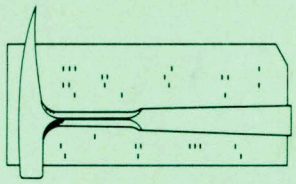

COMPUTER CONTRIBUTION 22
State Geological Survey
The University of Kansas, Lawrence
1968

EDITORIAL STAFF

Daniel F. Merriam, Editor

Assistant Editors

John C. Davis Owen T. Spitz

Associate Editors

John R. Dempsey
Richard W. Fetzner
James M. Forgotson, Jr.
John C. Griffiths
John W. Harbaugh
R.G. Hetherington
Sidney N. Hockens
J. Edward Klovan
William C. Krumbein
R.H. Lippert
William C. Pearn
Max G. Pitcher
Floyd W. Preston
Walther Schwarzacher
Peter H.A. Sneath

Editor's Remarks

This colloquium, fourth in a series on "Computer applications in the earth sciences", deals with simulation. To simulate is to "feign" or "imitate". Attempts at simulation by earth scientists, however, have not been particularly successful until recently. Prior to the development of computer simulation, geologic modeling was confined to small-scale physical models. Inherent in these models were problems of scaling material strengths and responses, and the problem of geologic time.

In other fields such as business, medicine, physiology, and the social sciences, simulation is in an advanced state. Geologists may do well then to adapt techniques already developed by other workers. A wide range of these techniques, presently available in engineering, geophysics, geography, and mathematics, is demonstrated here in the proceedings for the Colloquium on Simulation.

Although geologic modeling still is in an early stage of development, it offers a promising area of future research in earth science. Applications discussed in this colloquium include logging methods, salt-dome development, stochastic processes in stratigraphic analysis, sedimentation rates, and delta building. Little imagination is required to find other equally valid applications.

G. Bonham-Carter and J.W. Harbaugh state "The objectives of simulating natural systems are normally to test alternative models and to see how they react under various conditions; the natural system itself cannot be changed (unless it is partly man-influenced), only the model". Harbaugh (Mathematical simulation of marine sedimentation with IBM 7090/7094 computers: Kansas Geol. Survey Computer Contr. 1, 1966) was especially successful in developing a model to imitate the process of sediment transport and deposition within a sedimentary basin. Many other geological models were reported subsequently in the literature.

It is hoped that this colloquium will serve as a stimulant to those engaged in simulation and as an introduction to the technique for others. The colloquium is structured to allow maximum interchange of information between participants. We believe, as J.W. Harbaugh does, that "Mathematical simulation with digital computers offers important opportunities for geologists, opening the door to an experimental approach in fields where experimentation has, heretofore, been difficult or impossible" (Harbaugh, Computer simulation as an experimental tool in geology and paleontology, in Essays in paleontology and stratigraphy: Dept. Geol., Univ. Kansas, Sp. Publ. 2, 1967).

We are pleased to acknowledge help of our co-sponsors--the Computation Center, R.G. Hetherington, director, and R.J. Robinson, deputy director; and University Extension, R.F. Treece. J.C. Davis and O.T. Spitz of the Geological Survey and G.D. Shilling of the Computation Center have assisted with the preparations; Mrs. Laquetta Karch and the Geological Survey helped with the typing; W.E. Kukuk and R.W. Jaeger of the University Printing Service provided assistance in preparing the proceedings for publication.

Proceedings of other colloquia have been published as Geological Survey Computer Contribution 7 (classification), Computer Contribution 12 (trend analysis), and Computer Contribution 18 (time-series analysis). A list of Computer Contributions may be obtained by writing the Editor, Computer Contributions, Kansas Geological Survey, The University of Kansas, Lawrence, 66044.

COMPUTER APPLICATIONS IN THE EARTH SCIENCES:

COLLOQUIUM ON SIMULATION

Edited by

DANIEL F. MERRIAM

and

NAN CARNAHAN COCKE

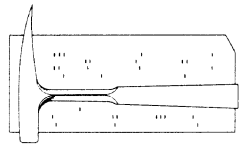

1968

CONTENTS

PATTERNS AND INFORMATION

by

Preston C. Hammer

Pennsylvania State University

INTRODUCTION

The electronic and computer age has led to many new interpretations of words previously in the language. The words analog, imitation, simulation, emulator, copy, model, reproduction, and duplication have more or less obvious relationships to each other in the present jargon. It would be interesting to try to sort out the rather large number of words tagging such concepts. Although I do not propose to attempt this here, I will illustrate how certain mathematical terms relate to the broad area of simulation. It is unfortunate, in my opinion, that the intuitive meanings of mathematical concepts have been swallowed by the day formalisms of algebra, logic, and ill-chosen axioms.

Despite numerous opportunities we have neglected in our work to show the relationships among the different fields of science and, as a result, there is a lack of transfer of information. In the space allocated, I will try to give an indication of what I mean.

APPROXIMATION SPACES AND SIMULATION

Topology, in one interpretation, may be called the study of closeness. Thus a neighborhood of a point contains all points considered to be close to the point. In simulation practice, for example, there is the system to be simulated and there is the system designed to simulate it. If you should ask how well the simulation imitates the original system, you have asked, equivalently, how close the simulation is to the original. Topological spaces have been axiomatized in such a fashion that they are insufficiently general to discuss simulation problems.

Any problem in which an object (e.g. a system, e.g. the universe) is to be modeled, simulated or imitated I choose to call an approximation problem. Usually, there is a set of objects to be approximated. Let me call such a set E. Now suppose p is an object in E and we wish to discuss approximations to it. At the outset, I find it convenient to be liberal so that you may adopt my system to your needs. Thus I will initially concede that any object q, of your choice, may be considered an approximation to p. For example, p may be the solar system and q may be a set of differential equations with appropriate initial values to be used to approximate the location of objects in the solar system. Here we have problems of patterns and information.

In our delightfully sloppy language I can say "solar system" and each of you will conjure up meanings for that pair of words. In one way we all know what the solar system is; in another, we have little information concerning its detailed structure. Thus your differential equation model will not be a model of the solar system but of the pattern you have discerned. This pattern may be called an abstraction from the solar system and is in itself only a shadow, or projection, of the "real" system. This pattern, while already too complex to treat by the differential equation approach is itself an approximation to the solar system. Thus the differential-equation system represents a simulation of an abstraction. If we convert the differential system into a form suitable for computation, yet another simulation takes place. When we enter the data and program into a computer, we have yet another approximation because the computer only simulates arithmetic operations. There are, naturally, many equation systems which may be used to approximate the solar system. When is one better than another?

Now I return to the set E of objects to be approximated and I ask: When will q be a good approximation to p? The following criteria are suggestive.

1. q must contain the essential information in p. (i.e. q must adequately preserve the pattern of p).
2. q must be within reach economically.
3. q must be better than p for the purposes in hand.

Of these criteria the first requires a criterion of closeness, information-wise. The second criterion is obvious and the third sometimes occasions raised eyebrows. Yet who looks for an approximation when the original will serve? It is obvious why a differential-equation system may be considered better than the solar system for purposes of forecasting eclipses and so on.

Being reasonable, practical people, we now say let v(p) be the set of all objects q which we wish to consider as possible approximations to p. The binary relation $[(p,q) : p \in E, q \in v(p)]$ I then call an approximation system. I do not yet call it a space because no criterion of preference is yet available to help choose an approximation for p. I hence assume an order (preference) relation

T(p) in v(p). If $(q_1, q_2) \in T(p)$ then I will say "q_1 is at least as good an approximation to p as q_2 is." Because each $q \in v(p)$ is just as good as q as an approximation to p, I may assume that T(p) is a reflexive, i.e. $(q,q) \in T(p)$ for each $q \in T(p)$. I will also make the assumption that $(q_1, q_2) \in T(p)$ and $(q_2, q_3) \in T(p)$ implies $(q_1, q_3) \in T(p)$ i.e. "q_1 better than q_2 and q_2 better than q_3 implies q_1 better than q_3" This is the property of transitivity (order). I call the ternary relation

$$A = [(p, q_1, q_2) : p \in E, (q_1, q_2) \quad T(p)]$$

an approximation space.

Concerning approximation spaces which are so simply defined, one might think that nothing can be said. On the contrary, every topological space is an approximation space but rather few approximation spaces are topological spaces. There are many treatises written on topological spaces. Are approximation spaces too general? I say that this definition, which I decided on last year after discussions with Professor D. G. Moursund, is the most specialized collection of systems which can be adapted to your needs but that for particular needs additional restrictions are easily inserted. The theory of these spaces and applications has barely begun.

The ideas apply to the approximations which are called language translations, and to simulations of all kinds. In many cases, as in language translation, the establishment of a precise preference relation is difficult.

Incidentally, in the above framework an approximation q_0 is v(p) is a best approximation provided $(q_0, q) \in T(p)$ for every $q \in v(p)$. Note that it is only a matter of interpretation to change from "at least as good as" to "at least as bad as" and I also have worst approximation defined by the same system.

FILTERS A LA MODE

Although approximation spaces have their roles, it often happens that conditions or criteria are given which select objects but which are not suitably interpreted as "closeness" conditions. Finding myself dealing with such criteria led me to generalize the concept of filter, using filters of chemistry, cigarettes, and electronics as the guide.

A filter, F, in a set M is any device which accepts or rejects each element of M. Then if A is the set of elements accepted by F then cA = M A is the set of elements rejected by F and (A, cA) is called the action of F.

Examples of filters abound in mathematics. Thus any set-property is a filter because it accepts elements of the set. Every equation or inequation is a filter accepting numbers, vectors, or functions which satisfy it. The Sieve of Eratosthenes is a filter. It accepts prime numbers and rejects composite numbers. A function is a collection of filters, (x,f) accepts fx from the range of f. A computing machine is a filter, (I,M) accepts M(I) = 0, the output, where I is the input.

It is seen easily that two filters F_1 and F_2 in M produce the conjunction filter which accepts $A_1 \cap A_2$ if F_1 accepts A_1 and F_2 accepts A_2. Simultaneous equations and axiom systems are conjunction filters. It is also readily seen that F_1, F_2 produce an equivalence relation in M where p is equivalent to q provided p and q are accepted or rejected together by F_1 and F_2. Every equivalence relation can be generated by a suitable collection of filters.

Although I will not here go into details, I may now point out that filter theory embraces approximation spaces because for a given p, an approximation space accepts sets close to p and rejects others. I have shown that the theory of filters also includes finite projective planes as well as topological spaces. The theory of filters, again, is open and on it a theory of machines may be based.

Of what importance can a theory of filters be in simulation? The approximation space aspect is obvious. However the process of making a model is a filtering process. The information we have concerning the solar system has been filtered whether we wish it or not, and the patterns we recognize are not by any means the only ones possible. They are mostly the patterns we have been trained to see. You doubt it?

Consider the word nowhere. Almost inevitably if you have been trained as I have you will read it: no where. But why not now here? The latter pattern is just as present in "nowhere" but many people I have asked have never seen it. Patterns which we recognize are the only ones we can use and we tend to recognize only those which we have been told to see. This is perhaps one reason why punning is such an important device of language learning - new patterns are brought out.

SIMULATION OF GEOLOGIC SYSTEMS: AN OVERVIEW

by

Graeme Bonham-Carter and John W. Harbaugh

Stanford University

ABSTRACT

Systems philosophy provides the theoretical framework linking diverse applications of computer simulation. Natural systems and man-made systems may be regarded as end members of a spectrum of system types. Simulation of man-made systems employs operations research techniques; the objectives of simulation are to optimize system design, and to test the performance of models under differing parameter settings. Simulation of natural systems cannot readily utilize specialized simulation languages, as these are designed primarily for industrial and business applications. The objectives of simulating natural systems are normally to test alternative models and to see how they react under various conditions; the natural system itself cannot be changed (unless it is partly man-influenced), only the model.

INTRODUCTION

With the explosive rise of simulation applications in a wide variety of fields (e.g. IBM, 1966), there is a need to sit back and take stock. A number of questions arise regarding the utility to geology of concepts and specific models developed in areas such as operations research and social science. For instance, can geologists make use of SIMSCRIPT or DYNAMO, two of many specialized simulation languages? Much of the simulation literature is concerned with topics such as queuing, inventory, routing of vehicular traffic and so on. Is the philosophy behind these studies similar to that employed say, in a simulation of deltaic sedimentation?

It seems to us that the common thread linking these diverse applications is the systems philosophy. Even if not explicitly stated, computer simulation of any process or collection of processes entails three basic steps: the definition of a system; the construction of a model; and the use of the model to imitate the behavior of the system (Fig. 1). Let us examine these steps a little more closely.

SYSTEMS, MODELS AND SIMULATION

We may define a system as a set of dynamically interrelated parts. If we change one part of a system, repercussions are felt in every other part ot the system. Thus the planets form a system; the atmosphere and lithosphere are both systems. A factory is a system and so is a supermarket. Each system must be defined by specifying its boundaries and identifying its components. Systems may be nested one within the other, depending upon how each is defined. For example, Figure 2 is a diagram illustrating a coastal system which might include components such as beaches, streams, deltas, and cliffs. Within this general system, one might want to consider a delta system, or on an even smaller scale, a single delta distributary as a system.

Systems may be either 'open' or 'closed' (Von Bertalanffy, 1950). Closed systems are those which have boundaries across which no import or export of energy or materials occurs (Von Bertalanffy, 1951). Systems are more commonly open, being continually affected by external factors, and in a state of dynamic equilibrium. Factories have inputs (e.g. raw materials) and outputs (e.g. finished products); their performance adjusts to the market need for products and the rate of inflow of materials. Similarly, a coastal system has inputs (e.g. streams, longshore currents) and outputs (e.g. turbidity currents); its performance, embodied as beaches, deltas, lagoons and so on is continually being adjusted to 'external' changes such as rates of sediment input, eustatic fluctuations and storms.

Because a system consists of an assemblage of complexly interrelated parts, it may be exceedingly hard to predict the effect of altering the state of a particular variable, or of changing the system structure. Man has first to simplify the system conceptually and to represent it with a model. Models are themselves artificial systems that attempt to portray the characteristics of some real system. Here we exclude iconic models, such as miniature aircraft.

Figure 1. - Three basic steps necessary for simulation of any process or collection of processes.

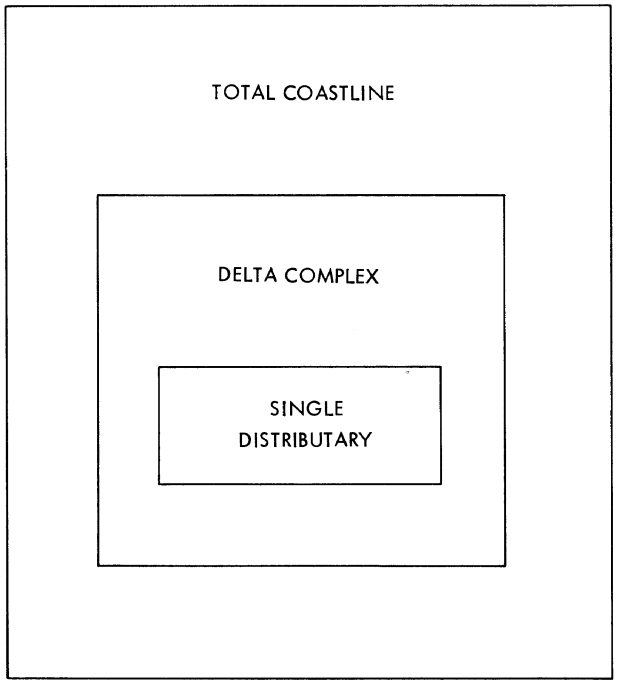

Figure 2.- Nesting of systems.

There are many types of models, such as conceptual and graphic models, but probably the most powerful and flexible way of representing a system is with mathematical or logical models. Mathematical models may be analytic and seek complete and precise solutions to certain aspects of systems; or they may be used for computer simulation, in which case 'solutions' are obtained by observing the model's 'performance' on a computer.

Simulation is the operation of the model of a system in such a way that the behavior of the system is reproduced as it moves through time. Simulation in operations research, social science, and natural science are all similar in that the basic steps of system definition, model construction, and model operation (simulation) are common to each. However, an important distinction can be made between man-made and natural systems, as these different types result in rather different computer models and objectives of study.

MAN-MADE VS. NATURAL SYSTEMS

A man-made system may be defined as a system created and controlled by man. An example is a factory whose components and structural organization are decided entirely by man, probably specialists in system design. If poorly designed, the factory may be hopelessly inefficient; the flow of materials and information must be routed so that delays and queues are cut to a minimum. A holdup in one part of a factory may have repercussions in every other part; a strike by the men in one department may freeze production throughout the plant.

A natural system is simply a system in which man plays no part. For example, the solar system is, so far, unaffected by any of man's activities. It operates under natural 'laws'. A delta is a geologic example of a natural system, although in this case man is able to modify the system if he wishes. In its untouched condition, a deltaic system operates under natural controls.

Between these end-members of 'natural' and 'man-made' systems, a whole spectrum of hybrid systems exists. These hybrids are very commonly the objects of simulation studies. Probably the best example is the study of man's influence in ecology. Natural ecological systems are delicately balanced by an exceedingly complex interlock of relationships. Simulation can help to answer questions about the possible repercussions of man's intrusion on this balance (Watt, 1966).

Simulation of Man-made Systems

Simulation studies of man-made systems are normally concerned with two basic types of question:

(1) How efficient is the structure of the system for handling the tasks for which it is constructed? The simulation seeks answers to these questions by making changes in system design and testing each design in a series of simulation experiments. Each new system configuration is tried by adjusting the model structure to match the system change and simulating the system behavior to see if performance is improved. For example, a city planner may wish to know the effect of excluding all passenger traffic from a city's center. With existing traffic loads, where would congestion points form, and what design would be best for minimizing holdups? Using a simulation model, alternative strategies may be explored thoroughly without going to the expense of real-life experiments. Notice, however, that changes in the real system structure are explored using the model; man-made systems can be changed, whereas pure natural systems cannot.

(2) The second type of question is related to the performance of a particular system under a variety of conditions. For instance, the city planner may want to know how the existing traffic control system in his city will perform under an increased traffic load. With a model of the system, a wide variety of computer experiments may be made to test the sensitivity of the system to changes in the controlling parameters.

A number of recent books have appeared that deal mainly with simulation of man-made systems, e.g. Mize and Cox (1968), Martin (1968), Evans, Wallace, and Sutherland (1967), and Naylor and others (1966).

Simulation of Natural Systems

The simulator of a natural system is faced

with slightly different problems. A natural system, if it is to remain so, cannot be altered or optimized by man. The purposes of simulation studies here are:

(1) To test alternative models of the system. Although the system design cannot be altered, it may be very instructive to try various model designs, to see which best approximates the system's behavior.

(2) Given a particular model, to explore the possible variations produced by altering or 'tuning' the input parameters. This objective is the same as (2) for man-made systems.

The process of trying alternative models is an iterative one. Normally during the course of model development, a number of alternatives will be tried, with a gradual improvement at each step. By the time a particular study is finished, earlier models may be forgotten because of their shortcomings, but they comprise an essential stage in this 'learning' process, in which the system/model fit is improved progressively.

GEOLOGIC SIMULATION: NATURAL SYSTEMS

A delta is a natural geologic system that has been studied by computer simulation (Bonham-Carter and Sutherland, 1967). The system to be modeled was defined as being that area in front of and including a single river distributary mouth, and thus constituted only a small subsystem of a whole deltaic complex. The main factors considered were the rates of river discharge, both water and sediment, the channel dimensions and the geometry of the marine basin into which the sediment settled. Offshore energy, tidal fluctuations, and other factors were not considered.

The principal objectives of the study were twofold:

(1) To assess the variations in deltaic deposition produced by altering the input parameters. For instance, how sensitive is the system to an increase in river depth, or to a change in grain size of the sediment? (2) To test Bates' (1953) hypothesis that a river flowing into the sea has a velocity structure similar to that found in a plane jet.

Initially, a static model was constructed that calculated the rate of deposition of sediment at each of a number of points in front of the channel mouth, using fixed rates of discharge, and a fixed composition of the sediment load. The total sediment load was represented by a number of nominal or statistical particles that were assumed to be traveling first parallel to the channel bottom then, having passed out of the channel mouth, to be following downward trajectories (Fig. 3). When these particles settled to the bottom, they fell into the cells of a horizontally placed accounting grid that recorded rates of deposition. The slope of the settling trajectories was assumed to be w/v, where

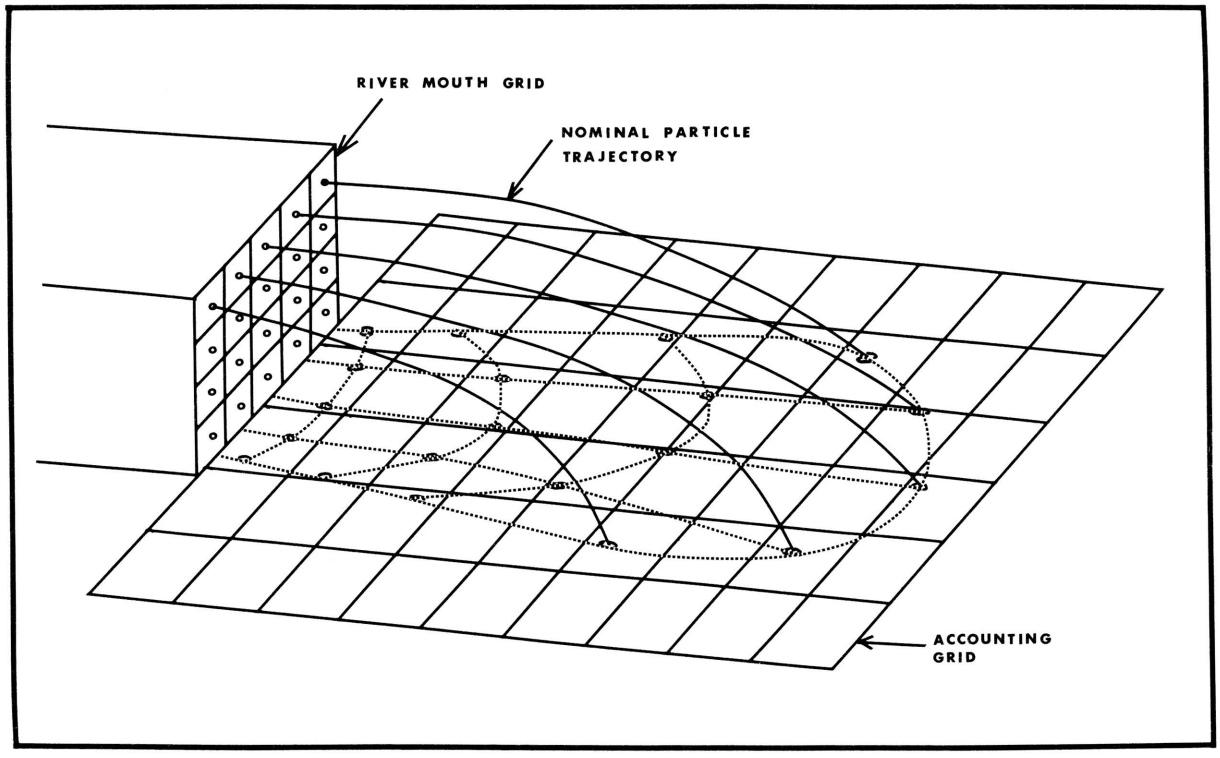

Figure 3.- Structure of delta simulation model, showing vertical river grid and horizontal accounting grid. Statistical particles issuing from center of each river grid cell are traced along settling trajectories until they settle into accounting grid cells.

w is the downward component of velocity (equal to minus the fall velocity of the particle concerned) and v is the forward velocity. The value of w was supplied as input; v could be determined at any point in front of the mouth assuming a model of flow that incorporated both Bates' plane jet hypothesis and variation in velocity with depth due to shear along the floor of the channel.

The sensitivity of this model to changes in grain size, river depth, river slope and other parameters was tested in a series of runs (Fig. 4). It was found that a narrow depositional area was produced, with very low angles of 'foreset' slopes, about 1/2°. It was argued that the narrowness of the 'fan' might have been caused by the rigid nature of the jet nozzle, like a fixed hose pouring water into a tub. Maybe in the natural system the flow direction oscillates from side to side, thus spreading sediment more widely. The computer model was modified accordingly to incorporate this effect (Fig. 5), although this 'rotation' effect is probably not the only mechanism responsible.

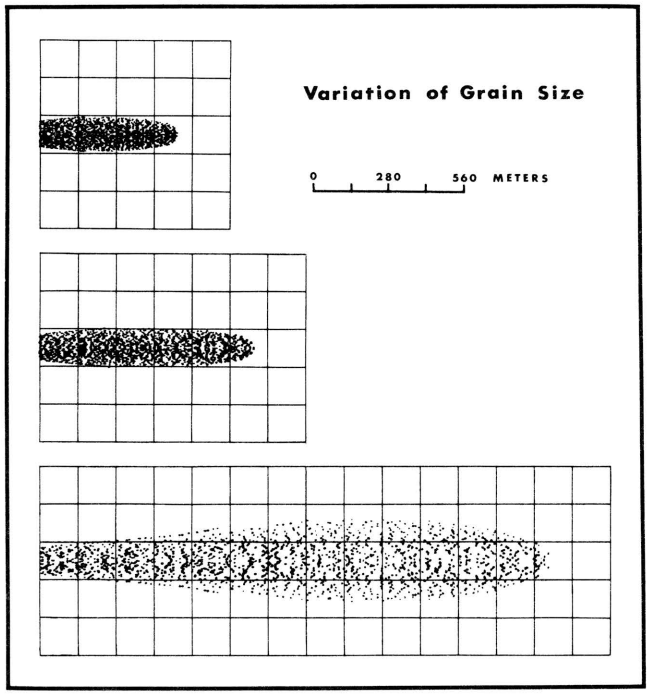

Figure 4.- Results from computer experiments using static model of delta. Fine points are terminal coordinates of statistical particles as they settled into horizontal accounting grid cells. River channel dimensions are 100 meters wide and 10 meters deep with average current velocity of 2m./sec. Three diagrams plotted by CALCOMP plotter, and record sensitivity of model to grain-size changes. Sediment diameters: 0.3 mm (upper), 0.2 mm (center), 0.1 mm (lower).

More serious, however, was the realization that this model was unable to explain the formation

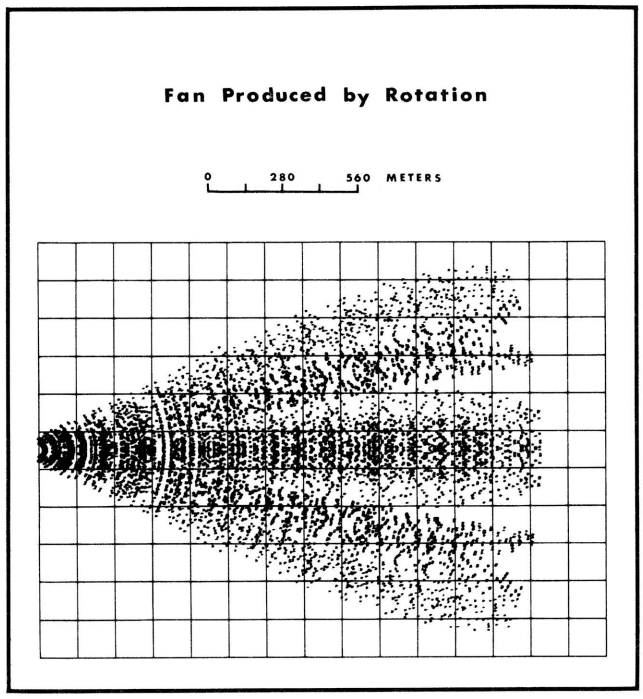

Figure 5.- Parameters for simulation run identical to those that produced lower diagram in Figure 4, except that main axis of flow rotated from side to side, using random number generator to determine each rotation position.

of distributary mouth bars or submerged natural levees marginal to the flow, as Bates (1953) had originally suggested. Furthermore, the static nature of this model prevented a response to sediment accumulation directly at the channel mouth. Rivers do not become completely blocked at the mouth, as would occur if these simulation runs were allowed to continue long enough.

The model was improved by making it dynamic and including a negative feedback control feature. The model structure was altered so that it could operate over a number of discrete time steps. At the termination of each increment, the state of the model was recorded and used as the starting conditions for the next time step.

As the grid cells around the river mouth filled with sediment, they eventually reached a level where no further net accumulation could occur, and depositional and erosional tendencies balanced. The elevation with reference to mean sea level of this equilibrium surface was called the limiting depth surface (L.D.S.) and was defined for each cell in the horizontal accounting grid. The duration of each time step of the model was defined as being the minimum time required for any cell to reach its L.D.S. value. Having reached the L.D.S., the cell became part of the delta 'platform' (Fig. 6). During subsequent time steps, sediment could no longer settle onto the delta platform, and the

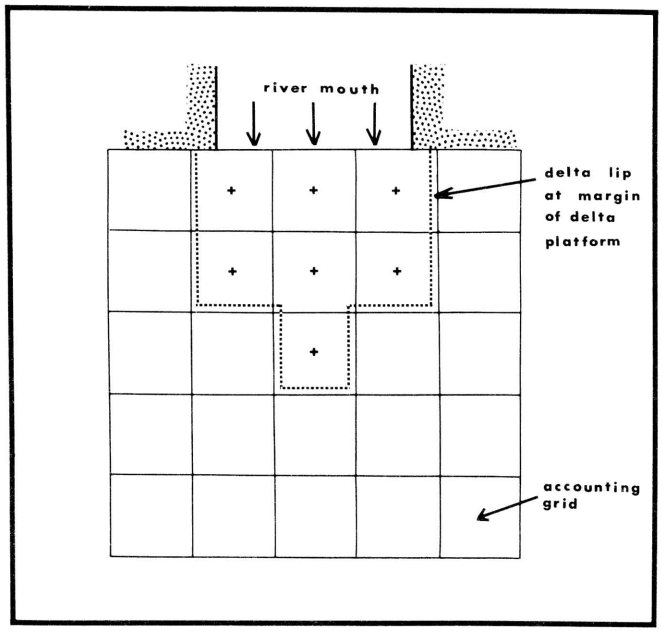

Figure 6.- As sediment accumulates in each accounting grid cell, sediment/water interface rises until equilibrium between erosion and deposition is reached. Once a cell fills to this point it becomes part of 'delta platform'. Statistical particles do not settle until they have crossed delta lip at margin of platform.

nominal particle trajectories remained horizontal until they crossed the delta 'lip' at the margin of the platform. Thus as time moved forward, the delta 'platform' moved outwards from the channel mouth. Deposition of sediment was controlled by the position of the delta lip, but the delta lip itself was controlled by deposition. Thus a negative feedback loop was able to keep the model under control (Fig. 7).

Using this model, it was found that 'deposits' possibly equivalent to a distributary mouth bar and submerged levees formed as predicted by Bates' hypothesis. Figure 8 illustrates a stratigraphic section (drawn by a CALCOMP plotter) through a simulated delta showing a distributary mouth bar.

To summarize, this simulation model was used for:

(1) Testing various models of a delta system encompassing deposition from a single distributary; shortcomings in the static model were found as a result of the first experiments; Bates' theory was found to produce a narrow fingerlike deposit that soon choked the channel mouth; the model was improved by making it dynamic.

(2) Testing delta response to changes in sediment type and channel dimensions.

Other published geologic simulation studies that fall into this 'natural systems' category include evaporite sedimentation (Briggs and Pollack, 1967), marine sedimentation (Harbaugh, 1966; Schwarzacher, 1966), salt dome development (Howard, 1967), sand grain evolution (Jizba, 1966), stratigraphic sequences (Potter and Blakely, 1967; Carr and others, 1966; Krumbein, 1967), brachiopod time-trend curves (Fox, 1967), petroleum reservoir behavior (Harbaugh, 1967; Breitenbach, 1964), interstitial water chemistry (Scholl and Johnson, 1967), and others.

GEOLOGIC SIMULATION: MAN-MADE SYSTEMS

In this short paper we will not discuss the simulation of geologically oriented man-made systems, except to point out a few of the major areas of application. Man-made systems generally have some criterion for measuring efficiency; this criterion is often economic. Simulation of man-made systems usually is done in order to test various system designs or operating characteristics, to find a strategy which minimizes cost, maximizes profits or optimizes some other criterion. This type of simulation is, therefore, an exceedingly important tool for decision-making.

The design of mining operations is one of the classic areas for operations research, and numerous simulation studies have been carried out in this area, e.g. Bucklen (1966), Manula (1966), Sanford (1965), Waring and Calder (1965), and many others.

Another very important simulation application is in the search for mineral deposits. With a priori

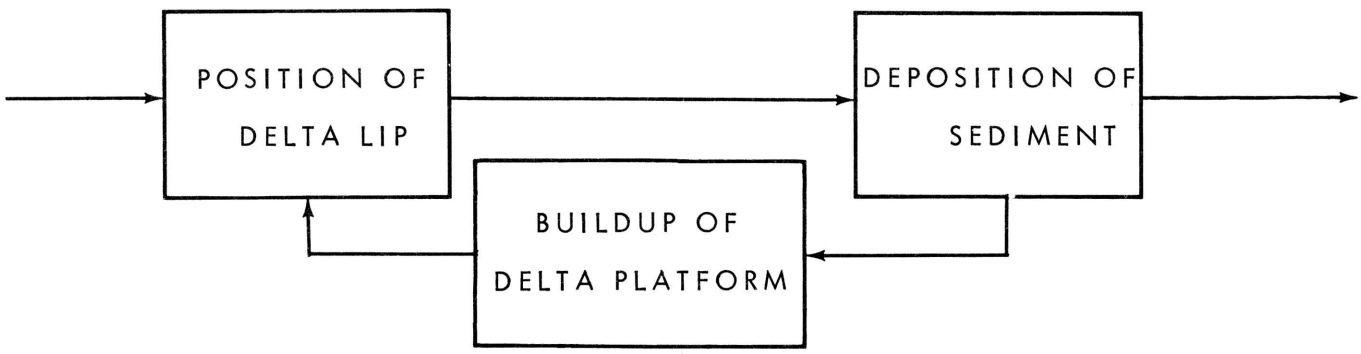

Figure 7.- Negative feedback loop showing interactive control between delta lip and sediment deposition.

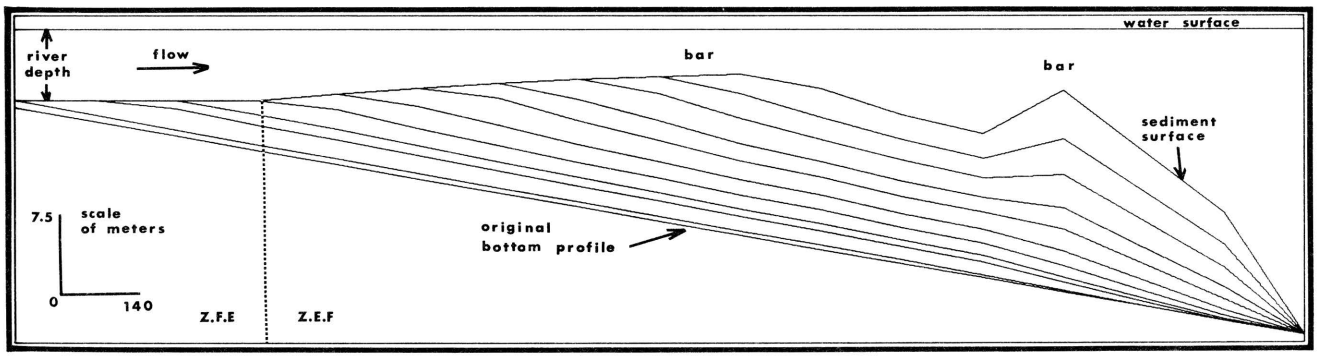

Figure 8. - Stratigraphic section along length of simulated delta, drawn by CALCOMP plotter with vertical exaggeration X18.7 from output using dynamic model. Sediment/water surface drawn in for each time increment, and appears as series of 'foreset' beds. Z.F.E. = Zone of Flow Establishment of jet velocity field; Z.E.F. = Zone of Established jet Flow.

knowledge of the frequency distributions of mineral 'targets', it is possible to test the success/failure ratio of a number of alternative exploration strategies (Griffiths and Drew, 1964). Individual prospects also may be 'mathematically drilled' by simulation in order to make an estimate of prospective reserves (Smith, 1968). Miesch, Connor, and Eicher (1964) have used a simulation approach to evaluate different sampling designs for geochemical surveys. These are examples of dominantly man-made systems (the search or sampling framework) with some 'natural' components (the rock composition variability).

A number of important simulation studies have been accomplished on dominantly natural systems, that have been modified by man for his own uses. For example, the design of water-resource systems has been the subject of extensive simulation studies (Hufschmidt and Fiering, 1966). In other areas, engineering geologists may wish to evaluate the effects of altering natural systems. For example, the following types of questions may arise:

(1) How will a change in a particular harbor design affect the stability of the local beaches?

(2) What effect will be produced on a particular water table by repeated drilling and pumping?

(3) How will dredging affect the siltation pattern in an estuary?

Using a simulation approach, questions of this type can be answered by employing simulation models of the system. The model can be modified, and man's probable influence studied before the real-life changes are made. In such cases, computer simulation may be an alternative or, better still, a supplement to physical scale modeling.

CONCLUSIONS

(1) Geologic systems may be usefully classified according to whether they are influenced by man, whether they are natural systems, or a hybrid between these two extremes.

(2) Simulation studies of man-made systems can make extensive use of techniques borrowed from operations research and allied fields. Considerable economic advantages are to be gained by using simulation for systems design and decision-making.

(3) Natural systems often require complex models for their simulation. Although specially designed simulation languages may be useful for modeling man-made geologic systems, the simulation of natural systems cannot generally make use of these programming aids. General purpose languages like FORTRAN are more useful.

(4) Systems principles are valuable for discerning the common ground underlying the simulation applications, both within geology and in other disciplines.

REFERENCES

Bates, C.C., 1953, Rational theory of delta formation: Am. Assoc. Petroleum Geologists Bull., v. 37, no. 9, p. 2119-2162.

Bonham-Carter, G.F., and Sutherland, A.J., 1967, Diffusion and settling of sediments at river mouths: a computer simulation model: Trans. Gulf Coast Assoc. Geol. Soc., v. 17, p. 326-338.

Brietenbach, E.A., 1964, Simulation of gravity drainage in oil reservoirs: Unpubl. doctoral dissertation, Stanford Univ.

Briggs, L.I., and Pollack, H.N., 1967, Digital model of evaporite sedimentation: Science, v. 155, no. 3761, p. 453-456.

Bucklen, E.P., 1966, Concepts of the VPI-OCR complex face simulator-basic logic for the simulation of work-time oriented systems, in Computers and operation research in mineral industries: Pennsylvania State Univ., 6th Ann. Symposium, v. 1, Min. Ind. Expt. Station Spec. Publ. 2-65, p. 11-114.

Carr, D.C., and others, 1966, Stratigraphic sections, bedding sequences, and random processes: Science, v. 154, no. 3753, p. 1162-1164.

Evans, G.W., Wallace, G.F., and Sutherland, G.L., 1967, Simulation using digital computers: Prentice-Hall, Englewood Cliffs, New Jersey, 224 p.

Fox, W.T., 1967, Simulation models of time-trend curves for paleoecologic interpretation, in Computer applications in the earth sciences, Colloquium on time-series analysis, D.F. Merriam, ed.: Kansas Geol. Survey Computer Contr. 18, p. 18-29.

Griffiths, J.C., and Drew, L.J., 1964, Simulation of exploration programs for natural resources by models: Colorado Sch. Mines Quart., v. 59, no. 4, p. 187-206.

Harbaugh, J.W., 1966, Mathematical simulation of marine sedimentation with IBM 7090/7094 computers: Kansas Geol. Survey Computer Contr. 1, 52 p.

Harbaugh, J.W., 1967, Computer simulation of petroleum accumulation in marine sediments: 7th World Petroleum Cong., Mexico City, v. 2, p. 625-632.

Howard, J.C., 1967, Dynamic mathematical simulation of salt-dome development (abs.): Geol. Soc. America Ann. Mtg., New Orleans, Nov. 1966, p. 104.

Hufschmidt, M.M., and Fiering, M.B., 1966, Simulation techniques for design of water-resource systems: Harvard Univ. Press, 212 p.

IBM, 1966, Bibliography on simulation: IBM Corp., 88 p.

Jizba, Z.V., 1966, Sand evolution simulation: Jour. Geology, v. 74, no. 5, p. 734-743.

Krumbein, W.C., 1967, FORTRAN IV computer programs for Markov chain experiments in geology: Kansas Geol. Survey Computer Contr. 13, 38 p.

Manula, C.B., and Kim, Y.C., 1966, Linear programming simulator for coal distribution problems, in Computers and operation research in mineral industries: Pennsylvania State Univ., 6th Ann. Symposium, v. 1, Min. Ind. Expt. Station Spec. Publ. 2-65, p. J1-J18.

Martin, F.F., 1968, Computer modeling and simulation: John Wiley & Sons, New York, 331 p.

Miesch, A.T., Connor, J.J., and Eicher, R.N., 1964, Investigation of chemical sampling problems by computer simulation: Colorado Sch. Mines Quart., v. 59, no. 4, p. 131-148.

Mize, J.H., and Cox, J.G., 1968, Essentials of simulation: Prentice-Hall, Englewood Cliffs, New Jersey, 234 p.

Naylor, T.H., Balintfy, J.L., Burdick, D.S., and Chu, K., 1966, Computer simulation techniques: John Wiley & Sons, New York, 352 p.

Potter, P.E., and Blakely, R.F., 1967, Generation of a synthetic vertical profile of a fluvial sandstone body: Trans. Soc. Petroleum Engineers AIME, Sept., 1967, p. 243-251.

Sanford, R.L., 1965, Stochastic simulation of a belt conveyor system, in Computers and computer applications in mining and exploration: College of Mines, Univ. Arizona, v. 1, p. D1-D18.

Scholl, D., and Johnson, W.L., 1967, Effects of diffusion on interstitial water chemistry in deltaic areas: preprint from 7th Intl. Sedimentological Congress.

Schwarzacher, W., 1966, Sedimentation in subsiding basins: Nature, v. 210, no. 5043, p. 1349-1350.

Smith, M.B., 1968, Estimate reserves by using computer simulation method: Oil and Gas Jour., v. 66, no. 11, p. 81-84.

Von Bertalanffy, L., 1950, Theory of open systems in physics and biology: Science, v. 111, no. 2872, p. 23-29.

Von Bertalanffy, L., 1951, An outline of general system theory: Jour. British Phil. Soc., v. 1, p. 134-165.

Waring, R.H., and Calder, P.N., 1965, The Carol mining simulator, in Computers and computer applications in mining and exploration: College of Mines, Univ. Arizona, v. 3, p. KK1-KK42.

Watt, K.E.F., 1966, Systems analysis in ecology: Academic Press, New York, 276 p.

COMPUTER SIMULATION OF TRANSGRESSIVE AND REGRESSIVE DEPOSITS WITH A DISCRETE-STATE, CONTINUOUS-TIME MARKOV MODEL

by

W.C. Krumbein

Northwestern University

ABSTRACT

The first-order, discrete-time, discrete-state Markov chain, with a one-step memory, has limitations in stratigraphic simulation. These relate in part to the lack of correlation, in terms of marker beds, from one simulation to another. This limitation can be reduced by setting up a Markov model in which the states are defined by the position of the strand during a transgression-regression cycle. In this way lateral continuity of the beds is preserved.

The simulation model presented in this paper is a continuous-time, discrete-state model based on transition rates instead of transition probabilities. It generates several equally spaced borehole or outcrop sections that show the kinds of deposits that are formed during each stage of the cycle. The transgressive-regressive littoral sand can be traced easily through the simulations. Steps involved in the transformation of a simple deterministic model to its stochastic counterpart are described.

INTRODUCTION

Simulations of stratigraphic sections commonly are based on transition probability matrices of first-order Markov chains with discrete time (or thickness) and discrete states, the latter being the lithologic components in the section. Each simulation is an independent event, and represents one "realization" from the infinite number of realizations that could arise from the underlying matrix of probabilities. This independence of the simulations, plus the one-step memory in the process, means that the vertical arrangement of individual beds may have no real relation to the stratigraphic marker beds that are an essential part of real-world stratigraphic sequences. These limitations may be partly overcome by use of higher order chains, such as Schwarzacher's recent use (1967) of a two-step memory, in which the states at time t_{r-30} and t_{r-1} are used to control the event at time t_r. The long memory part of the chain is related to the average thickness of the stratigraphic cycles, and hence tends to produce simulated sections with an overall similarity in cycle thickness.

For the first-order chain a sense of lateral continuity (and hence of stratigraphic correlation) can be introduced by setting up a model which establishes a forward and backward movement of the strand line as in transgressive-regressive cycles. Observation stations can be placed at convenient lateral positions to monitor the to-and-fro motion of the strand. Inasmuch as this motion is continuous rather than occurring as a series of discrete jumps, the model can be structured as a continuous-time Markov process, with either discrete or continuous states. This paper discusses a transgressive-regressive model in which the states are treated as discrete, and time is continuous. Models of this type permit the direct tracing of simulated marker beds from one monitoring position to the next, and they eliminate one of the major shortcomings of the conventional first-order chain as a simulation device.

In the first-order, discrete-time, discrete-state Markov chain, the transition probability p_{ij} is defined as the probability that the system under study will be in state j at time t_r, given that it was in state i at time t_{r-1}. In the simplest chain it is tacitly assumed that transitions occur at fixed discrete time intervals, $t = (t_r - t_{r-1})$, so that there is a transition with every click of a "Markovian clock." The transitions may be from a given state into itself, or from one state to another. The diagonal probabilities control the within-state transitions, and the off-diagonals control the between-state transitions.

In a transgressive-regressive cycle, it seems more realistic to think of time flowing continuously, during part of which (at any given geographic monitoring position), sandstone is deposited, followed by shale, and so on. In this situation, the pattern of transitions can be examined in terms of the length of time that the system remains in a given state, once it has entered that state. That is, interest shifts from the probability of a state change to the rate at which these changes occur.

The purpose of this preliminary report is to show how a relatively simple deterministic model with continuous time and continuous states can be converted into its stochastic equivalent. The mathematical relations between the transition-probability matrix, $[p_{ij}]$, of the discrete-time, discrete-state Markov chain and the transition-rate matrix, $[q_{ij}]$

of the continuous-time, discrete-state Markov model will be published as a Computer Contribution by the Kansas Geological Survey. The present report discusses principles underlying the models and includes some simulation output.

CONTINUOUS-TIME, CONTINUOUS-STATE MODEL

Figure 1 is a cross section normal to a straight coast for a greatly oversimplified model of a transgressive-regressive clastic wedge. The cycle starts with movement of the strandline from a position of maximum regression to one of maximum transgression, followed by regressive movement to the same starting position, whereupon the cycle repeats itself. This model is continuous in time and space, with all cycles of equal duration, and with no stillstands.

The three stratigraphic sections in Figure 1 indicate the kinds of deposits formed during a cycle. These consist of a belt of littoral sand in the shore zone, mud (marine shale) in the offshore water, and undifferentiated nonmarine deposits (lagoonal shale, coal, fluvial deposits, etc.) landward of the littoral sand. It is assumed that the deposits have thickness proportional to the time interval associated with each stage of the cycle, so that any horizontal line through the diagram is a time line. The model is also so constructed that the belt of littoral sand (i.e., the lateral width of the sand deposit along any horizontal line in Figure 1) is fixed in width throughout the cycle, whereas the marine shale extends indefinitely seaward and the nonmarine deposits extend indefinitely landward of the strandline sand. The fixed width of the sand belt is not unrealistic for a clastic wedge. The "marker bed" in this model is the time-transgressive littoral sand, shown in Figure 1 as outlining the cycles.

Historically, the concept of marine transgression and regression developed in part from detailed studies of many stratigraphic sections of the kinds illustrated, in which outcrops discrete in space provided the basis for inferring transgressive-regressive movements continuous in time and space. By re-discretizing the states in Figure 1, a simulation model can be set up in the framework of a Markov chain that develops discrete stratigraphic sections or boreholes at selected positions along the cross section of Figure 1.

CONTINUOUS-TIME, DISCRETE-STATE MODEL

In setting up the discretized model, we define

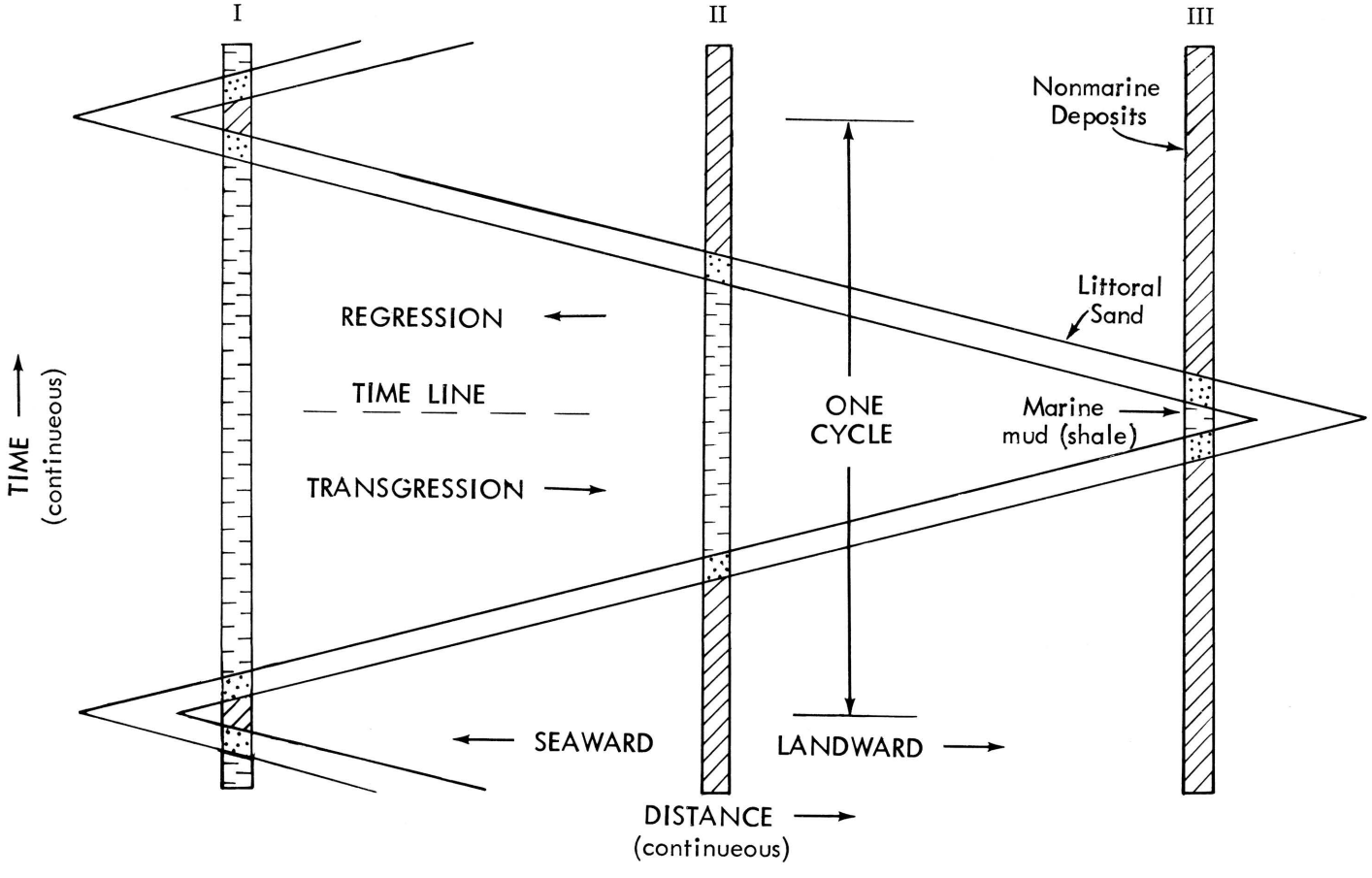

Figure 1.-Uniform transgressive-regressive cycle, showing pattern of sand through time, and three stratigraphic sections.

the states as successive positions occupied by the belt of littoral sand as the strandline moves forward and back. These positions are discretized by using the boreholes of Figure 1 as monitoring stations for observing the progress of the cycle. We now visualize the cycle in terms of the deposits formed during lateral migration of three environments that produce a band of littoral sand in the shore environment, with marine mud (shale) on its seaward side, and undifferentiated nonmarine deposits on the landward side.

Figure 2 shows the discretized model. The landward and seaward limits of the band of littoral sand are shown as successive segments at equally spaced time intervals, so placed that the position of the sand is unambiguously stated with respect to the three monitoring stations. These positions are boundaries between zones labeled A, B, C, and D from left to right. The state of the transgressive-regressive system is now defined by the position of the littoral sand within and between these zones. Thus, the first state (at the bottom of the diagram) is designated as AA because both sand limits lie in zone A. The second state is designated as AB because the sand limits straddle monitoring position I and hence the sand lies in both zones A and B. This procedure is followed through the cycle, with the regression states indicated as CD', CC', etc., as in Figure 2. This means that once state AB' is reached, the system moves to state AA for the next cycle.

For each state there is a definite lithology associated with each monitoring position. In state AA all three stations receive nonmarine deposits. In state AB position I receives littoral sand, and nonmarine beds continue at stations II and III. In state BB marine shale occurs at position I, but the littoral sand has not yet reached position II, so that this station and station III still receive nonmarine deposits. Thus, in a simulation experiment three stratigraphic sections or boreholes can be generated as the cycle proceeds, and each station receives an unambiguous deposit for each state of the system.

In order to make this model more realistic, allowance must be made for major or minor reversals in strandline movement during the progress of a cycle. Before this is done, however, it will be interesting to examine the transition rate matrix and its accompanying simulation output for the deterministic model of Figure 2. In this model each state is occupied for the same length of time, which means that the rates of moving from one state to the next are all equal, and the succeeding state is uniquely specified.

The $[q_{ij}]$ matrix for this simple case is shown in Table 1. This matrix has some special properties that deserve comment. Inasmuch as attention is concentrated on the time required to leave some state i and move to another state j, the diagonal elements can be eliminated; they are simply shown as X's in Table 1. The rate at which the system moves from state i to state j is indicated by the marginal values,

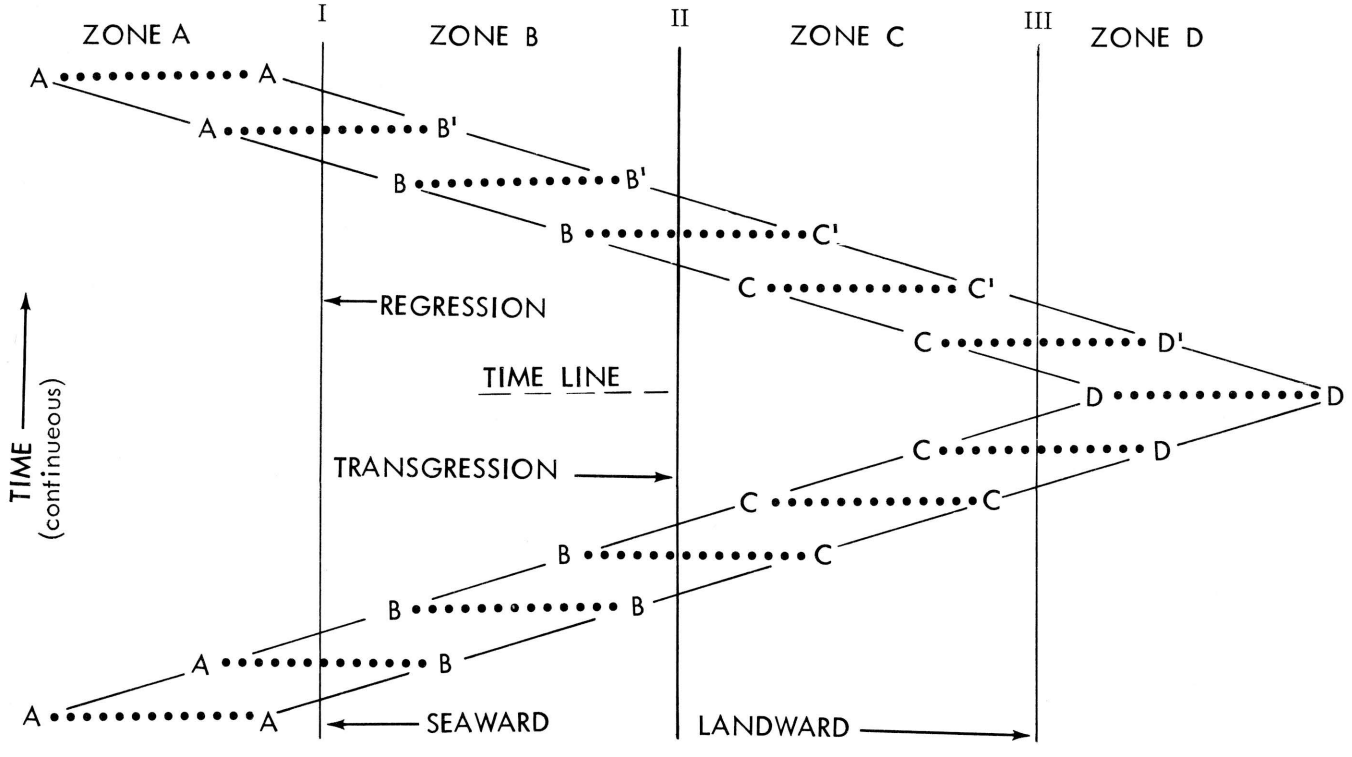

Figure 2.- Model of Figure 1 with discretized states showing position of littoral sand during progress of a cycle.

which represent the sum of the off-diagonal q_{ij}'s in a given row. These off-diagonals are proportional to the probabilities of moving to a specified state j. The row sums need not equal 1.0 as they do in a $[p_{ij}]$ matrix. An arbitrary rate of 4.0 units is used in Table 1; later this will be subdivided for the stochastic model.

Table 1 represents a completely deterministic scheme, in which the marginal rates are all equal, and the upper right-hand off-diagonal, with the same value, indicates that the probability is 1.0 (i.e., 4.0/4.0 = 1.0), that when the system leaves a given state i, it moves to the immediately adjacent state in the chain. The last row of the matrix represents the end of the cycle and the system returns to the initial state AA.

If we now assume that the rate of deposition is such that one unit of sediment thickness is deposited when the system is in any given state, the stratigraphic sections generated at each monitoring station are shown in Figure 3, which simulates one complete cycle. Horizontal lines are time lines, and diagonal lines in the figure indicate the continuous path of the littoral sand through the cycle. Simulation starts in state AA and proceeds systematically to AB', whereupon it returns to state AA as shown in the last line of the matrix in Table 1.

Table 1.- Matrix of transition rates for deterministic transgressive-regressive model.

Given State, i \ Succeeding State, j	AA	AB	BB	BC	CC	CD	DD	CD'	CC'	BC'	BB'	AB'	MARGIN
AA	X	4.0	0	0	0	0	0	0	0	0	0	0	4.0
AB	0	X	4.0	0	0	0	0	0	0	0	0	0	4.0
BB	0	0	X	4.0	0	0	0	0	0	0	0	0	4.0
BC	0	0	0	X	4.0	0	0	0	0	0	0	0	4.0
CC	0	0	0	0	X	4.0	0	0	0	0	0	0	4.0
CD	0	0	0	0	0	X	4.0	0	0	0	0	0	4.0
DD	0	0	0	0	0	0	X	4.0	0	0	0	0	4.0
CD'	0	0	0	0	0	0	0	X	4.0	0	0	0	4.0
CC'	0	0	0	0	0	0	0	0	X	4.0	0	0	4.0
BC'	0	0	0	0	0	0	0	0	0	X	4.0	0	4.0
BB'	0	0	0	0	0	0	0	0	0	0	X	4.0	4.0
AB'	4.0	0	0	0	0	0	0	0	0	0	0	X	4.0

MODIFIED MODEL WITH RANDOM REVERSALS

When reversals are introduced into the preceding model, additional entries are required in the rows of Table 1 to indicate that the preceding state can again be entered at any stage of the cycle. The conceptual model is shown in Figure 4 as a looped chain with forward and backward arrows that show the possible paths through the chain. We assume that progress through the chain from one state to the next (both in transgression and regression) is three times as likely as a reversal to the preceding state. The total rate for each state is kept at 4.0 units, but the value 3.0 is assigned to the forward

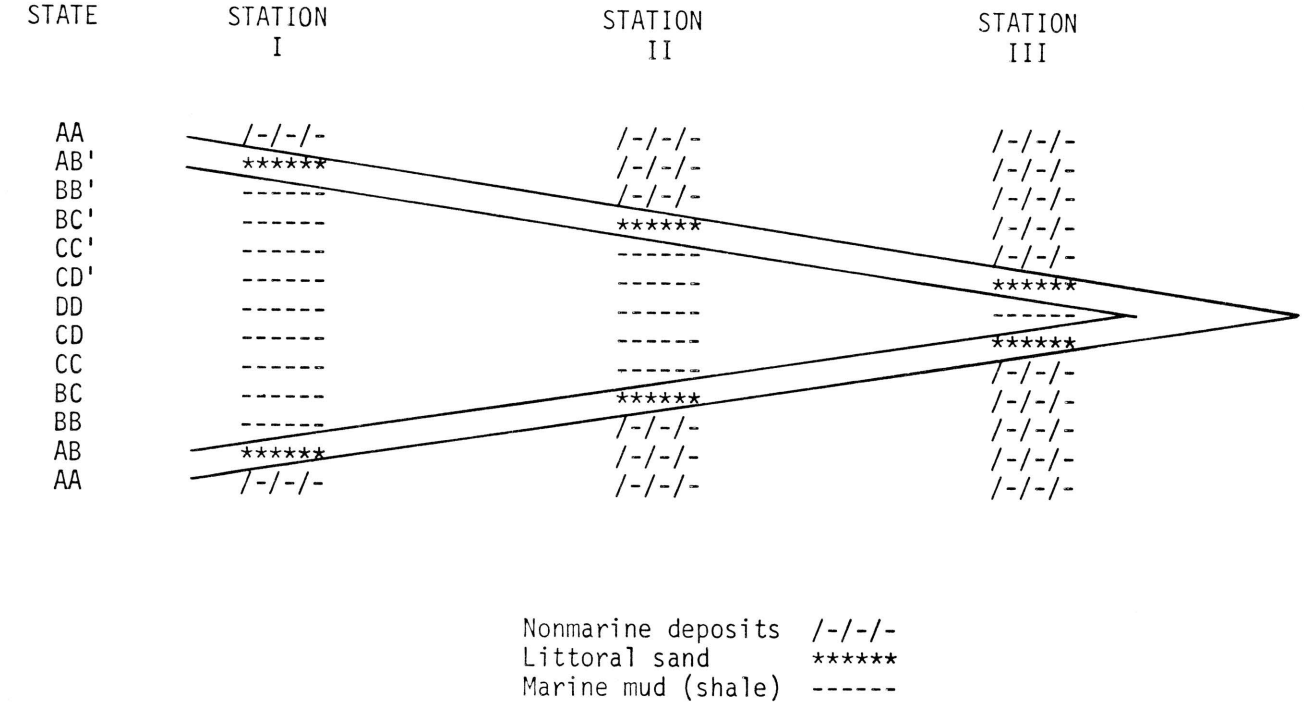

Figure 3.- Simulation of one cycle from matrix of Table 1. This is completely deterministic, and all simulated cycles would be the same.

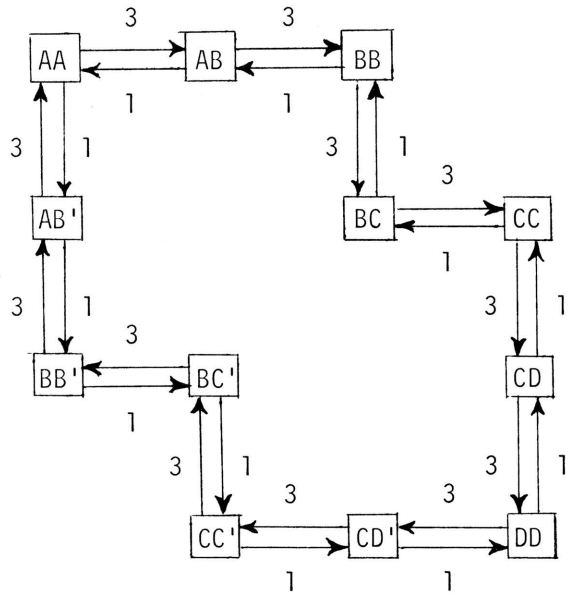

Figure 4.- Schematic diagram showing main flow of transgressive-regressive cycle, with relative rates of forward and backward motion.

arrows and 1.0 to the reverse arrows.

The chain in Figure 4 is arranged as a transition-rate matrix in Table 2. Marginal entries indicate total rates, and the individual q_{ij}'s are proportional to the probability of forward or backward movement. In implementing this model we again assume that one unit of thickness is deposited when the system is in any given state i, but now a new element enters the simulation. That is, although the total rate of moving from one state to another is 4.0 in each row of the matrix, the probability of moving to the succeeding state in the cycle is 3/4, whereas the probability of a reversal to the preceding state is 1/4.

A simulation run for this model is accomplished by starting in state AA, drawing a uniformly distributed one-digit random number in the range 1, 2, 3, and 4. If the number is 1, 2, or 3, the system moves forward (i.e., to state AB). If the number drawn is 4, the system moves backward to state AB', and so on through the simulation. Thus the model has become stochastic with respect to the succession of states, which are now controlled by probabilities throughout the chain. Figure 5 shows part of a simulation obtained by using Table 2 and random numbers for state changes.

Although this modified model has a stochastic element, the stochastic structure can be completed by now randomizing the total time occupied by each state. By adding this feature, the model introduces added variety into the cycles, in that it allows for the unpredictable variations that arise in real-world cycles under the combined influence of tectonic movements in the source area, changes in the nature and amount of detritus fed to the sea, changes in slope of the nearshore bottom, eustatic changes of sea level produced by tectonic events in ocean basins, etc. These underlying controls vary in space and time, and their combinations give rise to complex responses in the position of the strandlines at any given moment.

SIMULATION MODEL WITH RANDOMIZED TIME

The final modification to be made in the model is to randomize time as suggested in the preceding paragraph. To do so with this model, we select a uniformly distributed random number, U, in the range from 0 to 1, and take the natural log of its reciprocal, $\log_e(1/U)$. Then, if t_c represents the "time of change" from one state to another, we use the following relation to determine how long the system remains in a given state i:

$$t_c = \frac{\log_e(1/U)}{M_i} \quad .$$

Here M_i is the total rate for state i as indicated in the margin of the matrix. When observational data are used to set up the transition-rate matrix, it is found that a restricted range of random numbers gives the most "lifelike" simulations. In the present case, we used random numbers in the range 0.30 to 0.80 inclusive, for the t_c calculation. We again use the matrix of Table 2, to show how this simulation compares with the more deterministic models. (It may be mentioned in passing that U was kept constant in the simulation of Figure 5.)

The procedure for developing simulations involves the following steps: draw a random number

Table 2.- Matrix of transition rates for transgressive-regressive model with reversals.

		Succeeding State, j												
		AA	AB	BB	BC	CC	CD	DD	CD'	CC'	BC'	BB'	AB'	MARGIN
Given State, i	AA	X	3.0	0	0	0	0	0	0	0	0	0	1.0	4.0
	AB	1.0	X	3.0	0	0	0	0	0	0	0	0	0	4.0
	BB	0	1.0	X	3.0	0	0	0	0	0	0	0	0	4.0
	BC	0	0	1.0	X	3.0	0	0	0	0	0	0	0	4.0
	CC	0	0	0	1.0	X	3.0	0	0	0	0	0	0	4.0
	CD	0	0	0	0	1.0	X	3.0	0	0	0	0	0	4.0
	DD	0	0	0	0	0	1.0	X	3.0	0	0	0	0	4.0
	CD'	0	0	0	0	0	0	1.0	X	3.0	0	0	0	4.0
	CC'	0	0	0	0	0	0	0	1.0	X	3.0	0	0	4.0
	BC'	0	0	0	0	0	0	0	0	1.0	X	3.0	0	4.0
	BB'	0	0	0	0	0	0	0	0	0	1.0	X	3.0	4.0
	AB'	3.0	0	0	0	0	0	0	0	0	0	1.0	X	4.0

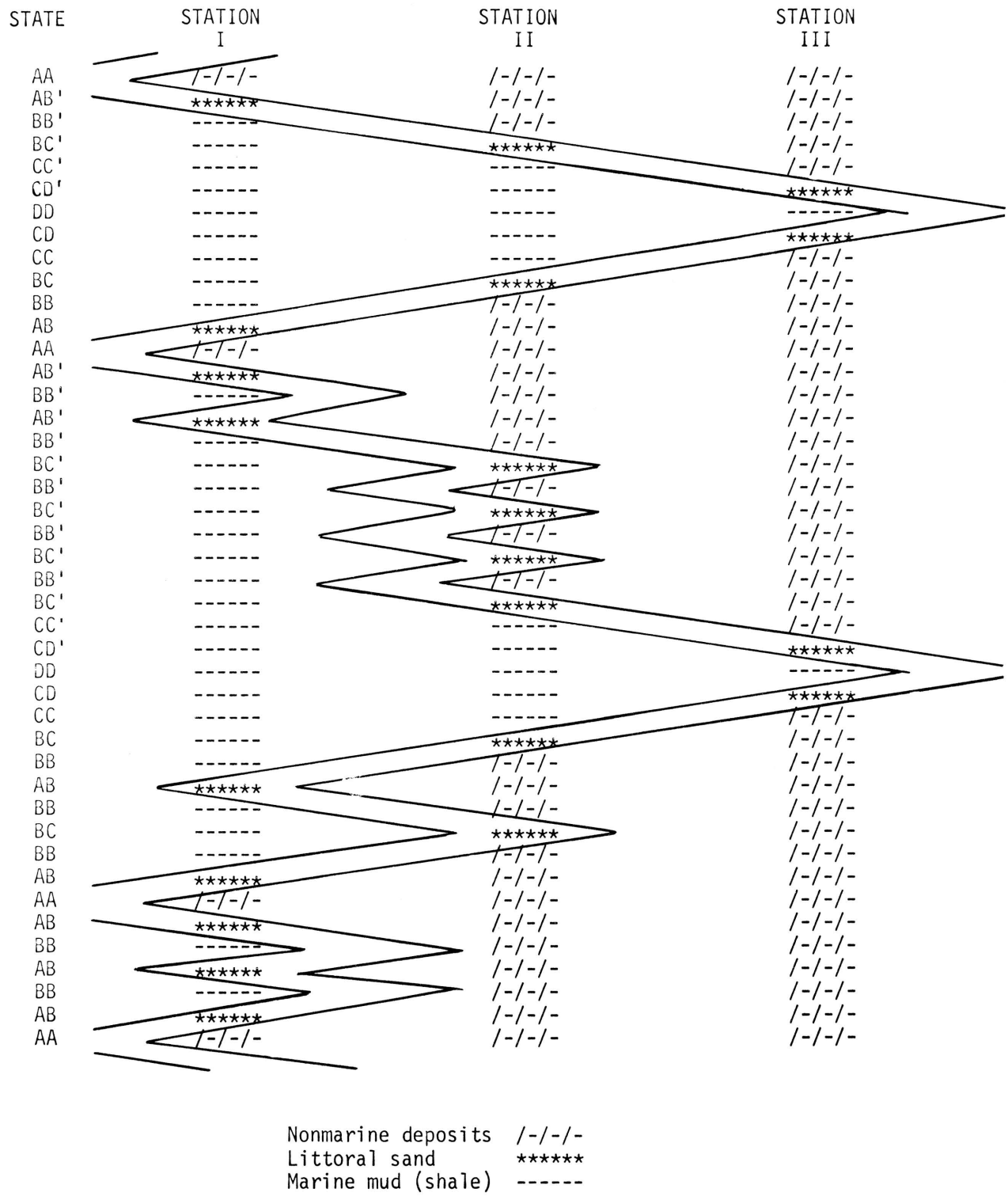

Figure 5.- Simulation of three stratigraphic sections from matrix of Table 2. This model permits reversals, but the time in each state remains constant.

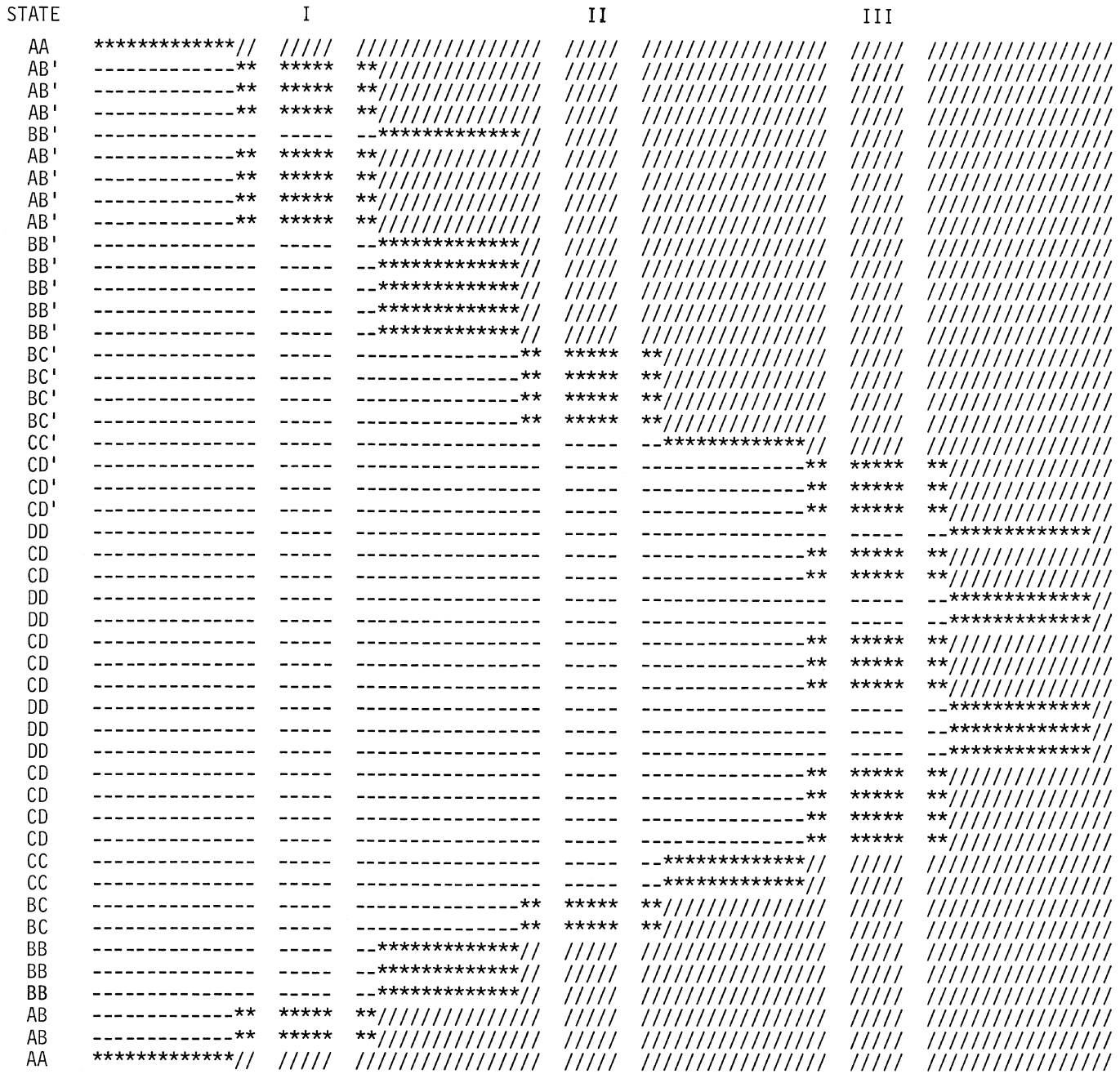

Figure 6.- Simulation of three stratigraphic sections from matrix of Table 2, with time in each state a random variable. This shows up in the different thickness associated with each state, indicated by state code on left.

from 0.30 to 0.80, compute its reciprocal and take the natural log. Divide this by the marginal rate for the state involved, to find how long the system remains in that state. Next, draw another random number to determine the state to which the system has moved, by using the individual q_{ij}'s as explained earlier to obtain the probabilities. Finally, select some interval of time to represent one unit of sediment thickness, to determine thickness of the deposit laid down during each state. For example, with the range of random numbers used here, the extremes of t_c will be 0.056 and 0.301 time units. We divided the difference into four parts and assigned a number of beds from 1 to 5 over this range. The following example gives two lines of computation:

State	U	$\log_e(1/U)$	t_c	No. of beds	Random no. for next state	State to which system moves
AA	0.66	0.412	0.103	2	57	AB
AB	0.54	0.615	0.154	3	80	AA

In this instance the system started in state AA with two units of sediment thickness, advanced to state AB with three thickness units, and reversed to state AA again. Normally one calls for say 500 state changes which will include a fairly large number of cycles. Our present limitation of no more than five thickness units per state change is wholly arbitrary, but with this restriction, a typical portion of simulated section is given in Figure 6, which shows the three stratigraphic sections generated.

The most striking difference between the simulations of Figure 5 and 6 is the variation in thickness of beds associated with a given state, as indicated by the codes on the left. The output here reconstructs the whole lateral pattern, with the monitoring stations edged by blank space. The discrete "jumps" of the shifting environments from one lateral position to the next are well illustrated; the thickness of the sand reflects the length of time that the system remains in a given state.

The arbitrary transition rates chosen for present examples serve mainly to show the added variety introduced by the stochastic model. The matrix of Table 2, as shown graphically in Figure 4, is still too simple for realistic simulations: if the random numbers that control state changes happen to fall properly, the system can regress to maximum transgression.

CONCLUSIONS

The organization of this report recapitulates the transition from a fully deterministic model to its stochastic counterpart. The final model still contains a kernel of determinism that controls the main pattern of transgression and regression, but as stated, it includes the sort of unpredictable fluctuation that is so commonly present in real-world cycles. In applied stratigraphic studies, the transition rate matrix can in some cases be set up directly from knowledge of rates of sedimentation. Commonly, however, it is more convenient to transform a $[p_{ij}]$ matrix to its $[q_{ij}]$ counterpart. This aspect of the model is discussed in the expanded report (Krumbein, in preparation) submitted for publication. A computer program for the transformation is included in that report, as is the stochastic transgressive-regressive program. Other topics related to extensions of the present model are developed in the later report, including the use of higher order Markov schemes.

I am much indebted to Professor John W. Tukey of Princeton University for enabling me, during the Spring of 1966, to participate in his Statistical Techniques Research Group, where many of the ideas in this paper, and the basic computer program, were developed.

REFERENCES

Krumbein, W.C., 1967, FORTRAN IV computer programs for Markov chain experiments in geology: Kansas Geol. Survey Computer Contr. 13, 38 p.

Krumbein, W.C., in preparation, FORTRAN IV computer programs for a continuous-time, discrete-state Markov model for stratigraphic simulation: Kansas Geol. Survey Computer Contr.

Schwarzacher, W., 1967, Some experiments to simulate the Pennsylvanian rock sequence of Kansas: Kansas Geol. Survey Computer Contr. 18, p. 5-14.

EXPERIMENTS WITH VARIABLE SEDIMENTATION RATES

by

Walther Schwarzacher

Queen's University, Belfast, Northern Ireland

INTRODUCTION

Attempts to simulate stratigraphical sequences have been made by Carr (1966), Krumbein (1967), and Schwarzacher (1967). These experiments showed that comparatively simple random processes may provide a descriptive model for the stratigraphical sections. Little has been learned, however, about the mechanics of sedimentation from such experiments. The reason for this is largely the complexity of natural processes. It is possible that some progress can be made by severely restricting the scope of such investigations, and in this contribution a limited problem is examined. How do fluctuating sedimentation rates affect the manner in which geological processes are recorded in the stratigraphical column? The problem can be best explained by the following example.

THE CONSTANT SEDIMENTATION RATE MODEL

We may consider the stratigraphical record as the end result of three stages. Stage 1 consists of the environment with changing conditions in time; stage 2 is the depositional process determined by a number of rules governing sedimentation rates, and stage 3 is the stratigraphical column with the lithological variation recorded along a vertical scale. As a practical example, let us assume that the environmental stage 1 can be described fully by three states, A, B, C, which represent conditions leading to three rock types, limestone, shale, and sandstone. We assume further that the three states in the time sequence appear at any time with equal probability, so the time series of events leading to the formation of the three rock types is described fully by the transition matrix,

$$W = \begin{bmatrix} \frac{1}{3} & \frac{1}{3} & \frac{1}{3} \\ \frac{1}{3} & \frac{1}{3} & \frac{1}{3} \\ \frac{1}{3} & \frac{1}{3} & \frac{1}{3} \end{bmatrix}$$

The sedimentation process shall be defined by three constant sedimentation rates, A:B:C = 1:2:3, meaning that in the same time in which one thickness of limestone is produced three thicknesses of sandstone could be laid down. The stratigraphical sequence generated by this mechanism can be deduced. Assume the initial stage was B:

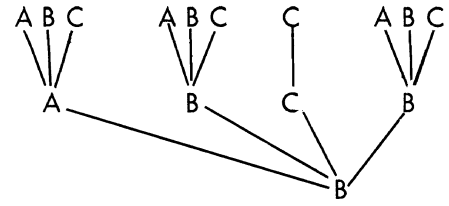

The possible sequences for two consecutive stages are shown in the above scheme.

The probability matrices for 1, 2, and 3 step transition are given by:

Step 1

$$\begin{bmatrix} \frac{1}{3} & \frac{1}{3} & \frac{1}{3} \\ \frac{1}{6} & \frac{4}{6} & \frac{1}{6} \\ \frac{1}{9} & \frac{1}{9} & \frac{7}{9} \end{bmatrix}$$

Step 2

$$\begin{bmatrix} \frac{1}{9} & \frac{4}{9} & \frac{4}{9} \\ \frac{5}{18} & \frac{5}{18} & \frac{8}{18} \\ \frac{4}{27} & \frac{7}{27} & \frac{16}{27} \end{bmatrix}$$

Step 3

$$\begin{bmatrix} \frac{4}{27} & \frac{7}{27} & \frac{16}{27} \\ \frac{5}{54} & \frac{20}{54} & \frac{29}{54} \\ \frac{16}{81} & \frac{28}{81} & \frac{37}{81} \end{bmatrix}$$

The series converges eventually to a matrix of the stable probability vector $[\frac{1}{6}, \frac{2}{6}, \frac{3}{6}]$. But this new series is no longer an independent random series as the states in the stratigraphical sequence depend on previous states. If we had chosen a first-order Markov process as the stage 1 environmental model, the Markov property would have been lost in the stratigraphical record. On the other hand, a pure cyclical stage 1 model given by the matrix,

$$\begin{bmatrix} 0 & 1 & 0 \\ 0 & 0 & 1 \\ 1 & 0 & 0 \end{bmatrix},$$

would have been unrecognizable unless up to six lags of stratigraphical data were calculated.

Because of its rigid conditions regarding sedimentation rates, the model is of limited use but is helpful in a first examination of observed transition matrices. For a test example, a composite section of Upper Pennsylvanian rocks of Kansas was used. The section was divided into 5-foot intervals, and each interval coded according to the lithology that occupied the greatest thickness within it. Four stages were differentiated; 1 = shale outside limestone for matrices; 2 = limestones, except Type 2; 3 = Type 2 limestone (R.C. Moore's classification, 1936), and 4 = shale inside limestone formations. The following matrix of transition probabilities was found:

$$\begin{bmatrix} .899 & .059 & .017 & .025 \\ .235 & .627 & .039 & .098 \\ .000 & .250 & .000 & .750 \\ .000 & .435 & .000 & .565 \end{bmatrix}.$$

Powering of this matrix gives the following stable probability vector: [.603, .256, .020, .121]. As an initial hypothesis we may assume that the average thickness of the lithologies is related to sedimentation rates of the rock types. Thus if we choose the sedimentation rate for Type 2 limestone as unity, we find that the ratios of the sedimentation rates are 1:2:3:4 = 30:13:1:6. That is, according to the hypothesis, outside shale is laid down 30 times as fast as Type 2 limestone, etc. We can now test different hypotheses regarding the stage 1 model. For example, the equal probability hypothesis of environmental time changes would lead to the transition matrix:

$$\begin{matrix} .975 & .008 & .008 & .008 \\ .002 & .994 & .002 & .002 \\ .250 & .250 & .250 & .250 \\ .042 & .042 & .042 & .874 \end{matrix},$$

which is obviously not close to the observed transition matrix. An environmental model of the form:

$$\begin{bmatrix} 0.00 & 1.00 & 0.00 & 0.00 \\ 0.90 & 0.00 & 0.00 & 0.10 \\ 0.00 & 0.25 & 0.00 & 0.75 \\ 0.00 & 0.90 & 0.10 & 0.00 \end{bmatrix},$$

leads to

$$\begin{bmatrix} .976 & .033 & 0. & .00 \\ .070 & .923 & 0. & .007 \\ .00 & .250 & 0. & .750 \\ .148 & .836 & 0. & .016 \end{bmatrix},$$

and although considerably closer to the observed matrix can not be much bettered under the assumption of constant sedimentation rates.

VARIABLE SEDIMENTATION RATE MODELS

It is altogether more realistic to assume that sedimentation rates are not constant but are in themselves random variables. The sedimentation rate may be thought of as a series of continuously alternating stages of deposition and erosion. We assume that at a certain time environmental conditions are such that a lithology W may potentially be deposited. At each time increment, erosion or deposition may take place. The probability of erosion following deposition is called α, and the probability of deposition after erosion is called β. These probabilities are assumed to be constants for each lithology-producing environment. The time sequence of erosion and deposition for a single lithology may be represented as dependent Bernoulli trials:

$$\begin{array}{l} \\ \text{Deposition} \\ \text{Erosion} \end{array} \begin{array}{c} \begin{array}{cc} \text{Deposition} & \text{Erosion} \end{array} \\ \begin{bmatrix} W_{11}(1-\alpha) & W_{11}\alpha \\ W_{11}\beta & W_{11}(\beta-1) \end{bmatrix} \end{array} \quad (1)$$

To satisfy the conditions of a transition matrix, W_{11} in this system must have the value of 1. There then exists an equilibrium given by the stable probability vector $[\frac{\beta}{\alpha+\beta}, \frac{\alpha}{\alpha+\beta}]$. The equilibrium gives us the proportion of time spent in the depositional and erosional phase during the stage W_1. Obviously for accumulation to occur, $\beta > \alpha$. The principle can be expanded to a multiple Markov chain in the following manner:

$$\begin{array}{c} \begin{array}{cccc} 1 & & 2 & \end{array} \\ \begin{bmatrix} W_{11}(1-\alpha_1) & W_{11}\alpha_1 & W_{12}(1-\alpha_2) & W_{12}\alpha_2 \ \ldots \\ W_{11}\beta_1 & W_{11}(1-\beta_1) & W_{12}\beta_2 & W_{12}(1-\beta_2) \ \ldots \\ W_{21}(1-\alpha_1) & W_{21}\alpha_1 & W_{22}(1-\alpha_2) & W_{22}\alpha_2 \ \ldots \\ W_{21}\beta_1 & W_{21}(1-\beta_1) & W_{22}\beta_2 & W_{22}(1-\beta_2) \ \ldots \\ \cdot & \cdot & \cdot & \cdot \ \ldots \\ \cdot & \cdot & \cdot & \cdot \ \ldots \end{bmatrix} \end{array} \quad (2)$$

A similar model has been proposed by Vistelius (1965) to explain specifically the sedimentation processes of turbidity currents. The Vistelius model specifies that only one thickness increment can be eroded prior to deposition whereas the present model can remain for several time increments in the depositional or erosional phase. Vistelius' argument regarding the Markov behavior of the resulting stratigraphical series, however, holds; that is, if states W_1, W_2, W_3, have been deposited in succession, $P\{W_3 \mid W_2, W_1\} = P\{W_3 \mid W_2\}$. Because of the possibility of missing steps in the stratigraphical series, the stratigraphical data may be unsuitable to reconstruct the environmental sequence. Vistelius was able to derive the matrix of transition probabilities in the stratigraphical sequence from the frequency of strata produced by his scheme. No such solution has been found as yet for this model but the equilibrium probabilities for the stratigraphical series can be determined and simulation models can be based on these probabilities.

Let the environmental development be represented by matrix [W]. The sedimentation parameters α, β for different lithologies in the long run will establish an equilibrium for deposition $\frac{\beta}{\alpha+\beta}$ and erosion $\frac{\alpha}{\alpha+\beta}$ written as vector π_δ and π_ϵ. The equilibrium of [W] will be given by $[W]^n$ where n is a

large number. The equilibrium vector for the generating matrix (2) is given by the product of the elements π_δ and π_ϵ and the elements of $[W]^n$ alternating in the following manner.

$$[W_{11}]^n_{\delta 1}\ [W_{11}]^n\pi_{\epsilon 1}\ [W_{12}]^n\pi_{\delta 2}\ [W_{12}]^n\pi_{\epsilon 2}\ \cdots$$

Now the probability that bed a in the stratigraphical section is followed by bed b is equal to the transition probability a→b and the probability that there has been an equal number of erosional and depositional steps in between the actual deposition of a and b. Thus the stable probability matrix of the stratigraphical series $[P]^n$ can be calculated and we find for instance:

$$[P_{11}] = [W_{11}]\pi_{\delta 1} \cdot \Sigma W_i\pi_{\delta i} \cdot \Sigma W_i\pi_{\ i}\ .$$

For example let [W] be the cyclical matrix:

$$W = \begin{bmatrix} 5 & 5 & 0 \\ 0 & 5 & 5 \\ 5 & 0 & 5 \end{bmatrix} \qquad W^n = \begin{bmatrix} \frac{1}{3} & \frac{1}{3} & \frac{1}{3} \\ \frac{1}{3} & \frac{1}{3} & \frac{1}{3} \\ \frac{1}{3} & \frac{1}{3} & \frac{1}{3} \end{bmatrix}$$

The parameters are $\alpha = .2, .1, 3, \beta = .6, .9, .4$; leading to the generating vector:

1		2		3	
δ	ϵ	δ	ϵ	δ	ϵ
.25	.083	.3	.033	.190	.143

and from this we obtain the stable vector for transition probabilities in the stratigraphical sequence:

$$P^n = [.336,\ .374,\ .290]\ .$$

An actual simulated run using this source model gave the first-order transition probabilities for the stratigraphical sequence as:

$$P = \begin{bmatrix} .433 & .540 & .027 \\ .084 & .481 & .433 \\ .550 & .052 & .398 \end{bmatrix}, \text{ and } P^{16} = \begin{bmatrix} .337 & .338 & .287 \\ .335 & .375 & .286 \\ .335 & .374 & .285 \end{bmatrix},$$

which is in good agreement with the predicted stable probabilities.

As an illustration for the working of the model we constructed the matrix:

$$W = \begin{bmatrix} .16 & .38 & .33 & .13 \\ .32 & .32 & .21 & .15 \\ .29 & .33 & .25 & .13 \\ .08 & .29 & .25 & .38 \end{bmatrix},$$

which in fact consists of standardized random numbers. Let us assume that this is the full description of the environmental history, for the sedimentary parameters we take $\alpha_{1\text{-}4} = [.1, .2, .3, .2]$ and $\beta_{1\text{-}4} = [.111, .674, .800, .436]$. The resulting stratigraphical sequence should have a constant probability vector of [.2207, .3486, .2556, .1749]. A simulated run under the same conditions gave [.2142, .3693, .2693, .1473]. Choosing instead a cyclical model given by the matrix:

$$\begin{bmatrix} 0 & 1 & 0 & 0 \\ 0 & 0 & 0 & 1 \\ 0 & 0 & 0 & 1 \\ .25 & .25 & .25 & .25 \end{bmatrix},$$

it gave a sequence with a stable probability of [.193, .403, .192, .212]. Note that this cannot be calculated as the above matrix does not converge with powering.

CONCLUSIONS

The model demonstrates that a stratigraphical sequence may be generated by a wide variety of time processes. Both deterministic and probability models of an environment can lead to similar Markov series in a stratigraphical sequence. However, by introducing the geological meaningful parameters of a and β we may be able to judge the plausibility of our environmental model. In the last example a decision may be based on the relative frequency of lithological types. Alternative models with a predetermined constant probability vector can be constructed by changing α and β. Not examined yet has been the thickness distribution of different beds which also can be simulated with the model.

REFERENCES

Carr, D.D., and others, 1966, Stratigraphic sections, bedding sequences, and random processes: Science, v. 154, no. 3753, p. 1162-1164.

Krumbein, W.C., 1967, FORTRAN IV computer programs for Markov chain experiments in geology: Kansas Geol. Survey Computer Contr. 13, 38 p.

Moore, R.C., 1936, Stratigraphic classification of the Pennsylvanian rocks of Kansas: Kansas Geol. Survey Bull. 22, 256 p.

Schwarzacher, W., 1967, Some experiments to simulate the Pennsylvanian rock sequence of Kansas: Kansas Geol. Survey Computer Contr. 18, p. 5-14.

Vistelius, A.B., 1965, Theory of formation of sedimentary beds: (English translation) Doklady Akad. Nank SSR, v. 164, no. 1, p. 158-160.

MONTE CARLO SIMULATION MODEL FOR PIERCEMENT SALT DOMES

by

James C. Howard

The Sun Oil Company Production and Research Laboratory

INTRODUCTION

Piercement salt domes intrude overlying sediments by upward displacement of salt from a buried source layer. Salt moves upward in response to a gravitational instability created by the density contrast between salt and heavier overburden. Dome morphology and growth rate depend on the density contrast between salt and overlying sediments, the bouyancy of the salt stock, the geothermal gradient and the strength of the overburden. The shape of the dome is influenced indirectly by the rate of basin subsidence.

Laboratory scale models of piercement salt structures have been constructed by Parker and McDowell (1955) and many others. By assuming viscous behavior for the salt and sediments, Selig (1965) and Biot and Ode' (1965) analytically described the nonpiercement stages of dome formation in theoretical models based on the laws of fluid mechanics. The physical and deterministic models do not illustrate the irregularities in dome shape such as salt ledges and spines, which may be observed in nature. A stochastic model, based on Monte Carlo or random walk techniques, more adequately accounts for the random components of variability in a transport phenomenon of the diffusion type. This has been demonstrated by Culling (1963) for soil creep, Litwiniszyn (1963) for subsidence in granular materials, Morrill (1965) and Yuill (1965) for population expansions, Harbaugh (1966) for growth of marine organism communities and Schenck (1963) for drainage basin evolution.

Halite crystals are deformed in part by intracrystalline gliding on preferred slip planes (Schwerdtner, 1965). From crystal to crystal the slip planes are assumed to be distributed randomly so that displacements made by a crystal form a sequence of independent random variables. Displacement of aggregates of crystals can be viewed in terms of a diffusion-type process.

The model is operated on an iterative basis by a set of assumed probability distributions that specify the likelihood of the salt-sediment interface displacing in different directions at successive increments of geologic time. By printing a series of vertical cross sections at any specified time increment, it is possible to observe the progressive changes in dome morphology. The model does not take into account the nature of deformation in the sediments or the development of caprock.

Acknowledgments.- I thank the officers of The Sun Oil Company Production and Research Laboratory for sponsoring the research and publication of this paper.

SYMBOLS USED

b	bouyancy
c	compaction
d_{com}	amount of compaction
d_{sed}	amount of sedimentation
d_{sub}	amount of subsidence
D	depth
g	gravitational constant
h	height of dome above its base
H	thickness of overburden
i	b, ρ, T, S
k_i	proportionality constant
LL_i	lower limit for the variate X_i
n	constant
$P[C]$	composite probability
$P[X_i]$	probability for the variate X_i
$P[NS]$	near surface end-member probability for X_i
$P[SL]$	source-bed level end-member probability for X_i
S	ultimate strength of sediment
$\bar{S}$	average sediment strength penetrated by salt
t	time
t_{lag}	time lag
T	temperature
TD	depth to the assumed present-day level of the salt layer
UL_i	upper limit for the variate X_i
v_{sed}	rate of sedimentation
w_i	weighting factors
$\bar{\omega}$	average growth rate of the dome
ρ	density
$\bar{\rho}$	average sediment density penetrated by salt
$\Delta\sigma$	differential stress between columns of salt and sediment

PARAMETERS AFFECTING SALT MOBILITY

Factors that are thought to exert the greatest

influence on the mobility of salt are depicted in Figure 1 as functions of depth. The nature of these curves will differ from one field situation to the next.

An estimate of the difference of sediment densities with depth can be obtained by applying a conversion factor to sonic-log velocities. Figure 1a is a modified version of a curve compiled by Nettleton (1934) for sediments in the Gulf Coast area. The bulk density of salt is approximately 2.2 gm/cm^3.

Bouyancy (Fig. 1b) is a cumulative effect that can be calculated from the product of the height of the dome and the density difference between the salt and overlying sediments. Bouyancy is zero before the dome begins to form and increases to a maximum when the dome reaches the level of minimum density contrast.

Gussow (1966) recognized the importance of the role of temperature in the mechanical behavior of salt. He stated that salt deforms plastically at temperatures in excess of 300° C, which requires approximately 25,000 feet of overburden, assuming a normal thermal gradient. Creep in halite probably occurs at lower temperature and pressure levels than indicated by many laboratory results, due to the weakening effect of geologic time. Guyod's (1946) experiments with electrolytic scale models suggest a linear thermal gradient in the sediments at distances sufficiently far from the dome so that the high heat conductivity of salt does not influence the gradient. The gradient flattens laterally with respect to the dome and the deviation from linearity becomes most pronounced directly above the dome as indicated in Figure 1c. Selig and Wallick (1966) confirmed Guyod's results in a theoretical model formulated around the heat flow equation. A geothermal gradient in the vicinity of a salt dome can be constructed from stabilized bottom-hole temperature measurements.

Figures 1d and 1e, published by Handin and Hager (1958), express the depth relationship of ultimate strength for the Barnes Sandstone and Muddy Creek shale. Even though these rocks are not from Gulf Coast assemblages, the curves are thought to be generally indicative of ultimate strength values for other sandstones and shales. Handin and Hager (1958) define ultimate strength as the greatest stress difference the material can withstand under given conditions of effective pressure, temperature and strain rate.

Processes which influence the shape of the dome include sedimentation, compaction and basin subsidence. The sedimentation rate is expressed as a function of time

$$v_{sed} = k\, t^{-1/n} \qquad (1)$$

This function will differ with geological setting. The amount of compaction is expressed in terms of the percentage of the original volume, as follows (equation 2):

$$c = H\left(1 - \frac{1}{1 + [1 - EXP(-kHt)]}\right) \qquad (2)$$

The amount of subsidence changes in response to the weight of the overburden. It is related to differences in the amounts of sedimentation and compaction.

$$d_{sub} = k\,(d_{sed} - d_{com}) \qquad (3)$$

PROBABILITY DISTRIBUTIONS

Nettleton (1934) used a continuous curve to describe the general form of a salt dome and its surrounding sink (Fig. 2). The curve can be approximated by straight-line segments and its shape defined by radii with respect to the axis of circular symmetry. Values for the radii are obtained from subsurface drilling, geophysical sources and scale-model studies. The top of the frustrum of the cone is equated to the estimated near-surface dome diameter. The flanks of the cone are determined by the estimated dips of the dome flanks. These are projected to the assumed source-bed level. The dimensions of the sink peripheral to the dome are estimated from laboratory model studies (Parker and McDowell, 1955). Material in the dome portion of the curve moves generally upward, whereas material in the sink regions migrates downward. Volume of salt in the dome is equivalent to that which is withdrawn from the salt source layer.

The curve is treated then as a probability density function with values ranging from zero to one. For each time interval, a random number is generated and its position along the abscissa is determined by the probability density function. At this randomly selected position, the specific direction of displacement of material at the salt-sediment interface is then computed.

In Figure 3, the relative likelihood of material displacing in different directions due to the separate influence of each physical parameter is represented qualitatively by vector diagrams at two levels -- near the surface and near the top of the source layer. For example, at the level of the salt bed, salt displaces only vertically or diagonally upward. Near the surface, sediment densities are less than salt density. Consequently, considering only the effect of density on salt mobility, at near-surface levels, salt tends to displace downward. Bouyant forces are directed upward and increase with the height of the dome. The distribution of isotherms in the salt and enclosing sediments (Selig and Wallick, 1966) suggests the likely directions of salt movement caused by the effects of temperature on mobility. Confining pressure is less near the surface than at the source bed. Near the surface, the salt tends to expand in the form of an overhang.

The position of the salt-sediment interface can be monitored at any instant in time. For a particular position on the interface at a fixed point

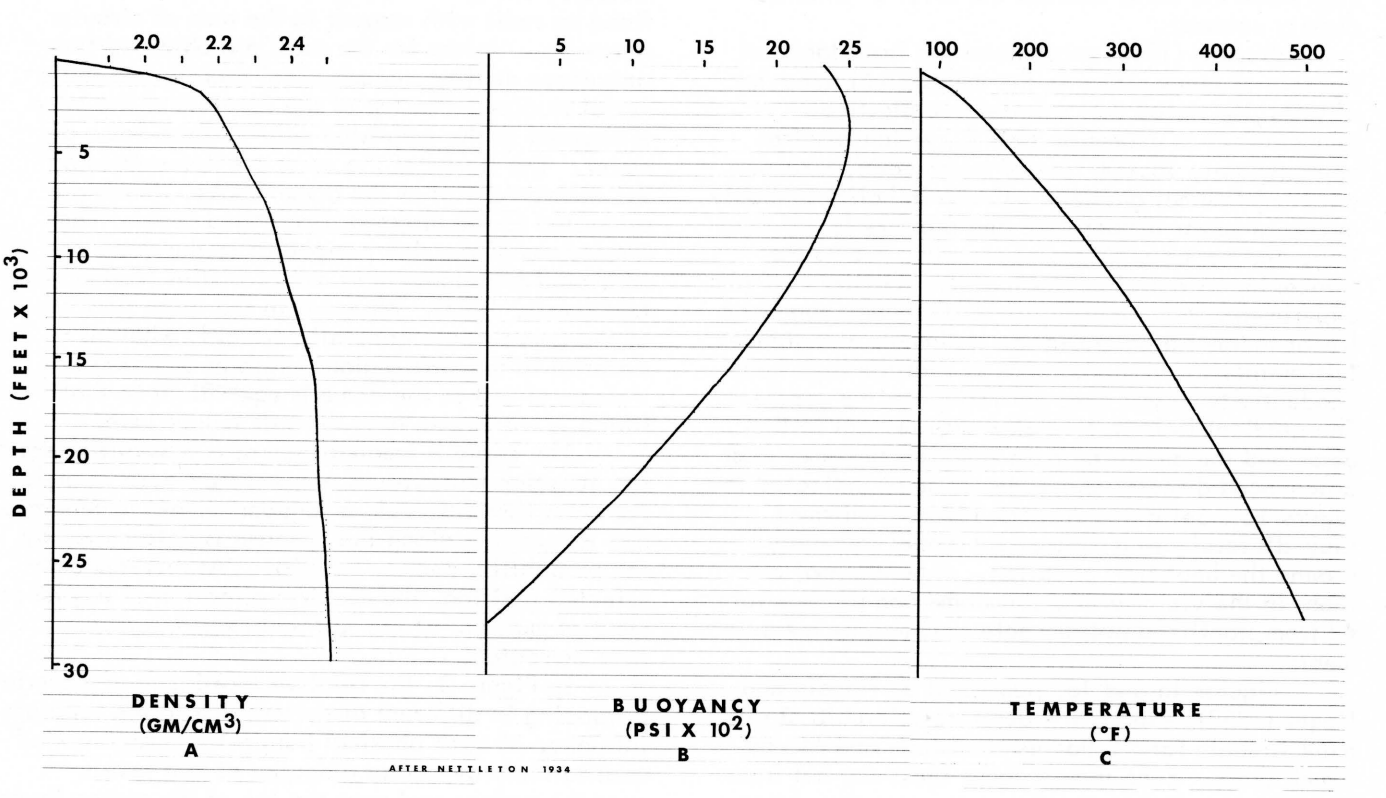
DEPTH (FEET X 10³)
2.0
2.2
2.4
5
10
15
20
25
30
DENSITY
(GM/CM³)
A
5
10
15
20
25
BUOYANCY
(PSI X 10²)
B
100
200
300
400
500
TEMPERATURE
(°F)
C
AFTER NETTLETON 1934

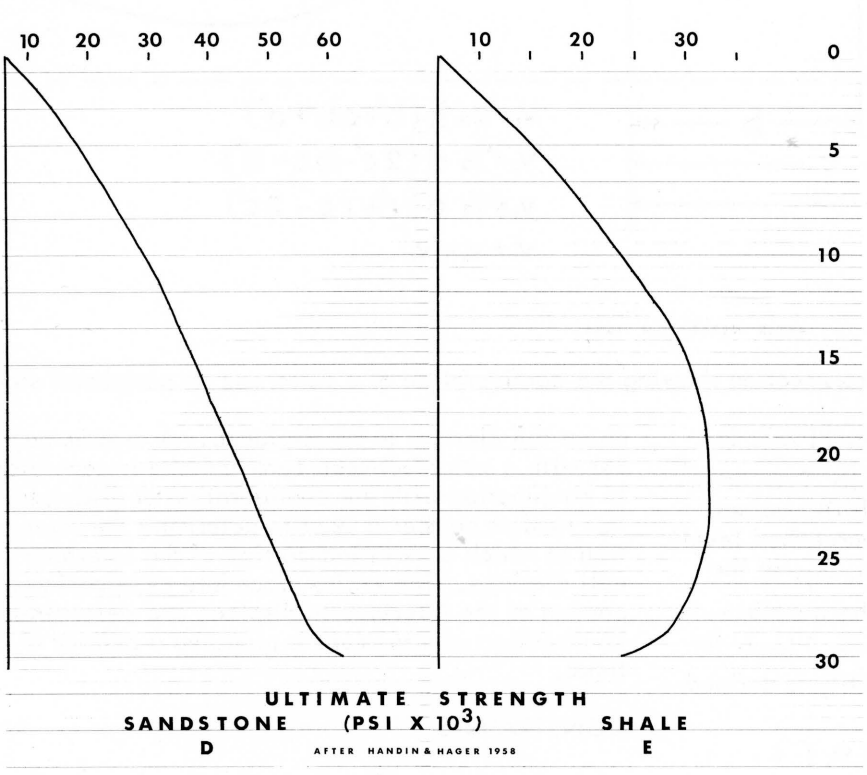

Figure 1.- Density, bouyancy, temperature and ultimate strength as functions of depth.

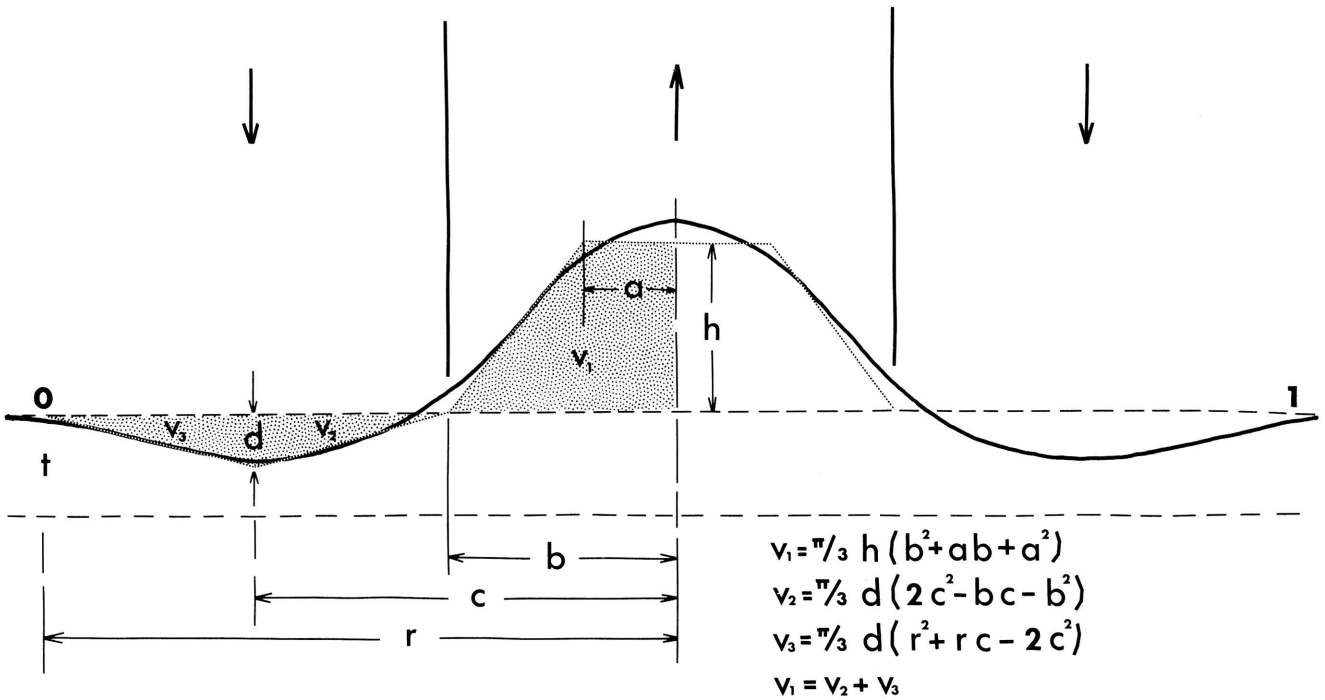

AFTER NETTLETON 1934

Figure 2.- Generalized vertical, cross section showing the configuration of a dome and its peripheral sink.

in time, a resultant probability value, $P[X_i]$, is calculated for each parameter, $i = \rho, b, T, S$, from a ratio of the two end-member probability values, $P[NS]$ (near surface) and $P[SL]$ (source-bed level). The ratio is proportional to the value, X_i, of the parameter at the specified depth of the interface with respect to the range of values $(UL_i - LL_i)$, for the parameter. The resultant probability is defined as

$$P[X_i] = (X_i - LL_i)/(UL_i - LL_i)\ P[SL] + [1 - (X_i - LL_i)/(UL_i - LL_i)]\ P[NS]. \quad (4)$$

The contribution of each distribution of probability values, $P[X_i]$, is related to the others by a weighting factor w_i from which a composite distribution of probability values, $P[C]$, is computed. The function relating the contributions of the parameters is unknown, making the choice of w_i arbitrary. The values utilized in the sequence portrayed in Figure 8 are determined as follows:

$$w_b = k_b\ (h/H),\ w_i = k_i\ (D/TD),\ \text{for } i = \rho, T, S \quad (5)$$

For each time increment, the composite distribution is represented by numerical values occupying a nine-cell, orthogonal grid, which is centered about the element to be displaced. A random number with a value between zero and one is generated. In conjunction with the configuration of grid values, this random number is used to determine the direction in which a specified portion of the interface will displace. The entire procedure of selecting a portion of the interface to displace and determining its direction of movement is repeated a number of times.

CONSTRAINTS

Certain specifications affecting the growth of the dome are incorporated in the model. Dome formation does not begin until the density of sediments deposited on top of the salt bed exceeds that of salt. Termination of dome development occurs when either of two conditions is met: (1) the salt supply is depleted, i.e., subsidence in the sink reaches the base of the salt layer (Fig. 5); (2) the differential stress

$$\Delta\sigma = (\rho_{sed} - \rho_{salt})\ gh \quad (6)$$

between a column of sediment and a column of salt of equal volume, as measured at the top of the salt layer, is less than the yield strength of salt, i.e., the salt no longer is deformed by flowage. Expansion of the salt stock to form an overhang is a common feature in the upper portion of salt domes in the Gulf

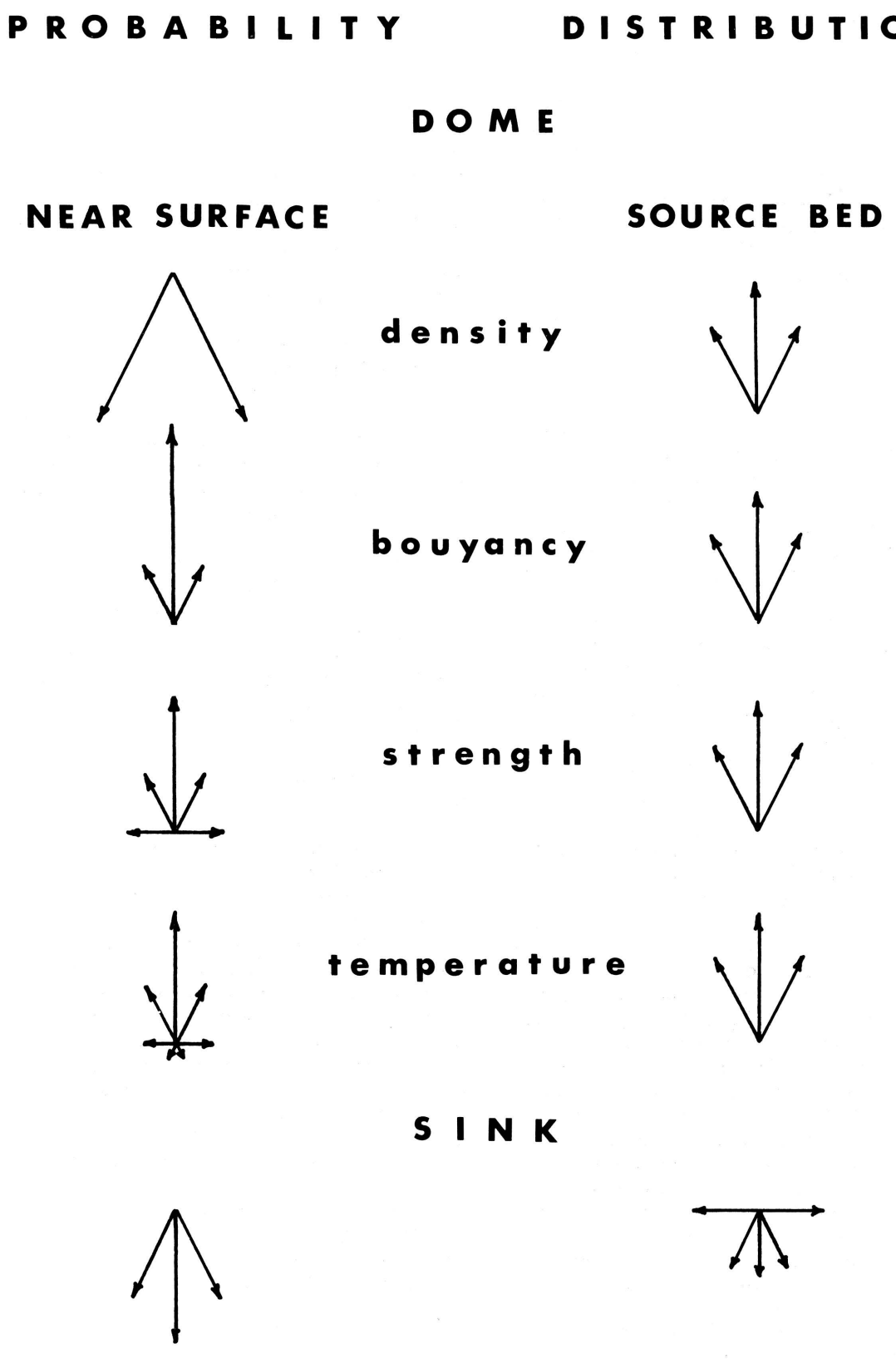

Figure 3.- End-member probability distributions in vector form.

Coast region (Fig. 4,5). Development of an overhang may be controlled in part by the strength of the enclosing strata. The free surface acts as a rigid boundary, which tends to flatten an approaching column of "plastico-viscous" salt (Fig. 7b). In the model, salt spreads laterally if the strength of enclosing sediments is less than an arbitrarily prescribed value. The lateral expansion continues for a period of time determined by the strength of the sediments, after which intrusion continues (Fig. 7c). The time lag is given by

$$t_{lag} = k\,S. \qquad (7)$$

RESULTS

The function in Figure 2 represents one set of variables which can be controlled from one test run to another. The same form of the function is used for all sequences shown here. The end-member probability distributions for the individual parameters (Fig. 3) constitute another set of variables. Irregularities on the gross form of the dome respond sensitively to changes in these distributions. For example some runs result in the development of abnormally long spines. Moderately developed spines are evident in Figures 4 through 8. A third source of variation is the interrelationship or weighting of the physical parameters. A variable set of weighting factors is employed to generate the dome sequence portrayed in Figure 8. Initially, $w_\rho > w_b > w_S > w_T$; as the dome evolves, w_b increases and bouyancy overshadows density contrast. As a result of the assumption that an overhang will tend to form if the strength of sediments penetrated by salt is less than a specified value, basin subsidence has a profound effect on the final form of the dome. The only difference in the controls used to generate the domes shown in Figures 6 and 7 is a slower sedimentation rate and consequently slower basin subsidence in Figure 6. Lateral growth is operable for a longer period of time in the sequence shown in Figure 6. Numerous salt ledges form. Although their lengths are unrealistic, ledges are observed in nature on the flanks of piercement salt domes and constitute potentially lucrative areas for oil and gas exploration. In Figures 7 and 8 the subsidence rates are identical. The end-member probability distributions and their degrees of weighting are different for the two experiments. The dome forming in Figure 8 is decidedly more tapered toward its apex and has entrained a considerable amount of country rock into the salt.

Figures 4 and 5 show results of a less elaborate model. In Figure 4, the only physical parameters represented are sediment density and temperature. In both figures, overhangs are developed distinctly in the upper regions of the dome. The overhang in Figure 4 is asymmetrical and spines begin to extend upward from it after a time lag. An asymmetrical drawdown which cuts off the salt supply to the dome is depicted in Figure 5. Asymmetrical sinks and overhangs are typical features of many Gulf Coast domes such as the Belle Isle dome in Louisiana. The asymmetry might be attributed to basinward sliding on down-to-the-basement faults, which causes uneven salt supply to the dome. In addition, a deviation in the growth axis of the dome would be expected. The sequences in Figures 4 and 5 suggest emplacement of the dome by means of an overhead stoping action due to the alternating advancement of spines. In support of this contention, country rock has been entrained into salt and can be observed in salt mines at the Belle Isle and Avery Island domes in Louisiana. A large spine projects from the top of the Jefferson Island dome, Louisiana. One interpretation of the feature is that it is an erosional remnant. However, "flow lines", delineated by dark anhydrite bands in the lighter colored halite, map conformably to the outline of the spine at its outer edge. This pattern could result from differential movement of the spine. Overhead stoping by spines as a mechanism of dome emplacement is mechanically more feasible than a postulated intrusion of a plug along a broad flat front.

Figures 6, 7, and 8 indicate that the top of the dome remains at approximately the same level through time and that the dome grows passively by downward extension of the stock during basin subsidence. Barton (1933) advanced this hypothesis for dome formation. Energy requirements for downbuilding of the stock are minimal. It seems plausible that active overhead stoping would become an important mechanism as soon as bouyant forces become well established.

Average growth rate of the dome sequence shown in Figure 8 is plotted versus time in Figure 9a. It is reasonable to assume that the growth rate increases with time as the dome overcomes friction between the salt and surrounding sediments as well as internal friction resulting from differential flowage of salt. At point A on the graph, the growth rate decreases, due to lateral spreading as the dome approaches the surface. The increase in $\bar{\omega}$ from point B to C is indicative of temporary vertical advance after a time lag. Figure 9b is a plot of the average sediment densities and strengths penetrated by the salt. The increase in $\bar{\rho}$ and $\bar{S}$ values conforms to the predominantly lateral motion of the salt. Figure 9c graphically illustrates the time variation of the amounts of sedimentation, compaction and basin subsidence for the dome sequence in Figure 8.

TESTING THE MODEL

One method of testing the validity of the model is to compute the gravity anomaly attributed to the final dome in the computer generated sequence (Fig. 10) and compare it with the gravity picture

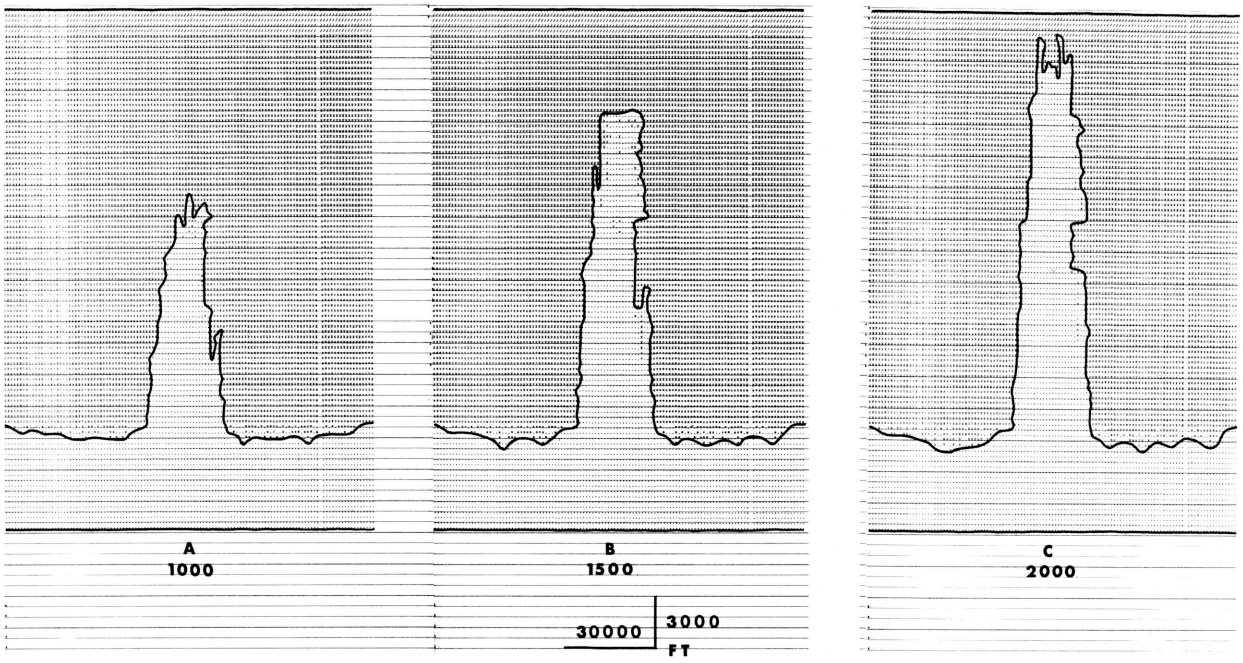

Figure 4.- Dome sequence: iterations 1000, 1500, 2000: salt is represented by . , sandstone by X, shale by = .

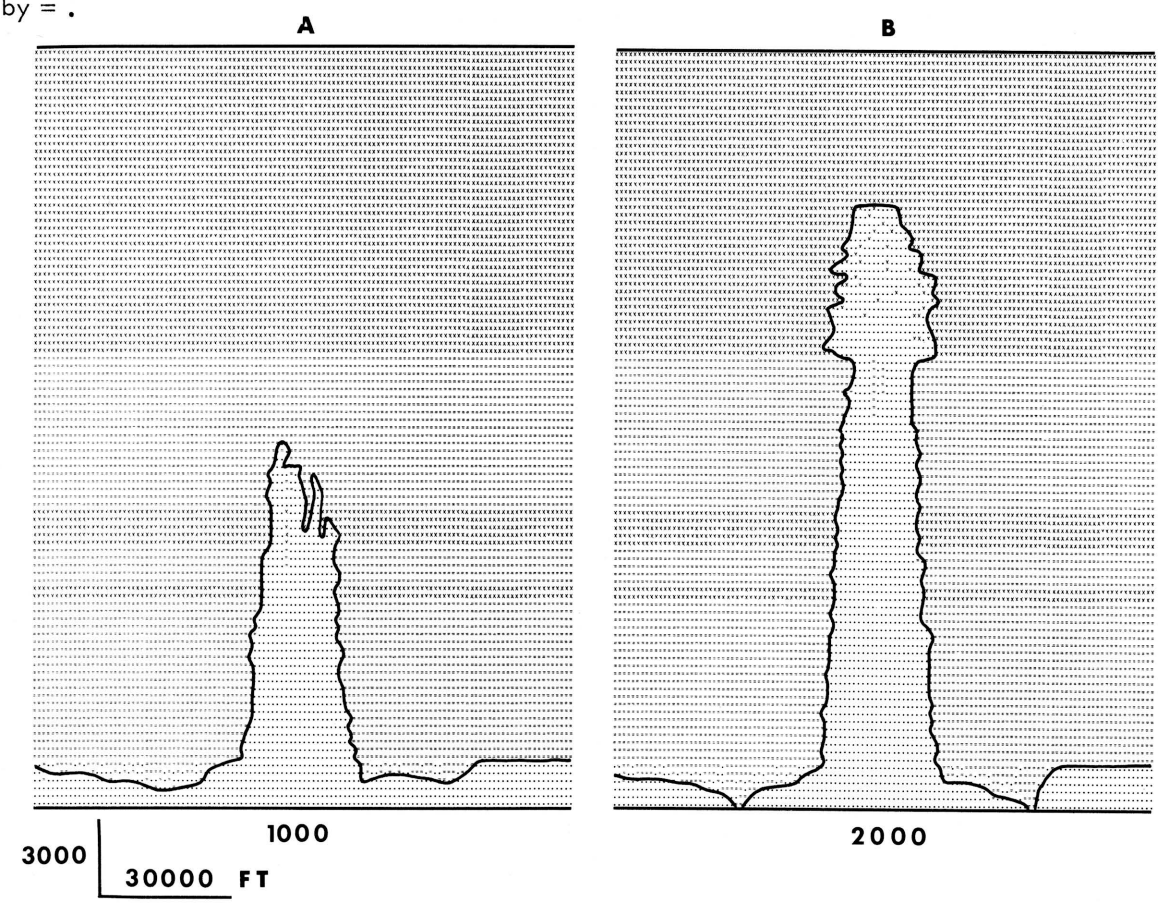

Figure 5.- Dome sequence: iterations 1000, 2000: salt is represented by . , sandstone by X, shale by = .

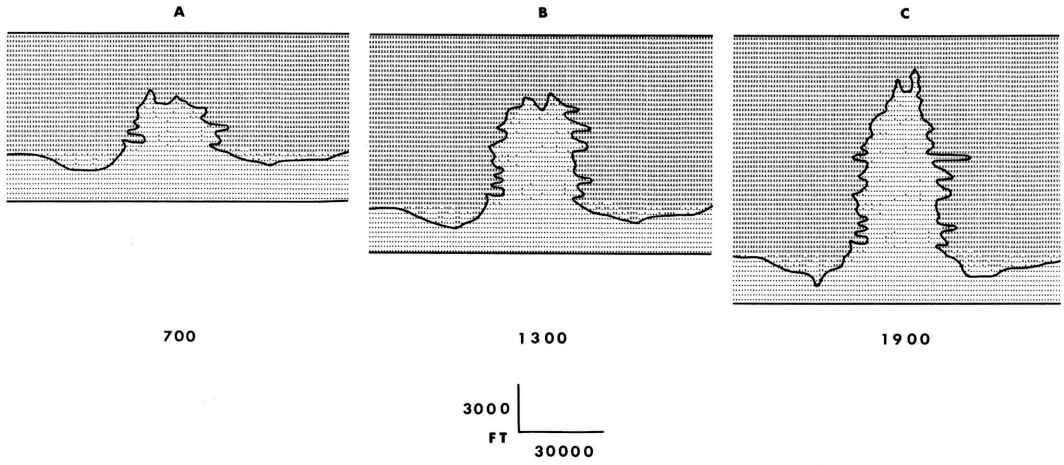

Figure 6.- Dome sequence accounting for sedimentation, compaction and basin subsidence: iterations 700, 1300, 1900.

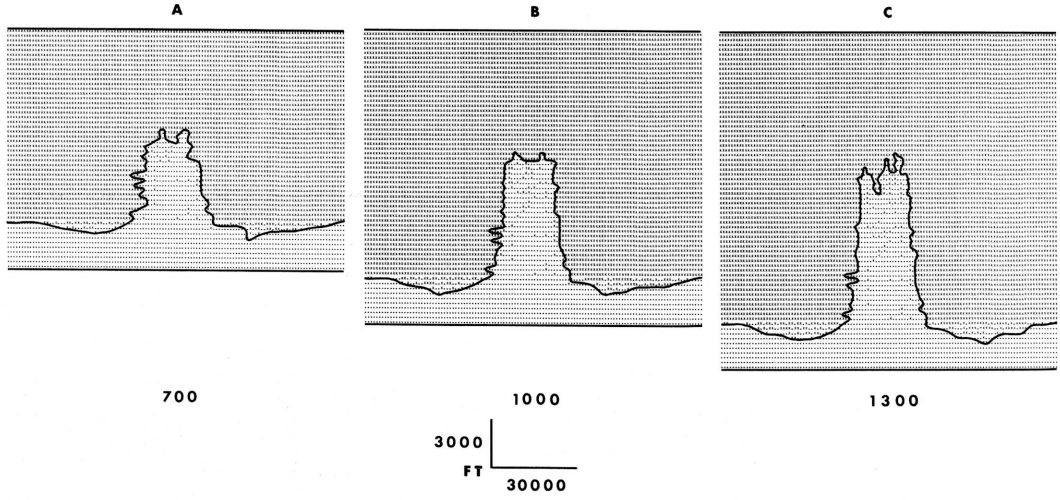

Figure 7.- Dome sequence: iterations 700, 1000, 1300: salt is represented by the symbol . and sandstone by X.

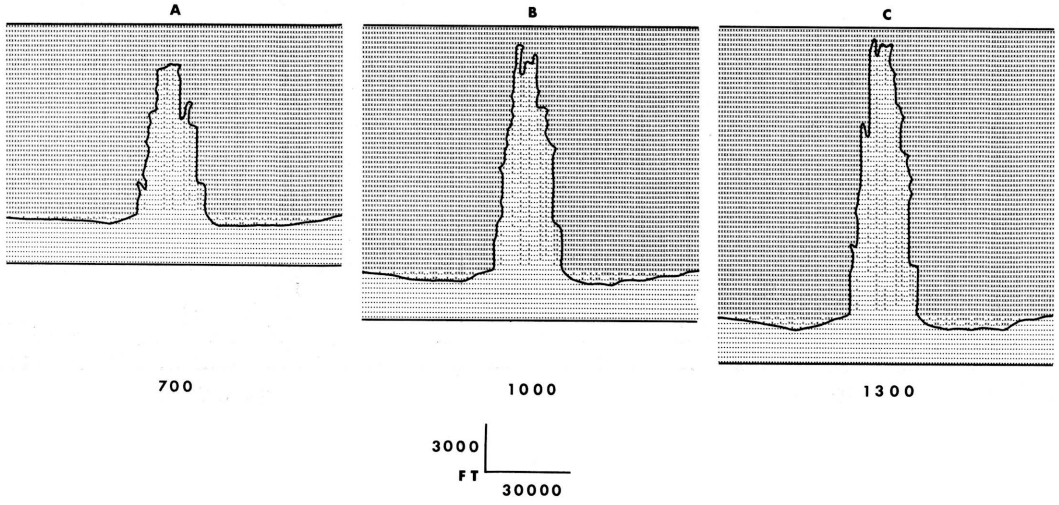

Figure 8.- Dome sequence with variable weighting factors: iterations 700, 1000, 1300.

Figure 9.- Mean growth rate (a), mean density and strength (b) sedimentation, compaction, subsidence (c) versus time.

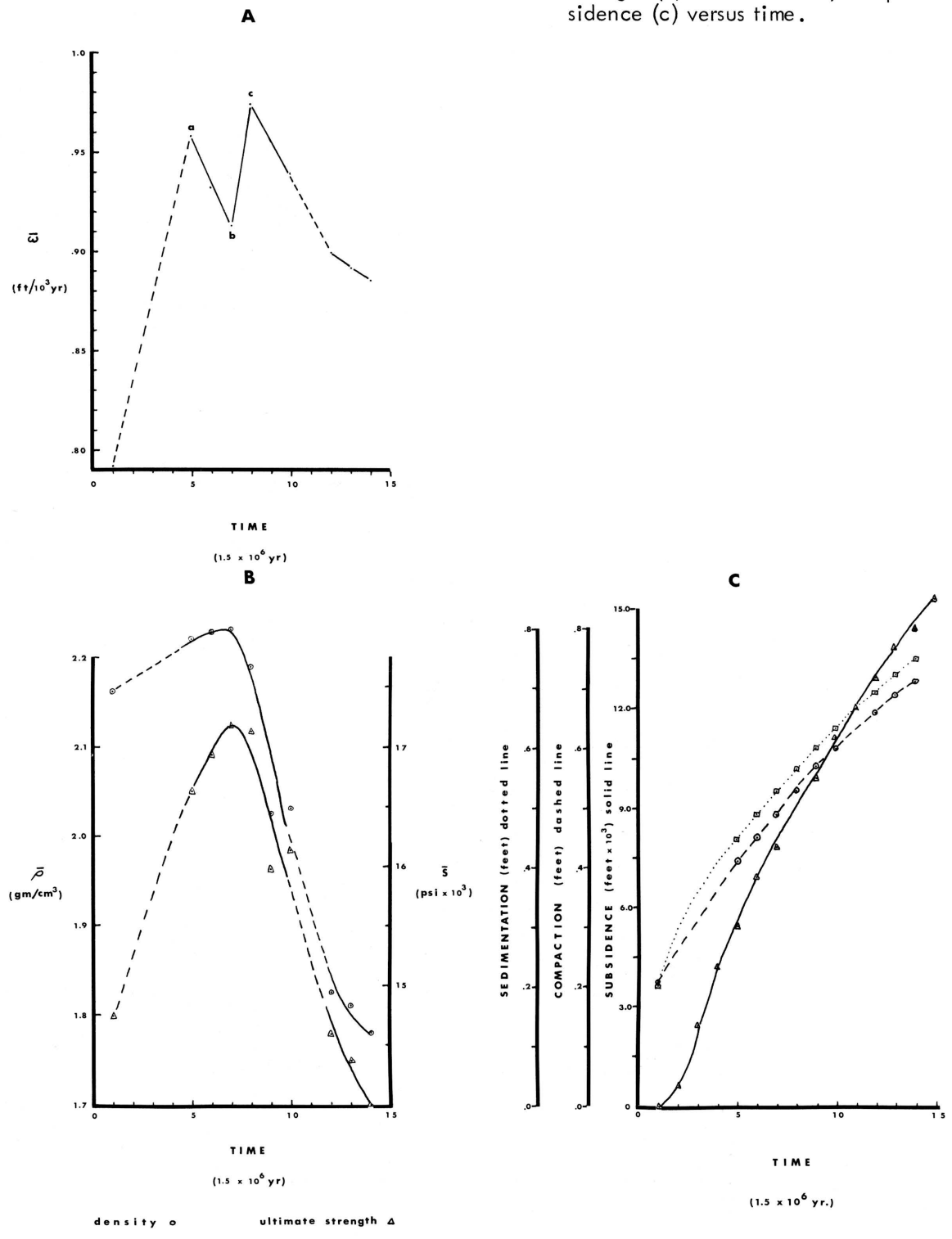

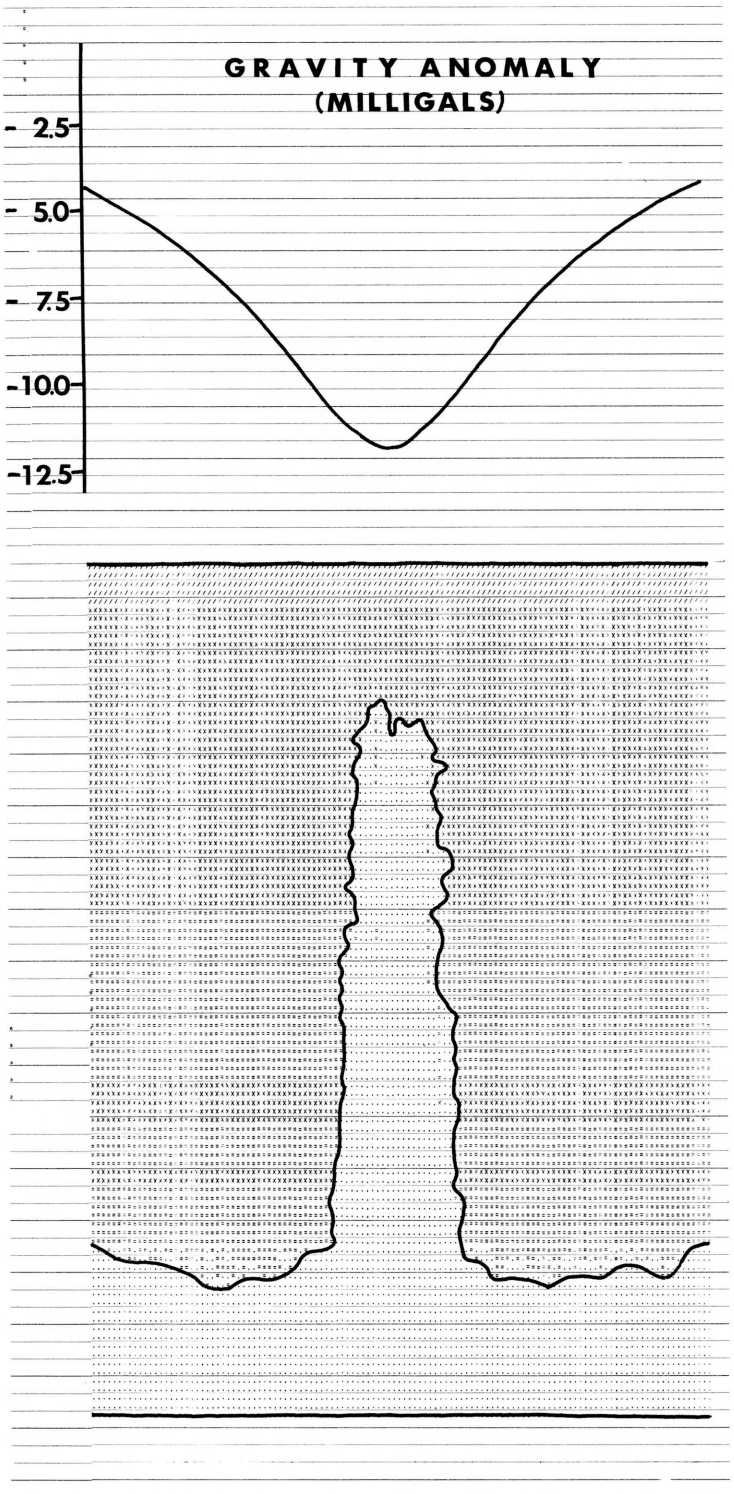

Figure 10. - Calculated gravity profile over computer generated salt dome.

observed for the real salt dome. If the fit is not good, the controls and initial assumptions, which comprise the foundation for the model, must be adjusted individually until a reasonable response is obtained. It should be possible to formulate a generalized model by testing a variety of contrasting but well-documented field localities. The model's potential prediction capabilities then could be applied to an unexplored area for which only a gravity survey exists.

CONCLUSIONS

Monte Carlo techniques provide a useful means of mimicking the progressive development of irregular protrusions on the flanks and tops of piercement salt domes. Coupled with symbolic display methods, stochastic simulation techniques can result in informative prediction capabilities. The model is embellished readily with elaborate and sophisticated changes designed to improve its similarity to reality. Monte Carlo techniques do not lead to a unique definition of the simulated system. Instead, the result expresses a probable or likely solution. There is no rigorous definition of the interrelationships among the physical parameters which comprise the system. The model, however, does provide clues as to the relative importance of different factors and processes and suggests the existence of certain mechanisms that are otherwise not intuitively obvious.

REFERENCES

Barton, D.C., 1933, Mechanics of formation of salt domes: Am. Assoc. Petroleum Geologists Bull., v. 17, no. 9, p. 1025-1083.

Biot, M.A., and Odé, H., 1965, Theory of gravity instability with variable overburden and compaction: Geophysics, v. 30, no. 2, p. 213-227.

Culling, W.E.H., 1963, Soil creep and the development of hillside slopes: Jour. Geology, v. 71, no. 2, p. 127-161.

Gussow, W.C., 1966, Salt temperature; a fundamental factor in salt dome intrusion: Nature, v. 210, no. 5035, p. 518-519.

Guyod, H.C., 1946, Temperature well logging: Pt. 2, Salt intrusions: Oil Weekly, v. 123, no. 9, p. 33-42; Pt. 3, Temperature distribution in the ground: Oil Weekly, v. 123, no. 10, p. 32-39.

Handin, J., and Hager, R.U., 1958, Experimental deformation of sedimentary rocks under confining pressure: tests at high temperature: Am. Assoc. Petroleum Geologists, v. 42, no. 12, p. 2892-2934.

Harbaugh, J.W., 1966, Mathematical simulation of marine sedimentation with IBM 7090/7094 computers: Kansas Geol. Survey Computer Contr. 1, 52 p.

Litwiniszyn, J., 1963, The model of a random walk of particles adapted to researches on problems of mechanics of loose media: Bull. De L'Acad. Polanaise des Sci., v. 11, p. 61-70.

Morrill, R.L., 1965, The Negro ghetto: problems and alternatives: Geographical Review, v. 55, p. 339-361.

Nettleton, L.L., 1934, Fluid mechanics of salt domes: Am. Assoc. Petroleum Geologists Bull., v. 18, no. 9, p. 1175-1204.

Parker, T.J., and McDowell, A.N., 1955, Model studies of salt dome tectonics: Am. Assoc. Petroleum Geologists Bull., v. 39, no. 12, p. 2384-2470.

Schenck, H., 1963, Simulation of the evolution of drainage basin networks with a digital computer: Jour. Geophysical Res., v. 68, no. 20, p. 5739-5745.

Schwerdtner, W.M., 1965, Preferred orientation of halite in a "salt seismogram": in 2nd Symposium on salt: No. Ohio Geol. Soc., v. 1, p. 70-84.

Selig, F., 1965, A theoretical prediction of salt dome patterns: Geophysics, v. 30, no. 4, p. 633-643.

Selig, F., and Wallick, G.C., 1966, Temperature distribution in salt domes and surrounding sediments: Geophysics, v. 31, no. 2, p. 346-361.

Yuill, R.S., 1965, A simulation study of barrier effects in spatial diffusion problems: Michigan Inter-Univ. Community of Math. Geog., Discussion Paper 5, 47 p.

GEOCHEMICAL AND LOGGING APPLICATIONS OF A COMPUTER SIMULATED NEUTRON ACTIVATION SYSTEM

by

V. Charyula
Tulsa University

and

M.K. Horn
Cities Service Oil Company

ABSTRACT

A computer program is presented for simulating gamma-ray energy spectra of neutron activated elements. Input parameters of the program are: mass of the sample, abundance, half life, gamma energies and activation cross section of the element, duration of irradiation and time of detection. The output is the individual spectra of each isotope in the sample and the composite spectrum of the sample. By means of this program, it is possible to simulate neutron activation experiments for different rock samples under varying conditions of irradiation and detection times.

INTRODUCTION

In neutron activation analysis, a sample of material is first irradiated with neutrons, thus causing the sample to be radioactive. Each isotope of the elements contained in the irradiated sample has a specific mode of decay characterized by the half-life, the energy and the type of radiation. By monitoring these characteristic radiations and by comparing them with some known standards, the isotopes and the elements in the sample can be quantitatively determined. Thus, activation always consists primarily of two steps: irradiation and detection. Chemical separation of a sample is an additional step occasionally.

A computer method is presented here that allows one to simulate the activation experiment. Specific geochemical examples are presented. Simulation of rock and mineral irradiation and detection is especially useful because of the complex mixing of the spectra derived from various chemical elements found in lithologic species. The simulated spectra offer the geochemist rapid means of choosing optimum irradiation and monitoring times for the actual activation analysis experiment. For the simulation, a geochemical model of the lithologic type is needed to approximate the various element concentrations that are expected in the sample. Geochemical models based upon material balances (Horn and Adams, 1966) are used to estimate expected chemical element concentrations. Of course, other concentration models may be used for the simulation input.

PROGRAM INPUT, OUTPUT, AND LOGIC

Input

The input to the simulation program consists of (1) irradiation, (2) sample, and (3) detection factors, all of which affect the character of resultant spectra.

Irradiation factors include neutron flux and irradiation time.

Sample factors include sample volume, sample bulk density, estimated elemental concentrations in sample, isotope percentages, activation cross sections appropriate to the neutron energy, half-lives, gamma energies of isotopes, and branch ratios.

Detection factors including detection time, time of detection start, detection efficiency, channel number, and maximum energy to be detected, are included.

Output

The output consists of any or all of the following as desired:

Printouts of Compton distribution, photopeak distribution, and the sum of the two, given per channel and per element. If more than one element is input, the composite energies per channel are also printed.

Plotter displays of the spectrum of the individual elements used as input. If more than one element is input, the composite spectra is also plotted.

Program Logic

The program consists of a main routine and three subroutines:

The main routine (1) reads and prints input, (2) prints individual isotopic data, (3) converts time units, and (4) prints results of synthetic gamma-ray spectra.

The first subroutine computes saturation

activity, A_s,

$$A_s = (V\rho pfN_o\varepsilon\sigma\Phi)/M \qquad (1)$$

where

V = volume of sample,
ρ = bulk density of sample,
p = ppm of element,
f = isotopic percentage,
N_o = Avogadro's number,
ε = detector efficiency
σ = activation cross section,
Φ = neutron flux, and
M = atomic weight.

The significance of the saturation activity is that it represents the activity produced by an infinitely long irradiation, i.e., the maximum producible activity for the isotope under consideration.

The second subroutine (1) computes the total activity of the sample during the detection time; and (2) assigns the activity, thus computed, to the various detection channels representing Compton continuum, photopeaks, and their pair peaks.

The third subroutine controls the plotting display. In our applications, an online CALCOMP 563 drum plotter is used. CRT displays also could be used.

Some features of this subroutine are:

Computation of the total activity (Fig. 1).- The activity, I, of a sample exposed to a neutron flux, Φ, for a time T_I, at time T after irradiation stops is given by:

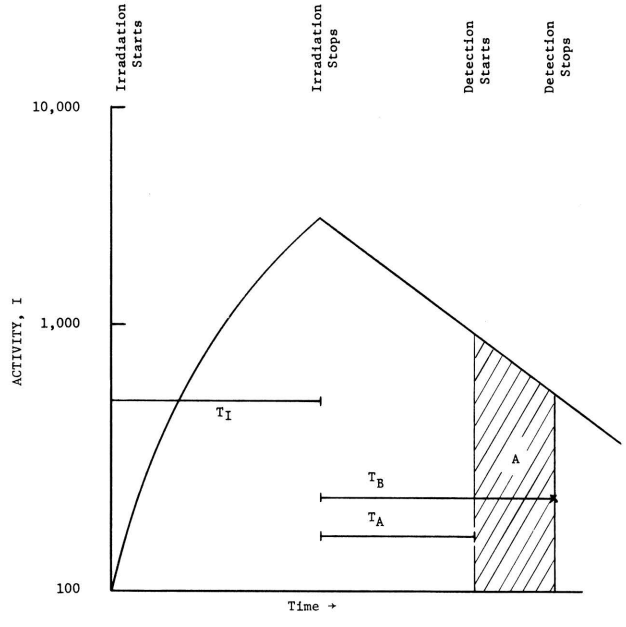

Figure 1.- Activation as function of time, T_I = time of irradiation, $T_B - T_A$ = detection time.

$$I(T) = A_s \cdot (1-e^{-\lambda T_I}) \cdot e^{-\lambda T} \quad , \qquad (2)$$

where

λ = decay constant of product nuclide, and
A_s = saturation activity (equation 1).

Assume detection starts at time T_A after irradiation stops, and stops at time T_B. The number of counts accumulated during the detection interval $T_B - T_A$ is given by integrating equation (2) with respect to the time T, between time limits of T_A and T_B:

$$A = \int_{T_A}^{T_B} I(T)dT = \int_{T_A}^{T_B} \left\{ A_s \cdot (1-e^{-\lambda T}) \cdot (e^{-\lambda T}) \right\} dT,$$

and

$$A = \frac{A_s \cdot (1-e^{-\lambda T_I}) \cdot (e^{-\lambda T_A} - e^{-\lambda T_B})}{\lambda} \qquad (3)$$

Equation (3) gives the total number of counts detected during the time interval $(T_B - T_A)$. These counts are the sum of the counts due to Compton scattering, pair production, and photopeaks. The distribution of the total counts to the proper channels is explained in the following paragraphs.

Distribution of Total Counts Into Appropriate Channels

Pair production.- If the gamma energy is greater than 1.02 Mev two peaks, at energies given by $(E_\gamma - 0.51)$ Mev and $(E_\gamma - 1.02)$ Mev should occur. The contribution due to this effect can be treated in the same manner as in the case of photo electric and Compton effect. To account for the pair production effect, the steps in the program are as follows.

If the energy of the gamma given in the data is greater than 1.02 Mev, then the two energies at which they occur are calculated. These two energies are treated as if due to two additional gammas, i.e., they give rise to Compton continuum and photopeaks. The number of counts detected due to pair production depends on the product of two factors, viz. branching ratio of the primary gamma and the probability of occurrence of each peak. The branching ratio is a factor which accounts for the fraction of activity due to the gamma ray under consideration as compared with the entire activity of the parent nucleus. This value is posted on the data card. It is, in general, complicated to find the probability of occurrence of pair peaks. However, for the present work, an empirical relation has been derived by observing the occurrence of such peaks due to single energy gammas (Heath, 1964). The empirical formulae are found to be as follows:

Probability of occurrence = $e^{1.25 E_\gamma}$, for

$E_{pair} = E_\gamma - 0.51$, and (4)

Probability of occurrence = e^{E_γ}, for

$E_{pair} = E_\gamma - 1.02$. (5)

Photo peaks. - Photo peaks are obtained due to the interaction of primary gammas as well as pair-production photons, with the crystal. To obtain the number of counts due to the photo electric effect from the total counts, the latter is multiplied by the photofraction. Photofraction, PHF, is defined as the ratio of area under the photo peak to the area of entire spectrum. PHF is a function of energy of the gamma ray as well as the size of the crystal. An empirical relation has been derived, for use in this program, from the published values of PHF vs. energy for a sodium iodide crystal of size 3" dia. X 3" long. This relation is found to be

$$PHF = e^{-E_\gamma} . \quad (6)$$

This empirical formula is within about 10 percent of the published values (Heath, 1964).

The number of counts due to the photo electric effect, PC, is, therefore, given by,

PC = (A) x (PHF) x (Branch ratio of E_γ). (7)

The photo counts, PC, are distributed in a Gaussian fashion around the peak energy, E_γ, of the gamma ray, by means of the following formula,

$$PC(n) = (PC) \frac{1}{(2\pi\bar{n})^{1/2}} e^{-\frac{(\bar{n}-n)^2}{2\bar{n}}} , \quad (8)$$

where PC(n) = number of photo counts in any channel n

$n = 0, 1, \ldots . \bar{n}, \bar{n}+1, \ldots . 2\bar{n}$,

$\bar{n}$ = The number of channels on either side of the channel corresponding to the peak height of the spectrum, n_p, and

$$n_p = \frac{E_2}{\text{channel width}} - 1.0 .$$

To determine the number of channels on either side of the peak, $\bar{n}$, the following computational steps are needed.

In terms of the full width at half maximum, 2w, which is explained in the next paragraph, $\bar{n}$ is obtained, by comparing the number of counts at peak and half-the-peak, as follows:

$$\bar{n} = \frac{w^2}{2 \log e^2} = \frac{w^2}{1.386} \quad (9)$$

Full width at half maximum, f.w.h.m., is the width of the spectrum in energy units at half the maximum (i.e., peak) counts. The resolution of the peak is defined as f.w.h.m. The resolution is a function of gamma energy. From the published values (Heath, 1964) of energy vs. resolution, R, an empirical relation, given below, has been derived for use in this program,

$$R = \frac{10^{(0.819 - 0.327 \log_{10} E_2)}}{100} . \quad (10)$$

In terms of R, and the channel, n_p, corresponding to the peak, $\bar{n}$ is given by

$$\bar{n} = 1 + \left[\frac{(n_p)(R)}{2} + 1 \right]^2 / 1.386 \quad (11)$$

The photo counts are distributed according to equation (8) in channels between $n_p - \bar{n}$ to $n_p + \bar{n}$.

Compton distribution. - Compton continuum is due to the primary gammas as well as due to the photons produced in the pair production process. The activity due to the Compton effect of any single photon (either primary gamma or the pair production photons) is the difference between the total activity and the activity due to photo-electric effect. Therefore, the Compton activity, CA is given by

CA = A(1-Photo Fraction) (Branch ratio of E_γ). (12)

The Compton activity is distributed uniformly in all the channels, from channel 1 to the channel giving the Compton edge, which is the channel number corresponding to the maximum energy, E_c, lost by a photon in Compton collision, given by

$$E_c = \frac{E_\gamma}{(1 + \frac{mc^2}{2E_\gamma})} . \quad (13)$$

Other processes, such as back scatter and annihilation spectra, have not been considered as they are of secondary importance. In practice one is more interested in a spectrum in which the Compton continuum is as fully suppressed as possible while the photo and pair peaks are predominant. From this point of view, the assumptions made and the semi-empirical nature of the program seem to be valid.

An experimentally obtained curve from Heath's work (1964) is compared with that obtained from this program in Figure 2. In this case the full energy peak has been normalized.

GEOCHEMICAL AND LOGGING APPLICATIONS TO ACTIVATION SIMULATION

A few applications of generated synthetic

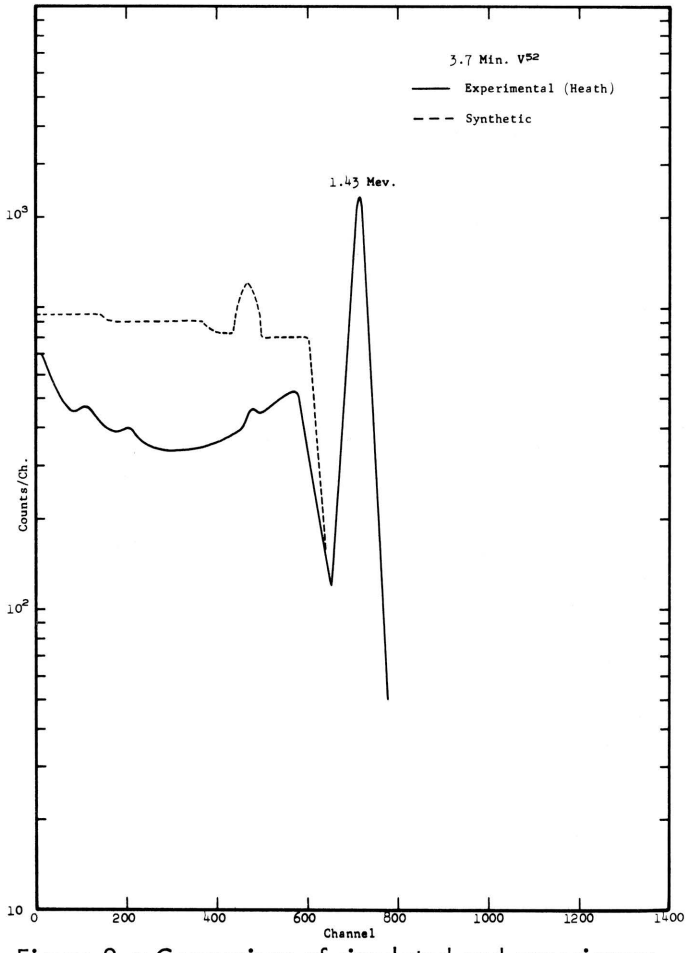

Figure 2.- Comparison of simulated and experimental activation in spectrum, V^{52}.

gamma spectra will be discussed in the following section. Three typical cases have been considered, viz. borehole in situ irradiation, shale cutting activation and the exploration of manganese nodules.

Borehole Irradiation

With the advent of borehole neutron generators, fast neutron fluxes of the order of 10^8 n/cm^2 sec. are now available. Some investigations (Caldwell, and others, 1963; Hoyer and Rumble, 1965) have employed these to identify the capture gamma rays or to measure the thermal neutron life times in media of interest to the oil and gas industry. However, the application of thermal neutron activation analysis for exploratory purposes seems to have been little investigated. An experiment has been simulated by means of the computer program described in the previous section, to represent the irradiation of formations consisting of either shales or carbonates or sandstones. The assumptions and the analysis of the results of the simulated experiment are described below.

It is assumed that a thermal neutron flux of 10^7 n/cm^2 sec. is available to irradiate a spherical volume of 1 meter in diameter. The irradiation time is taken to be 2 minutes. Detection starts 3 minutes after irradiation stops and lasts for one minute. The maximum energy range is taken to be 3.2 Mev which is uniformly divided into 160 channels. Because the geometry of the system and other parameters that contribute to the efficiency of the detection are not precisely known, the detection efficiency is taken to be unity. As more information on the detector efficiency becomes available, it can be incorporated into the program. The values of most probable composition of the samples, viz. shales, carbonates and sandstones, are taken from Horn and Adams (1966). Other nuclear data are obtained from Reactor Physics Constants (1963). Gamma-ray spectra thus obtained are shown in Figure 3.

From Figure 3, it can be seen that, in general, there is more activity exhibited by carbonates than by either shales or sandstones. The ppm of Mg in carbonates is 45,300 whereas it is 16,400 in shales and only 8,100 in sandstones. The high content of Mg^{27} coupled with the fact that the irradiation and detection times are 2 minutes and 5 minutes respectively, which happen to be optimum for Mg^{27} with half-life of 9.45 minutes, accounts for the predominance of Mg peaks in carbonates. With shales, however, the Al content is 80,000 ppm compared to 32,000 in carbonates and only 8,970 ppm in sandstones; thus the peaks due to Al^{28} are predominant. Sandstones in which Si content is high, viz. 35,900, do not strikingly exhibit the peak due to Si^{31} because the isotopic percentage of Si^{31} is low, being 30 percent; and also the activation cross section is low. Moreover, what little activity is due to Si^{31} is suppressed by the peak due to Al^{28} at the same energy (1.26) because the irradiation times chosen are more favorable for Al^{28} (half-life of 2.3 minutes) as opposed to Si^{31} (half-life of 2.65 hours).

Thus, even from a single irradiation of a short duration the nature of the three types of rocks can be clearly seen. Further, various detection times would lead to more conclusive results. It also may be noted that from a mixture of nearly 80 isotopes this method has reduced the number of elements of prominence considerably.

Shale Cutting Activation

Another application of the neutron activation method is the analysis of rock samples obtained from drill cuttings. This is advantageous in that there is no restriction on the time element and the conditions under which the tests would be performed. Hence, it may be possible to design the experiments

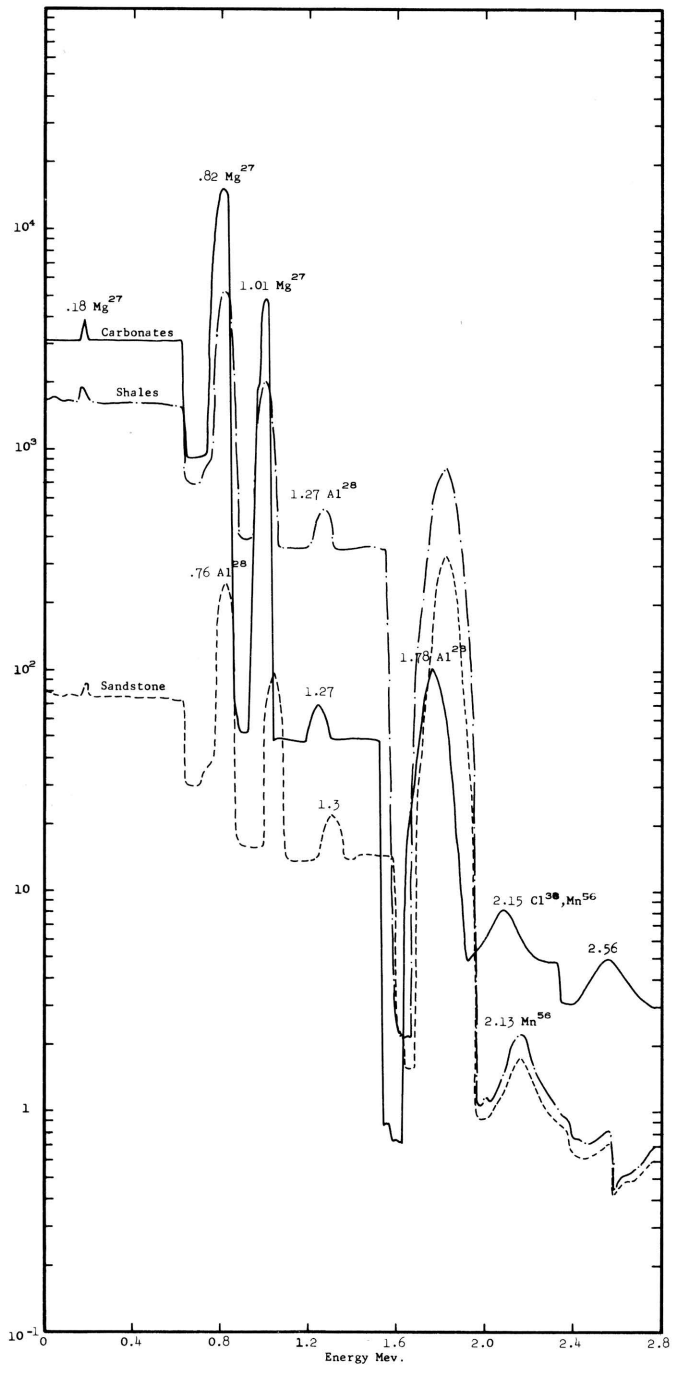

Figure 3.- Thermal neutron activation of shales, carbonates, and sandstones, irradiation time 2 min., detection after 3 min., 0.02 Mev/ channel.

to give the required information. As an example, a shale cutting of the composition given in Table 1 is used as a sample. The conditions of the simulated experiment are that the available thermal neutron flux is 10^{14} n/cm^2 sec., (which is possible from nuclear reactors) and the irradiation time is 30 minutes. The activity was monitored by simulation for seven days at intervals of 24 hours. The resulting spectra are seen in Figure 4. The posted values of half-lives and peak energies are shown in Table 2.

Manganese Nodules

Data pertaining to the composition of the manganese nodules have been obtained from Mero (1964). Results obtained from a simulated 2 minute exposure of manganese nodules to a thermal neutron flux of 10^7 n/cm^2 sec. and detection of the activity after 1 minute and 1 hour are shown in Figure 5. As a comparison, the spectra due to pelagic clays of same sample volume and identical experimental conditions are shown on the corresponding figures.

The peaks of interest in each instance are shown in Table 3.

From the spectrum obtained 1 minute after irradiation, it can be seen that the two media do

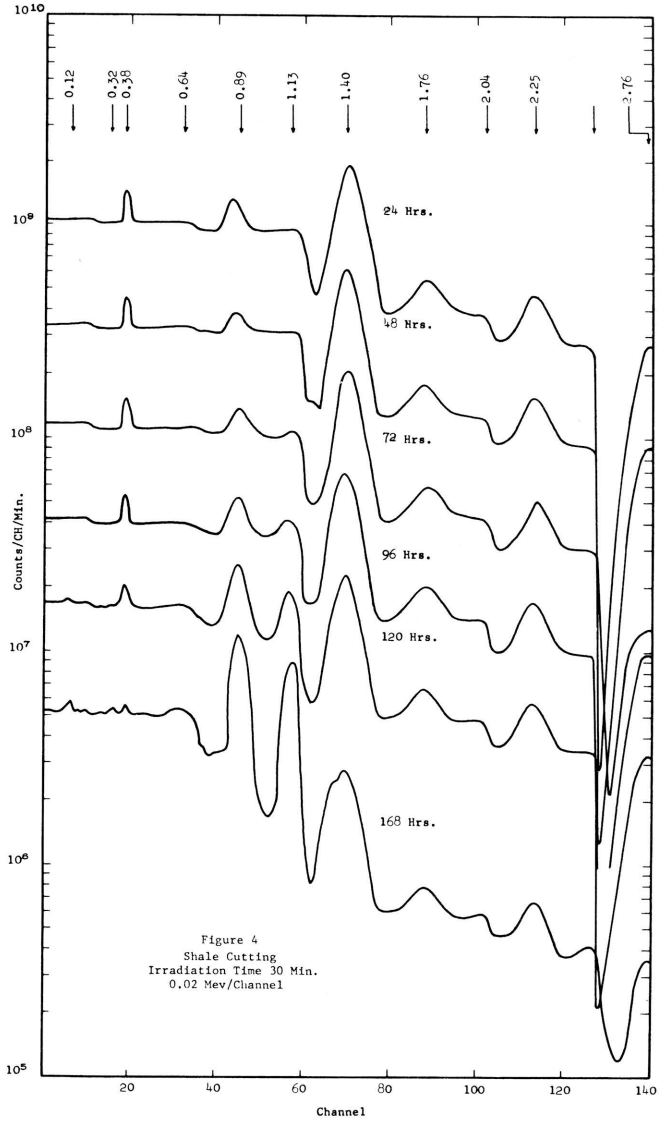

Figure 4.- Shale cutting, irradiation time 30 min., 0.02 Mev/channel.

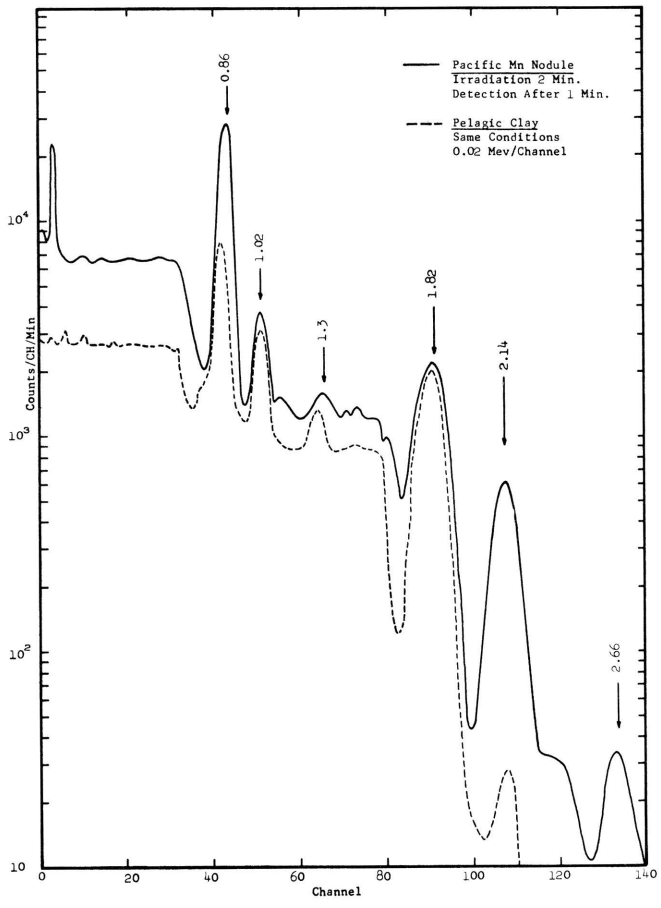

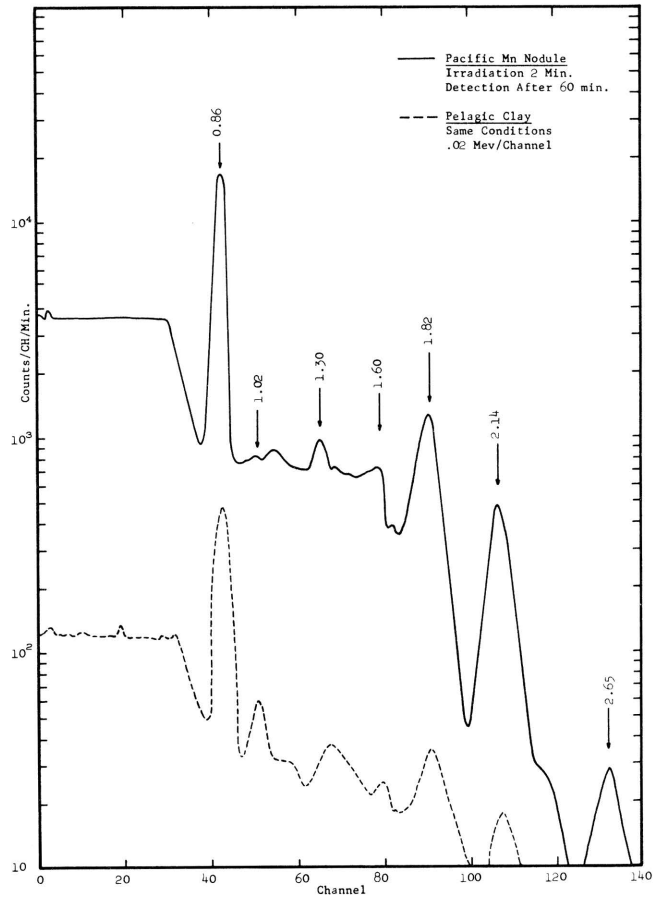

Figure 5.- Comparison of peaks of interest for manganese nodules and pelagic clays: a, detection after 1 min.; b, detection after 60 min.

not give radically different results, although the activity due to the clays is less than that due to the nodules. However, the difference in the two media becomes obvious from the spectra obtained 1 hour after irradiation has taken place. The clays, which have higher contents of Al which has short half-life, exhibit less activity by far than the nodules which have a high concentration of Mn with longer half-life. Moreover, the activity due to both Al and Mg in the nodules would have decayed substantially, if not entirely, so that the peak at 0.86 is entirely due to the presence of Mn.

Table 1.- Composition of a shale cutting.

Element	ppm.
Mn	523
Na	3,028
Fe	23,481
Sc	29.2
La	25.0
Co	81.0
Cu	125

Table 2. - Posted values of half-lives and peak energies.

Isotope	Half-Life	Peak Energies (Mev.)	Pair Peaks
Mn 56	2.6 hrs.	2.12, 1.81, 0.84	1.1, 1.61, 1.3, 0.79
Na 24	15.0 hrs.	2.76, 1.38	1.74, 2.25, 0.87, 0.36
Fe 59	45.1 days	1.29, 1.10, 0.19	0.78, 0.27, 0.59
Sc 46	85.0 days	1.12, 0.89	0.61, 0.11
La 140	40.0 hrs.	2.57, 0.92	2.06, 1.55
Co 60	5.3 yrs.	1.17, 1.33	
Cu 64	12.87 hrs.	1.34	

Table 3. - Comparison of peaks for manganese nodules and pelagic clays.

MANGANESE NODULES

Element	ppm.	Half-Life	Peak Energies	Pair Peaks
Mn 56	242,000	2.6 hrs.	0.845 1.81 2.13	 0.79, 1.3 1.01, 1.52
Mg 27	17,000	9.4 min.	0.834 1.01 0.181	---
Al 28	29,000	2.3 min.	1.78	1.06, 1.57

PELAGIC CLAYS

Element	ppm.	Half-Life	Peak Energies	Pair Peaks
Mn 56	5,820	2.6 hrs.	0.845 1.81 2.13	 0.79, 1.3 1.01, 1.52
Mg 27	15,200	9.45 min.	0.834 1.01 0.181	
Al 28	84,200	2.3 min.	1.78	1.06, 1.57

REFERENCES

Caldwell, R.L., Baldwin, W.F., Bargainer, J.D., Berry, J.E., Salaita, G.N., and Sloan, R.W., 1963, Gamma ray spectroscopy in well logging: Geophysics, v. 28, no. 4, p. 617.

Heath, R.L., 1964, Scintillation spectrometry, gamma-ray spectrum catalogue: U.S. Atomic Energy Comm., Washington, D.C.

Horn, M.K., and Adams, J.A.S., 1966, Computer-derived geochemical balances and element abundances: Geochimica et Cosmochimica Acta, v. 30, p. 279-297.

Hoyer, W.A., and Rumble, R.C., 1965, Field experience in measuring oil content, lithology and porosity with a high-energy neutron-induced spectral logging system: Jour. Petroleum Tech., v. 17, no. 7, 301 p.

Mero, J.L., 1964, The mineral resources of the sea: Elsevier Pub. Co., Amsterdam, 312 p.

Reactor Physics Constants (2nd ed.), ANL-5800, 1963: U.S. Atomic Energy Comm., Washington, D.C.

ON THE INTERPRETATION OF STATE VECTORS AND LOCAL TRANSFORMATION OPERATORS

by

Henry N. Pollack
University of Michigan

"The purpose of computing is insight, not numbers."
R.W. Hamming (1962)

Krumbein (1967), in a paper on Markov chain experiments, remarks that an important by-product of such experiments is that the scientist comes to view his observations as a set of states that succeed each other in some patterned way, and that the pattern of succession, if it can be discovered, can lead to a fuller understanding of the underlying geological process. In the short essay to follow, I wish to focus attention on the origin, characteristics, and interpretation of a small group of patterns of succession.

Let us consider a single-valued function of one space variable and time, $Z = f(X,t)$. We may identify this function as a topographic profile, with the value of the function being the elevation of the land surface at location X and time t. The passage to subsequent states may then admit to an interpretation in terms of geomorphic processes. To obtain a later state of this profile, one can hypothesize the nature of the change, and give it expression in terms of a differential equation involving the local time rate of change of elevation $\partial Z/\partial t$. This can then be integrated over time to yield a later state. Some simple illustrative models follow:

I. $\frac{\partial Z}{\partial t} = -(\text{random})$

elevation decrement is random in location and magnitude.

II. $\frac{\partial Z}{\partial t} = -a$

elevation decrement is constant everywhere; regional subsidence.

III. $\frac{\partial Z}{\partial t} = -bZ$

elevation decrement is proportional to local elevation; higher regions suffer more severe denudation than lower regions.

IV. $\frac{\partial Z}{\partial t} = -c\left|\frac{\partial Z}{\partial X}\right|$

elevation decrement is proportional to local slope.

V. $\frac{\partial Z}{\partial t} = d\,\frac{\partial^2 Z}{\partial X^2}$

elevation decrement is proportional to local curvature; mass "diffuses" from hills to valleys.

In the above, a, b, c, and d are positive constants. Models II, III, and IV are taken from Scheidegger (1961) while model V can be recognized as the classical diffusion equation.

Let us now select from the profile a "state vector", i.e., a finite sample of elevations $Z_1, Z_2, \ldots Z_i, \ldots Z_n$ at a set of discrete points $X_1, X_2, \ldots X_i, \ldots X_n$. For convenience let $\Delta X = X_i - X_{i-1}$ be a constant spacing. Similarly, using superscripts, let $Z_i^1, Z_i^2, \ldots Z_i^j$ be the values at point X_i at times $t_1, t_2, \ldots t_j$, with $\Delta t = t_j - t_{j-1}$. The partial derivatives may then be approximated by appropriate differences,

$$\frac{\partial Z}{\partial t} \simeq \frac{Z_i^{j+1} - Z_i^j}{\Delta t}\ , \quad \frac{\partial Z}{\partial X} \simeq \frac{Z_{i+1}^j - Z_{i-1}^j}{2\Delta X}\ .$$

Future states of the profile predicted by each of the processes above are

I. $Z_i^{j+1} = Z_i^j - (\text{random})\,\Delta t$

II. $Z_i^{j+1} = Z_i^j - a\Delta t$

III. $Z_i^{j+1} = Z_i^j - (b\Delta t)Z_i^j$

IV. $Z_i^{j+1} = Z_i^j - \frac{c\Delta t}{2\Delta X}\left|Z_{i+1}^j - Z_{i-1}^j\right|$

V. $Z_i^{j+1} = Z_i^j + \frac{d\Delta t}{(\Delta X)^2}\,(Z_{i-1}^j + Z_{i+1}^j - 2Z_i^j)$

The coefficient $d\Delta t/(\Delta X)^2 = \delta$ must satisfy $\delta \leq 1/2$ for the difference equation to represent adequately the diffusion process. Each of the above is of the form

$$Z_i^{j+1} = \text{constant} + \sum_{m=-1}^{m=1} W_{i,m}\, Z_{i+m}^{j} \quad , \qquad (1)$$

where the $W_{i,m}$ are the appropriate coefficients of the Z_{i+m}^{j}. The future value at a point is obtained as a sum of weighted present values at the point and its adjacent neighbors, plus an additional increment independent of the present profile values. The generation of a new state, then, is seen to be accomplished by performing a moving weighted sum operation on the present state vector. The weights and constant term for each of the processes are tabulated in Table 1, and illustrative examples of some of these processes acting on a common original profile are shown in Figure 1.

It is, of course, a relatively easy undertaking to hypothesize a geomorphic process in terms of a differential equation, which in turn can be cast into the form of a moving weighted sum operation. The inverse task, that of inferring a differential equation (and ultimately a process) from some given or empirical operator, is usually more difficult. For example, one might ask what process, if any, is implied in the generation of a new state by passing a present state through the common three point weighted moving average operation frequently employed as a data "smoother." The operation can be written

$$Z_i^{j+1} = \frac{\sum_{m=-1}^{m=1} C_{i,m}\, Z_{i+m}}{\sum_{m=-1}^{m=1} C_{i,m}} \quad ,$$

and when the operator is symmetrical ($C_{i,-1} = C_{i,1}$), this expands to

$$Z_i^{j+1} = \frac{C_{i,\pm 1}}{\Sigma C_{i,m}} \left(Z_{i-1}^{j} + Z_{i+1}^{j}\right) + \frac{C_{i,0}}{\Sigma C_{i,m}} Z_i^{j} \quad .$$

In the notation of Table 1, this expression has $W_{i,-1} = W_{i,1} = C_{i,\pm 1} / \Sigma C_{i,m}$ and $W_{i,0} = C_{i,0} / \Sigma C_{i,m}$. One may note that this operation is equivalent to diffusion if $C_{i,\pm 1} / \Sigma C_{i,m} = \delta$ and $C_{i,0} / \Sigma C_{i,m} = 1 - 2\delta$. Satisfaction of the first condition guarantees satisfaction of the second; thus a necessary and sufficient condition for weighted moving average "smoothing" to be equivalent to diffusion is $C_{i,1} = C_{i,-1} = \delta \Sigma C_{i,m}$. When δ is constrained by the inequality $\delta \leq 1/2$, the condition $C_{i,1} = C_{i,-1} \leq 1/2\, \Sigma C_{i,m}$ is obtained. One can convince himself that every symmetric operator satisfies that condition independent of the central weight, provided only that $C_{i,m}, C_{i,0} \geq 0$. Commonly employed smoothing schemes, such as the three point equal weight (1,1,1) and the three point binomial weight (1,2,1) moving averages are seen to be diffusion operators. Thus we have arrived at a process interpretation of a frequently utilized class of local digital operators.

It is also worthwhile to note that for systems in which future states are generated by operations requiring values at adjacent sites (as in IV, V above), some provision must be made for modification of the procedure at the ends of the interval. Without pursuing the topic in detail, suffice it to say that the nature of this procedure also plays an important role in the eventual state of the system. Just as boundary conditions extract uniqueness from the general solution of a differential equation, so does the interval endpoint procedure attach its signature to the state vector (for a clear exposition of this relationship, see Lanczos, 1961, chap. 4).

Krumbein (1967) has remarked that "in the classical deterministic model, the state of the system in time and space can be exactly predicted from knowledge of the functional relation specified by the underlying differential equation." Such knowledge, with its attendant predictive capability, is one of

Table 1.- Weights and constant term for processes of models I-V.

Model	Constant	$W_{i,-1}$	$W_{i,0}$	$W_{i,1}$	Remarks
I.	$-(\text{random})\Delta t$	0	1	0	
II.	$-a\Delta t$	0	1	0	
III.	0	0	$(1-b\Delta t)$	0	
IV.	0	$\pm c\Delta t/2\Delta X$	1	$\mp c\Delta t/2\Delta X$	Choice of signs as $Z_{i+1}^{j} \gtrless Z_{i-1}^{j}$
V.	0	δ	$1-2\delta$	δ	$\delta \leq 1/2$

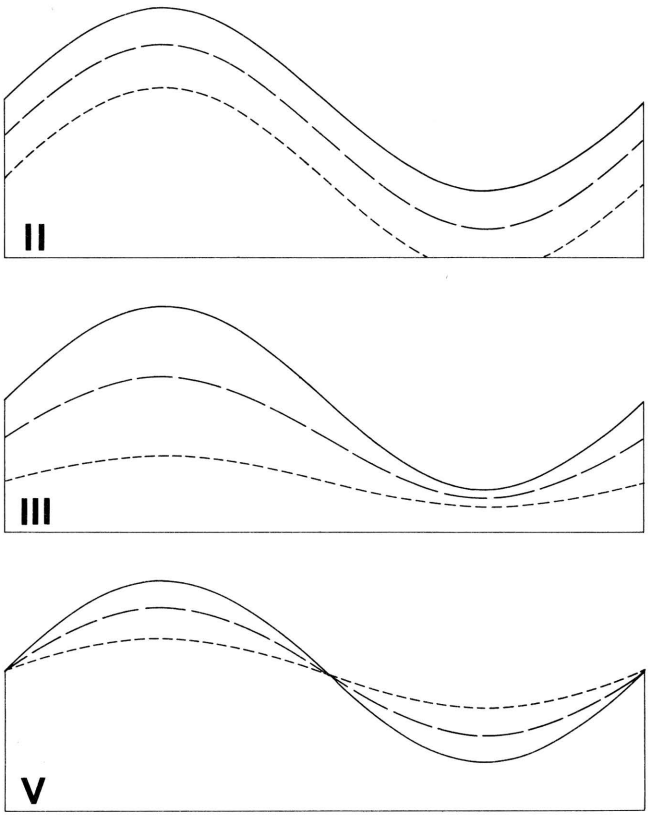

Figure 1.- Modification of sinusoidal profile according to models II, III, and V. Solid lines are common original profile, dashed lines are subsequent profiles.

the fundamental goals of science. By exploring, as we have here, the links between state vectors, local transformation operators, and associated differential equations, attention is drawn to that vital transition zone where assemblages of observations become identifiable as states of some process. Probing of this transition zone will hopefully enable the science of geology to advance from a state of statistical characterization to one of deterministic prediction.

REFERENCES

Hamming, R.W., 1962, Numerical methods for scientists and engineers: McGraw-Hill, New York, 411 p.

Krumbein, W.C., 1967, FORTRAN IV computer programs for Markov chain experiments in geology: Kansas Geol. Survey Computer Contr. 13, 38 p.

Lanczos, C., 1961, Linear differential operators: D. Van Nostrand and Co., New York, 564 p.

Scheidegger, A.E., 1961, Theoretical geomorphology: Springer-Verlag, Berlin, 327 p.

Tobler, W.R., 1966, Numerical map generalization: Michigan Inter-Univ. Community of Math. Geog., Discussion Paper 8, 13 p.

Tobler, W.R., 1967, Of maps and matrices: Jour. of Regional Sci., v. 7, no. 2, (supplement), p. 275-280.

APPENDIX

The generation of a future state vector by the weighted sum operation of equation (1) can be thought of as the following matrix operation (Tobler, 1966, 1967):

Z^{i+1} = constant + Z^i . S where Z^i is the present (1 x n) state vector and S an (n x n) matrix of the form

$$S = \begin{bmatrix}
\text{Special} & & 0 & 0 & 0 & 0 & . & 0 & 0 & 0 & 0 \\
W_{-1} & W_0 & W_1 & 0 & 0 & 0 & . & 0 & 0 & 0 & 0 \\
0 & W_{-1} & W_0 & W_1 & 0 & 0 & . & 0 & 0 & 0 & 0 \\
0 & 0 & W_{-1} & W_0 & W_1 & 0 & . & 0 & 0 & 0 & 0 \\
0 & 0 & 0 & W_{-1} & W_0 & W_1 & . & 0 & 0 & 0 & 0 \\
. & . & . & . & . & . & . & . & . & . & . \\
0 & 0 & 0 & 0 & 0 & 0 & . & W_{-1} & W_0 & W_1 & 0 \\
0 & 0 & 0 & 0 & 0 & 0 & . & 0 & W_{-1} & W_0 & W_1 \\
0 & 0 & 0 & 0 & 0 & 0 & . & 0 & 0 & \text{Special} &
\end{bmatrix}$$

SOLUTION OF PARTIAL DIFFERENTIAL EQUATIONS USING A GENERAL PURPOSE ANALOG COMPUTER

by

K.A. Bishop

The University of Kansas

The acquisition of information concerning physical entities, phenomena, or processes by any means other than direct measurement involves what might be called the simulation or analog concept. Regardless of whether one is interested in the precise time of the next equinox or the performance of a prototype aircraft, a model of the situation is exercised. Two basic assumptions underlie the application of any model (1) the validity of its description of the physical situation, and (2) the economy resulting from its exercise in contradistinction to direct measurement of the required information.

Models may take on many forms, such as a wind-tunnel version of the prototype aircraft or iron filings on a sheet of paper to elucidate two dimensions of the force field surrounding a permanent magnet, but the most common form is the mathematical statement of physical laws that apply in a particular situation. These expressions generally consist of combinations of algebraic, differential, and integral equations, with appropriate boundary conditions and constraints.

Application of the general purpose analog computer as a simulator may be viewed as a second level of hierarchy of the modeling concept. Consider the following situation. It is desired to evaluate the hypothesis that a large amplitude secondary pressure pulse, which has been identified as the cause of the destruction of the SL-1 nuclear reactor, was the result of steam generated by heat transfer from particles of the melted core falling through the water moderator (Green and others, 1965). It is obvious that the hazards involved, coupled with the cost of a reactor installation, preclude experimental replication. Further, the implied experiment involves measurement of heat fluxes or their inference based on measured surface temperatures, Newton's cooling law, and estimated film heat transfer coefficients.

Whereas direct measurement is out of the question, the mathematical expression of the applicable laws, i.e., Fourier's and Newton's heat transfer laws, is well known. Even so, the uncertainty as to the magnitude of the film heat transfer coefficient, due to questions of boiling regime, raises the spectre of an immense computational task if either the analytical or numerical solution to the requisite partial differential equations is employed.

The general purpose analog computer consists of a large number of operational amplifiers, potentiometers, integration networks, etc., which may be interconnected (programmed) in a configuration such that its behavior is described by a set of equations similar to those describing the heat transfer problem under consideration. Further, measurement of voltages existing at different points in the circuit as a function of time is more economical than solving the differential equation model of the physical situation.

It is apparent that the untenable proposition of making extremely difficult measurements involving the destructive testing of nuclear reactors has been replaced by that of making direct measurements of a physical analog.

For the purpose of this discussion, it is appropriate to narrow the scope of the problem to solve a partial differential equation on an analog computer. In order to accomplish this it can be stated simply that Green and others (1965) made measurements of the surface temperature of a sphere moving through a water bath and its subsequent cooling in still air. The measurement was made by photographing an oscilloscope trace which was generated by a thermocouple attached to a metallic sphere. This trace is shown in Figure 1.

The sharply decreasing initial portion of the trace corresponds to the surface temperature trajectory while the sphere was under water. The sharp

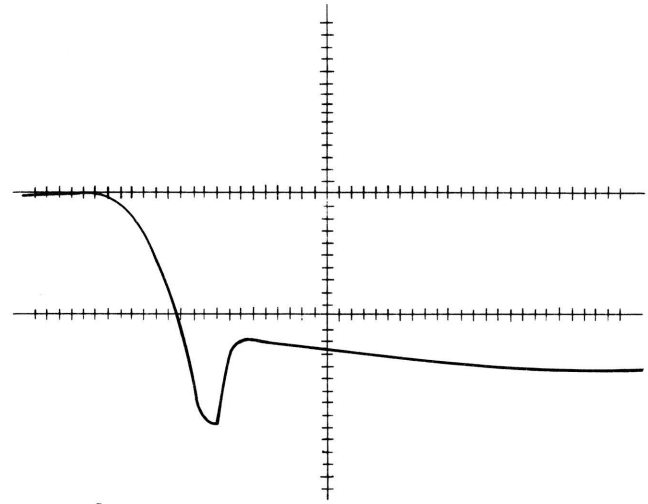

Figure 1. - Transient surface temperature response. Scale: 1 mu/cm (vertical), 0.1 sec/cm (horizontal).

rebound corresponds to the emergence of the sphere from the water and reflects change from conduction to convection as the rate limiting phenomenon. The slight drooping of the tail indicates that while film heat transfer coefficients in still air are small they are finite. Rather than consider the problem of evaluating the hypothesis, consider the simulation involved in reproducing the trajectory of Figure 1.

THE MATHEMATICAL MODEL

An energy balance over a differential element of volume gives rise to the partial differential equation

$$\frac{\partial \theta}{\partial t} = \alpha \nabla^2 \theta \qquad (1)$$

where θ is temperature; t is time; α is the thermal diffusivity; and ∇^2 is the Laplacian operation. This assumes that $\alpha \neq \alpha$ (position, time). Further, the rate of heat transfer from the surface is given by the expression

$$q = hA(\bar{\theta} - \theta) \qquad (2)$$

where h is the Newton cooling parameter (which is a function of both position and time); A is surface area; and $\bar{\theta}$ is the temperature of the water. Two cases were considered: (1) temperature as a function of radius and time, and (2) temperature as a function of radius and one angular dimension. For these cases the model equations are

$$\frac{\partial \theta}{\partial t} = \frac{\alpha}{r^2} \frac{\partial}{\partial r}\left[r^2 \frac{\partial \theta}{\partial r}\right] \qquad (3)$$

$$\frac{\partial \theta}{\partial t} = \alpha \left\{ \frac{1}{r^2} \frac{\partial}{\partial r}\left[r^2 \frac{\partial \theta}{\partial r}\right] + \frac{1}{r^2 \sin \phi} \frac{\partial}{\partial \phi}\left(\sin \phi \frac{\partial \theta}{\partial \phi}\right) \right\} \qquad (4)$$

Taylor series expansion of the deviations of temperature with respect to space dimensions in terms of finite differences leads to a set of ordinary differential equations. The general interior equations for the two cases considered are

$$\left.\frac{d\theta}{d\eta}\right|_{r = n\Delta r} = \left.(1 + \frac{1}{n})\theta\right|_{r = (n+1)\Delta r} - 2\theta\Big|_{r = n\Delta r} + \left.(1 - \frac{1}{n})\theta\right|_{r = (n-1)\Delta r} \qquad (5)$$

$$\left.\frac{d\theta}{d\eta}\right|_{\substack{\phi = m\Delta\phi \\ r = n\Delta r}} = \left\{ \left.(1 + \frac{1}{n})\theta\right|_{\substack{\phi = m\Delta\phi \\ r = (n+1)\Delta r}} - \left(2 + \frac{2}{n^2(\Delta\phi)^2}\right)\theta\Big|_{\substack{\phi = m\Delta\phi \\ r = n\Delta r}} + \left.(1 - \frac{1}{n})\theta\right|_{\substack{\phi = m\Delta\phi \\ r = (n-1)\Delta r}} + \left(\frac{2 + \Delta\phi \cot(m\Delta\phi)}{2n^2(\Delta\phi)^2}\right)\theta\Big|_{\substack{\phi = (m+1)\Delta\phi \\ r = n\Delta r}} + \left(\frac{2 - \Delta\phi \cot(m\Delta\phi)}{2n^2(\Delta\phi)^2}\right)\theta\Big|_{\substack{\phi = (m-1)\Delta\phi \\ r = n\Delta r}} \right\} \qquad (6)$$

where η is a dimensionless variable which involves α and Δr.

Analog Computer Notation

A general purpose analog computer is a collection of operational amplifiers, summing networks, integration networks, potentiometers, multipliers, function generators, etc. For the purpose of this study, we need only consider the first three elements in this list.

I. Coefficient potentiometers multiply a voltage by an arbitrary constant, $0 < k < 1.0$. Its operation is shown symbolically:

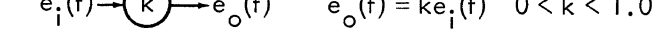

II. Operational amplifiers equipped with summing networks sum voltage signals. Their operation is shown symbolically:

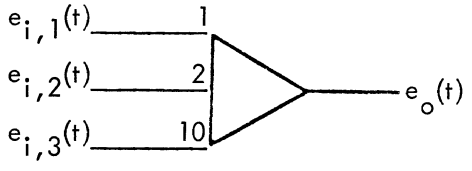

$$e_o(t) = -[e_1(t) + 2e_2(t) + 10\, e_3(t)]$$

or in general $e_o(t) = -\sum_i G_i e_{i,i}$ where G_i is the input gain for a particular signal.

III. Operational amplifiers equipped with integration networks integrate voltage signals with respect to time. Their operation is shown symbolically

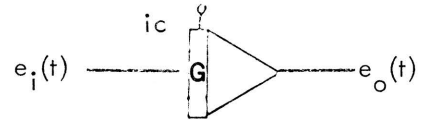

$$e_o(t) = -\left[G \int_0^t e_i(t)\,dt + ic\right]$$

where $ic = -e_o(0)$.

Because summing networks are input networks and integration networks are feedback networks they may be and are combined in this application.

Application to the Case $\theta = \theta(r\eta)$

For this case, the partial differential equation (1) with boundary constraining equation (2) is replaced by the set of ordinary differential equations of the form of equation (5) in which the subscripts, n, refer to grid points shown

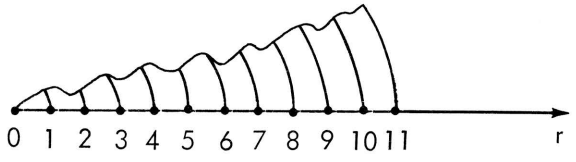

namely

$$\frac{d\theta_1}{d\eta} = 2[\theta_2 - \theta_1] \qquad \theta_1(0) = k$$

$$\frac{d\theta_2}{d\eta} = 3\theta_3/2 - 2\theta_2 + \theta_1/2 \qquad \theta_2(0) = k$$

$$\frac{d\theta_3}{d\eta} = 4\theta_4/3 - 2\theta_3 + 2\theta_2/3 \qquad \theta_3(0) = k$$

$$\frac{d\theta_{10}}{d\eta} = 11\theta_{11}/10 - 2\theta_{10} + 9\theta_9/10 \qquad \theta_{10}(0) = k$$

$$\theta_{11} = \begin{cases} 0.913\,\theta_{10} - 33.6 & 0 \le \eta \le T \\ \theta_{10} & \eta > T \end{cases} \quad (7)$$

where T is the value of η at which the medium surrounding the sphere changes from liquid to vapor, i.e., the film heat transfer coefficient becomes comparatively insignificant. The analog computer program is shown in Figure 2.

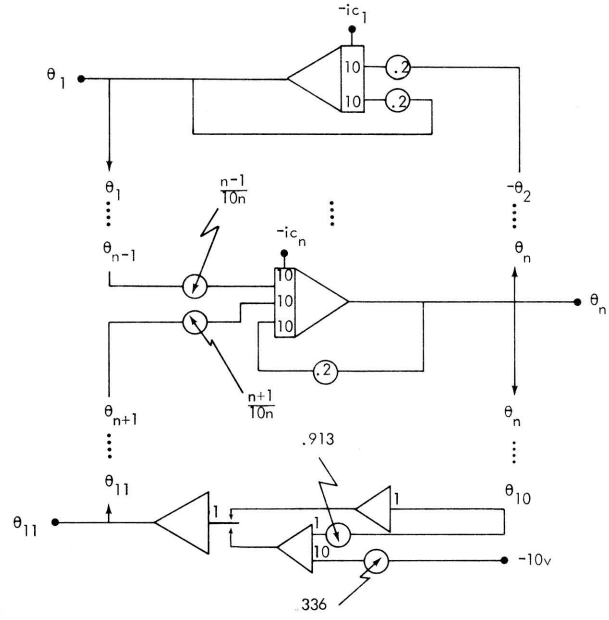

Figure 2.- Analog program for $\theta(r,\eta)$

Results of the computations are presented in Figure 3. The traces are plots of temperature as a function of time for parameters of radial position. The lowest trace in Figure 3 corresponds to the temperature at the surface of the sphere, i.e., a simulation of the experimental work of Green and others (1965) in Figure 1.

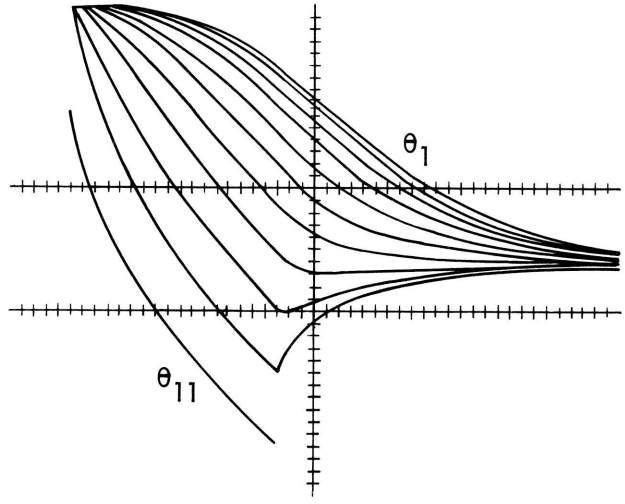

Figure 3.-Temperature profile for eleven radial grid model. Scale: 6/5 dimensionless sec/unit (horizontal); 10 dimensionless degrees/unit (vertical).

Application to the Case $\theta = \theta(r, \emptyset, t)$

For this case the partial differential equation (1) with boundary constraint equation (2) is replaced by the set of ordinary differential equations of the form of equation (6) in which the subscripts, m,n refer to grid points.

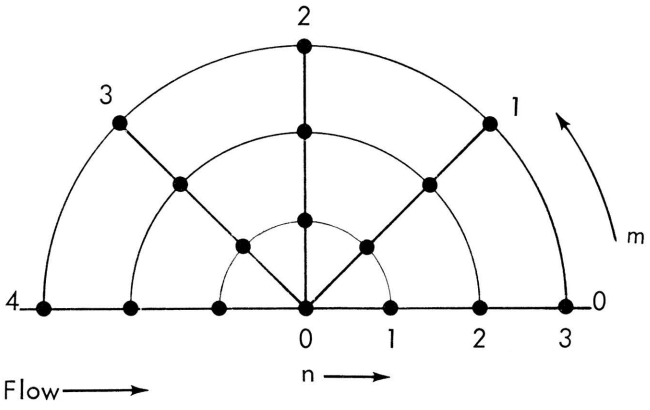

In contradistinction to the previous case, the hydrodynamics of the physical situation can be brought into play. Moving pictures show a vapor cloud partially covering the surface, thus decreasing the heat transfer rate at the trailing edge. This vapor cloud is sketched

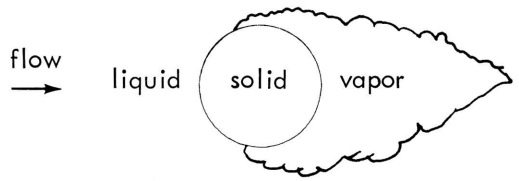

In order to introduce this information to the simulation, the boundary conditions listed were instituted.

$q = hA(\bar{\theta} - \theta)$	grid m = 3, 4; n = 3 $\eta \leq T$
$q = 0$	grid m = 3, 4; n = 3 $\eta > T$
$q = 0$	grid m = 0, 1, 2; n = 3 all η

(8)

The boundary conditions were applied to the two-space dimension model given in equation (6). Note that the symmetry about a line through the center of the sphere and parallel with the flow direction suggested by the shape of the vapor cloud has also been included in the model.

The programmed equations are:

$$\frac{d\theta_{0,1}}{d\eta} = 2\theta_{0,2} - 8.484\theta_{0,1} + 6.484\theta_{1,1}$$

$$\frac{d\theta_{0,2}}{d\eta} = -2.621\theta_{0,2} + 0.5\theta_{0,1} + 2.121\theta_{1,2}$$

$$\frac{d\theta_{4,1}}{d\eta} = 2\theta_{4,2} - 8.484\theta_{4,1} + 6.484\theta_{3,1}$$

$$\frac{d\theta_{4,2}}{d\eta} = -2.621\theta_{4,2} + 0.5\theta_{4,1} + 2.121\theta_{3,2}$$

$$\theta_{0,3} = \theta_{0,2}$$

$$\theta_{1,3} = \theta_{1,2}$$

$$\theta_{2,3} = \theta_{2,2}$$

$$\theta_{3,3} = \begin{cases} .653\theta_{3,2} - 130 & 0 \leq \eta \leq T \\ \theta_{3,2} & \eta > T \end{cases}$$

$$\theta_{4,3} = \begin{cases} .653\theta_{4,2} - 130 & 0 \leq \eta \leq T \\ \theta_{4,2} & \eta > T \end{cases} \qquad (9)$$

$$\frac{d\theta_{m,n}}{d\eta} = \text{equation (6) for } m = 1,2,3;\ n = 1,2.$$

A general interior grid point would be programmed as shown in Figure 4.

Results of the computation are presented in Figures 5, 6, 7, 8, and 9. Each of these presents traces of temperature as a function of time at various radii for a particular value of the angular parameter. Figures 5, 6, and 7 show small variations of temperature due to the small rate of heat transfer to the vapor cloud. Figures 8 and 9 show the enhanced rebound upon emergence from the liquid which was exhibited in Figure 1.

The limitation of the analog approach to solving partial differential equations becomes obvious from considerations of this case. This limitation, of course, is that all analog equipment is used in parallel, thus an almost trivially small grid system taxes all but the largest analog installations.

This problem has been solved at the Argonne National Laboratory analog facility. The two-space dimension case which involved seven angular parameters and seven radial parameters required 43 integrators, in excess of 120 operational amplifiers and in excess of 200 coefficient potentiometers--in short, more than 75 percent of the facility's capability was tied up for this problem.

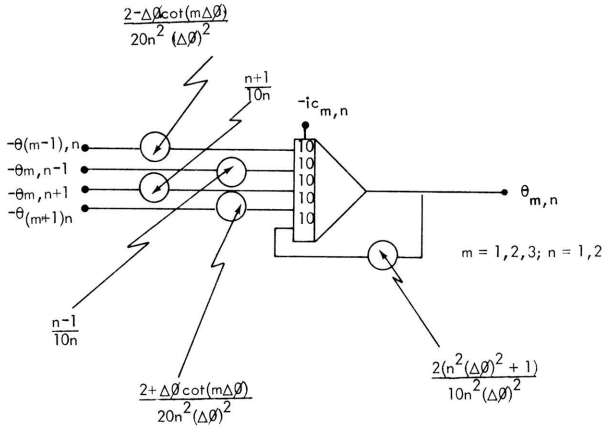

Figure 4.- Symbolic representation of typical interior grid point.

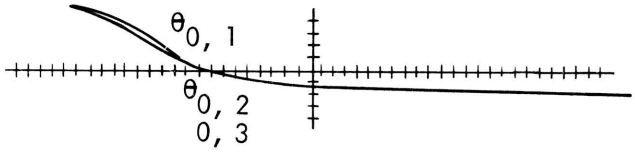

Figure 5.- Temperature profile two-space dimension model m = 0. Scale: 1 dimensionless sec/unit (horizontal); 10 dimensionless degrees/unit (vertical).

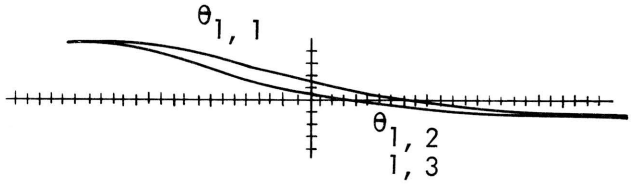

Figure 6.- Temperature profile two-space dimension model m = 1. Scale: 1 dimensionless sec/unit (horizontal); 10 dimensionless degrees/unit (vertical).

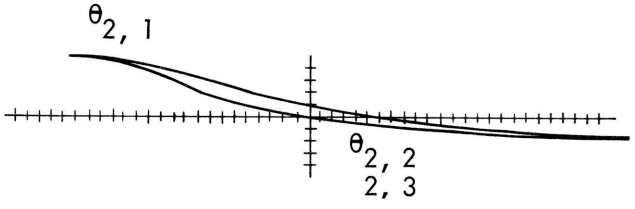

Figure 7.- Temperature profile two-space dimension model m = 2. Scale: 1 dimensionless sec/unit (horizontal); 10 dimensionless degrees/unit (vertical).

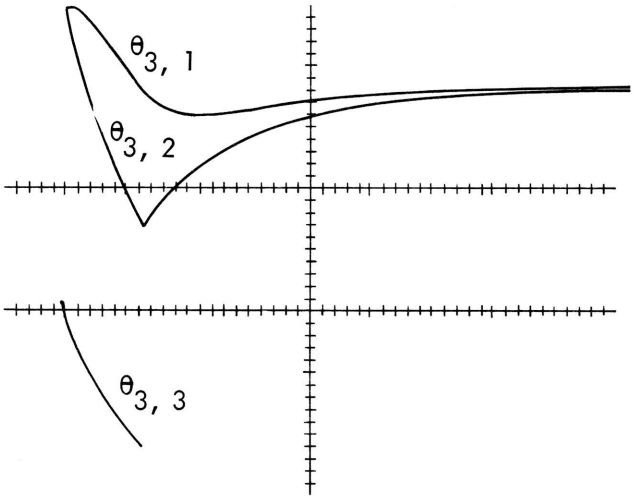

Figure 8.- Temperature profile two-space dimension model m = 3. Scale: 1 dimensionless sec/unit (horizontal); 10 dimensionless degrees/unit (vertical).

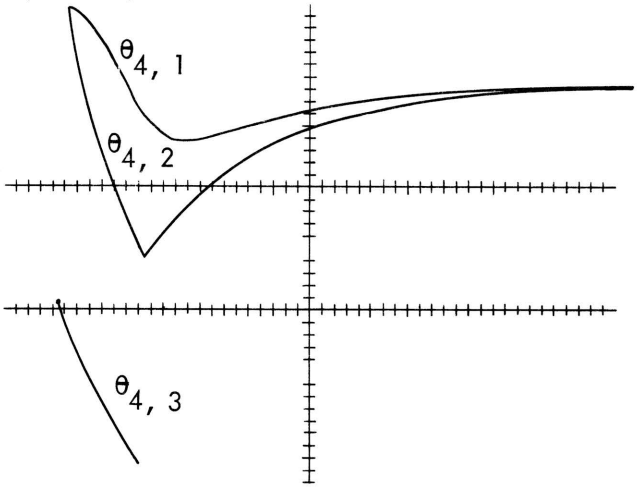

Figure 9.- Temperature profile two-space dimension model m = 4. Scale: 1 dimensionless sec/unit (horizontal); 10 dimensionless degrees/unit (vertical).

CONCLUSIONS

The general purpose analog computer may provide rapid solutions to relatively coarse grid net simulations of systems described by partial differential equations. The parallel use aspect of components in analog simulation precludes the use of this technique for large problems.

REFERENCE

Green, N.W., and others, 1965, Study of heat transfer from a sphere moving through water: Argonne Natl. Laboratory Report, 108 p.

MATHEMATICAL MODELING OF RESERVOIR BEHAVIOR

by

C.F. Weinaug

The University of Kansas

INTRODUCTION

The purpose of this paper is not to present new information, but to show a well-known simulation technique for gas reservoirs in the hope that these methods might be applied to different geological processes. Before the advent of large-scale, digital computers, it was not possible to obtain approximate solutions to the differential equations that describe physical changes in the geological environment, such as folding, faulting, etc. Now, solutions to some types of differential equations, describing plastic-elastic deformation, and fluid flow, are obtained by difference equation techniques. As an illustration, the method is applied to gas fields, and the differential equation developed. This equation is then converted into a set of difference equations, which can be solved by a digital computer. Results of the solution are shown here.

Acknowledgments.- I thank John R. Dempsey of Northern Natural Gas Company, who wrote the programs, and Northern Natural Gas Company for providing computer facilities. I also thank Humble Oil and Refining Company for giving me time to attend the conference and present this paper.

MATHEMATICAL DEVELOPMENT

In the case of gas flow in porous media, a small element of the media is taken, as shown in Figure 1. For the case in which flow is limited to the x direction, the product of density, velocity, and cross-section area yields the rate, weight per unit time, at which fluid flows into the element.

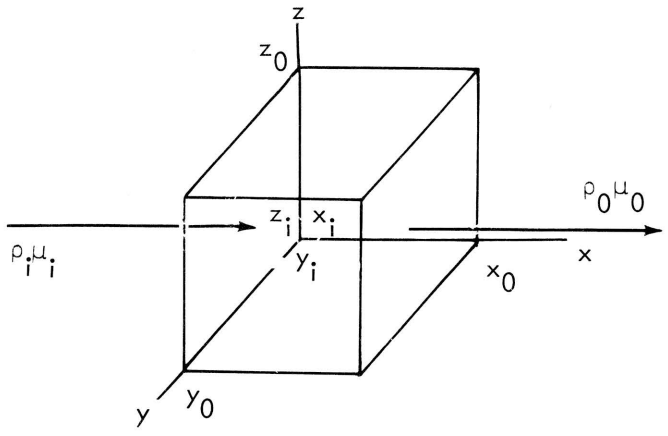

Figure 1.- Example of gas flow in porous media.

$$\rho_i U_i \ (y_0 - y_i) \ (z_0 - z_i)$$

where

ρ_i = density of entering fluid,

U_i = velocity of entering fluid, and

$(y_0 - y_i)(z_0 - z_i)$ = area through which fluid enters and leaves the element.

In a like manner, the rate at which fluid leaves the element is described by

$$\rho_0 U_0 \ (y_0 - y_i) \ (z_0 - z_i)$$

where

ρ_0 = density of fluid leaving element,

and

U_0 = velocity of fluid leaving element.

Because mass must be conserved in this situation, the net flow of fluid into, and out of, the element must equal the accumulation of fluid in the element with respect to time.

$$\text{Input-Output} = \text{Accumulation} \qquad (1)$$

In a time span, $t_2 - t_1$, the difference between the rate flow in and out, multiplied by the elapsed time, will yield the right side of equation (1).

$$[\rho_i U_i (y_0 - y_i)(z_0 - z_i) - \rho_0 U_0 (y_0 - y_i) \cdot (z_0 - z_i)] \ [t_2 - t_1] = \text{Accumulation} \qquad (2)$$

In mathematical parlance, it is customary to rearrange equation (2) to get equation (3),

$$(\rho_0 U_0 - \rho_i U_i)(y_0 - y_i)(z_0 - z_i)(t_2 - t_1) = \text{Accumulation} \qquad (3)$$

The accumulation within the element can be calculated from the product of the change in density during the time span and the volume of the element.

$$\phi (\rho_{t_2} - \rho_{t_1})(x_0 - x_i)(y_0 - y_i)(z_0 - z_i) = \text{Accumulation}, \qquad (4)$$

where

ϕ = fractional porosity,

ρ_{t_2} = density within the element at end of time period,

ρ_{t_1} = density within the element at beginning of time period, and

$(x_0 - x_i)(y_0 - y_i)(z_0 - z_i)$ = volume of element.

Equation (4) is substituted into equation (3) to give equation (5)

$$(\rho_0 U_0 - \rho_i U_i)(y_0 - y_i)(z_0 - z_i)(t_2 - t_1) =$$

$$\phi(\rho_{t_2} - \rho_{t_1})(x_0 - x_i)(y_0 - y_i)(z_0 - z_i). \quad (5)$$

Both sides of equation (5) may be divided by $(t_2 - t_1)(x_0 - x_i)(y_0 - y_i)(z_0 - z_i)$ to yield equation (6)

$$\frac{(\rho_0 U_0 - \rho_i U_i)}{x_0 - x_i} = -\phi \frac{(\rho_{t_2} - \rho_{t_1})}{t_2 - t_1} \quad (6)$$

If the element and time span are reduced in size until $(x_0 - x_i)$ and $(t_2 - t_1)$ approach zero, equation (6) may be replaced by the partial differential euqation,

$$\frac{\partial(\rho U)}{\partial x} = -\phi \frac{\partial \rho}{\partial t} . \quad (7)$$

The above development can be repeated for the more general case where flow is in any direction. In this case, the flow is broken into components of the coordinate system. Thus, there would be ρU terms for the y and z directions, as well as the x direction on the right-hand side of equations (2), (5), (6), and (7), whereas the left-hand side would remain unchanged. The result, for the general case, is known as the equation continuity,

$$\frac{\partial \rho U}{\partial x} + \frac{\partial \rho U}{\partial y} + \frac{\partial \rho U}{\partial z} = -\phi \frac{\partial \rho}{\partial t} \quad (8)$$

Density and velocity terms in equation (8) may be replaced by terms that are easier to measure. The gas law equation is used to predict density,

$$PV = ZnRT_a \quad (9)$$

where

P = pressure,

V = volume,

Z = compressibility factor to correct for real gas deviation from ideal gas law,

n = number of moles of gas,

R = universal gas law constant, and

T_a = absolute temperature.

Also

ρ = weight per unit volume,

$\frac{\rho}{M}$ = moles per unit volume,

where M = molecular weight of the gas, then

$$P(1.0) = Z \frac{\rho}{M} R T_a, \text{ and } \rho = \frac{PM}{ZRT_a} \quad (10)$$

For the velocity terms, Darcy's law is used.

$$U_x = \frac{K_x}{\mu} \frac{\partial P}{\partial x}; \; U_y = \frac{K_y}{\mu} \frac{\partial P}{\partial y}, \text{ and}$$

$$U_z = \frac{K_z}{\mu} \frac{\partial P}{\partial z} \quad (11)$$

where

U_x = velocity in x direction,

U_y = velocity in y direction,

U_z = velocity in z direction,

K_x = permeability in x direction,

K_y = permeability in y direction,

K_z = permeability in z direction, and

μ = viscosity.

The indicated substitution gives

$$\frac{\partial \frac{PM}{ZRT} \frac{K_x}{\mu} \frac{\partial P}{\partial x}}{\partial x} + \frac{\partial \frac{PM}{ZRT} \frac{K_y}{\mu} \frac{\partial P}{\partial y}}{\partial y} +$$

$$\frac{\partial \frac{PM}{ZRT} \frac{K_z}{\mu} \frac{\partial P}{\partial z}}{\partial z} = \phi \frac{\partial \frac{PM}{ZRT}}{\partial t} \quad (12)$$

In the case of a gas reservoir, temperature and molecular weight may be considered constant throughout the formation. For this reason, these two terms and the universal gas law constant are cancelled in equation (12) to give,

$$\frac{\partial \frac{K_x}{\mu} \frac{P}{Z} \frac{\partial P}{\partial x}}{\partial x} + \frac{\partial \frac{K_y}{\mu} \frac{P}{Z} \frac{\partial P}{\partial y}}{\partial y} +$$

$$\frac{\partial \frac{K_z}{\mu} \frac{P}{Z} \frac{\partial P}{\partial z}}{\partial z} = -\phi \frac{\partial \frac{P}{Z}}{\partial t} \qquad (13)$$

This is the basic equation that mathematically describes the flow of gas within a formation. The equation contains only two assumptions. First, gas density can be described by equation (10), and second by Darcy's law. Both of these assumptions have been proven by large volumes of experimental data. Thus, solutions of equation (13) will simulate and predict the behavior of gas within a reservoir during the production process. It is impossible at this time, however, to obtain rigorous mathematical solutions. Also, the irregular geometry of gas reservoirs would limit the application of the solutions.

In order to overcome the limitations of present mathematical knowledge, equation (13) is simplified and then restated as a difference equation which will approximate closely the original differential equation.

For equation (13), it is convenient to multiply the right-hand side by $\frac{P}{P}$, and assume that Z does not change much with a small change in time.

$$\frac{\partial \frac{K_x}{\mu} \frac{P}{Z} \frac{\partial P}{\partial x}}{\partial x} + \frac{\partial \frac{K_y}{\mu} \frac{P}{Z} \frac{\partial P}{\partial y}}{\partial y} + \frac{\partial \frac{K_z}{\mu} \frac{P}{Z} \frac{\partial P}{\partial z}}{\partial z}$$

$$= -\phi \frac{P \partial P}{PZ \partial t} \qquad (14)$$

Further, remembering that

$$P \partial P = 1/2 \, \partial P^2 ,$$

then equation (14) becomes

$$\frac{\partial \frac{K_x}{\mu Z} \frac{\partial P^2}{\partial x}}{\partial x} + \frac{\partial \frac{K_y}{\mu Z} \frac{\partial P^2}{\partial y}}{\partial y} +$$

$$\frac{\partial \frac{K_z}{\mu Z} \frac{\partial P^2}{\partial y}}{\partial z} = -\phi \frac{\partial P^2}{PZ \partial t} \qquad (15)$$

In many problems involving gas, it is not necessary to fully consider the changes of P with respect to z, because the areal changes in thickness may be included in the x, y, and T terms,

$$\frac{\partial \frac{K_x T}{\mu Z} \frac{\partial P^2}{\partial x}}{\partial x} + \frac{\partial \frac{K_y T}{\mu Z} \frac{\partial P^2}{\partial y}}{\partial y} =$$

$$-\phi \, T \frac{\partial P^2}{PZ \partial t} , \qquad (16)$$

where

T = thickness

Before forming a difference equation, the area to be studied is divided into a number of parts. This is accomplished by overlaying or superimposing a graph on a map of the area, as shown in Figure 2.

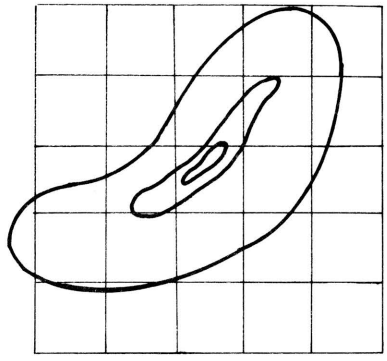

Figure 2.- Superimposed map.

The intersection of the coordinate lines forms the mesh- or grid-point map indicated in Figure 3.

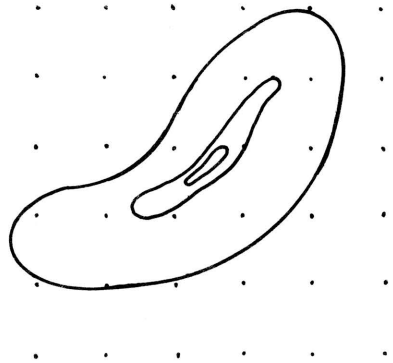

Figure 3.- Mesh-point map.

In order to remember the different points, they are numbered as indicated in Figure 4.

1, 1	1, 2	1, 3	. . . .	1, n
2, 1	2, 2	2, 3	. . . .	.
3, 1	3, 2	3, 3	. . . .	.
.				.
.				.
.				.
.				.
.				.
m, 1				m, n

Figure 4.- Mesh-point numbers; n = maximum number of points in x direction, and m = maximum number of points in y direction.

To write a difference equation, a mesh point and its four surrounding points are selected as indicated in Figure 5.

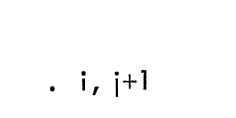

Figure 5.- Generalized mesh-point locations for difference equation.

Here j indicates position along the x axis, and i the corresponding position on the y axis. One other designation is needed for the time. Because time will be considered in a series of steps, the position within these steps is given by L. It should be noted that i, j, and L are itergers, or whole numbers.

This numbering system is a convenient method to indicate position of any property on the map by using positions as subscripts. For example, Pi, j, and L indicate pressure at the i and jth position and Lth time step.

Using these subscripts, a difference equation is formed from equation (16) remembering that

$$\lim_{(x_2-x_1)\to 0} \frac{y_2 - y_1}{x_2 - x_1} = \frac{\partial y}{\partial x} , \qquad (17)$$

thus

$$\frac{\partial P^2}{\partial x} \cong \frac{P^2_{i,\,j-1,\,L+1} - P^2_{i,\,j,\,L+1}}{x_{i,\,j+1} - x_{i,j}} \quad \text{or}$$

$$\frac{P^2_{i,\,j,\,L+1} - P^2_{i,\,j-1,\,L+1}}{x_{i,\,j} - x_{i,\,j-1}} \qquad (18)$$

Because the difference in pressures squared is taken over an interval, the indicated multiplying term is averaged over the interval.

$$\frac{K_x T \partial P^2}{\mu Z \partial x} \cong \frac{1}{2}\left[\left(\frac{K_x T}{\mu Z}\right)_{i,\,j,\,L} + \left(\frac{K_x T}{\mu Z}\right)_{i,\,j-1,\,L}\right] \cdot \left[\frac{P^2_{i,\,j,\,L+1} - P^2_{i,\,j-1,\,L+1}}{x_{i,\,j} - x_{i,\,j-1}}\right] \qquad (19)$$

or

$$\frac{K_x T P \partial P^2}{\mu Z \partial x} \cong \frac{1}{2}\left[\left(\frac{K_x T}{\mu Z}\right)_{i,\,j+1,\,L} + \left(\frac{K_x T}{\mu Z}\right)_{i,\,j,\,L}\right] \cdot \left[\frac{P^2_{i,\,j+1,\,L+1} - P^2_{i,\,j,\,L+1}}{x_{i,\,j+1} - x_{i,\,j}}\right] \qquad (20)$$

To complete the process for the first term in equation (16), the difference of the right-hand sides of equations (19) and (20) is divided by the average distance.

$$\frac{\partial \frac{K_x T}{\mu Z}\frac{\partial P^2}{\partial x}}{\partial x} \cong \left\{ \frac{1}{2}\left[\left(\frac{K_x T}{\mu Z}\right)_{i,\,j+1,\,L} + \left(\frac{K_x T}{\mu Z}\right)_{i,\,j,\,L}\right] \left[\frac{P^2_{i,\,j+1,\,L+1} - P^2_{i,\,j,\,L+1}}{x_{i,\,j+1} - x_{i,\,j}}\right] - \frac{1}{2}\left[\left(\frac{K_x T}{\mu Z}\right)_{i,\,j,\,L} + \left(\frac{K_x T}{\mu Z}\right)_{i,\,j-1,\,L}\right]\left[\frac{P^2_{i,\,j,\,L+1} - P^2_{i,\,j-1,\,L+1}}{x_{i,\,j} - x_{i,\,j-1}}\right] \right\} \left\{ \frac{1}{\frac{1}{2}(x_{i,\,j+1} - x_{i,\,j-1})} \right\} \qquad (21)$$

It can be seen that the y-direction term is given by equation (22).

$$\frac{\partial \frac{K_y T \partial P^2}{\mu Z \partial y}}{\partial y} \cong \left\{ \frac{1}{2}\left[\left(\frac{K_y T}{\mu Z}\right)_{i+1,\,j,\,L} \left(\frac{K_y T}{\mu Z}\right)_{i,\,j,\,L}\right] \left[\frac{P^2_{i+1,\,j,\,L+1} - P^2_{i,\,j,\,L+1}}{Y_{i+1,\,j,\,L} - Y_{i,\,j,\,L}}\right] - \frac{1}{2}\left[\left(\frac{K_y T}{\mu Z}\right)_{i,\,j,\,L} + \left(\frac{K_y T}{\mu Z}\right)_{i-1,\,j,\,L}\right]\left[\frac{P^2_{i,\,j,\,L+1} - P^2_{i-1,\,j,\,L+1}}{Y_{i,\,j} - Y_{i-1,\,j}}\right] \right\} \left\{ \frac{1}{\frac{1}{2}(Y_{i+1,\,j} - Y_{i-1,\,j})} \right\} \qquad (22)$$

In a like manner, the right-hand side of equation (16) can be differenced.

$$-\phi T \frac{\partial P^2}{P Z \partial T} \cong \left[-\phi_{i,\,j}\, T_{i,\,j} \frac{1}{(PZ)_{i,\,j,\,L}}\right] \cdot \left[\frac{P^2_{i,\,j,\,L+1} - P^2_{i,\,j,\,L}}{t_{L+1} - t_L}\right] \qquad (23)$$

Equations (21), (22), and (23) are substituted into equation (16) to give equation (24),

$$\left\{\frac{1}{2}\left[\left(\frac{K_x T}{\mu Z}\right)_{i,\,j+1,\,L}+\left(\frac{K_x T}{\mu Z}\right)_{i,\,j,\,L}\right]\left[\frac{P^2_{i,\,j+1,\,L}-P^2_{i,\,j,\,L}}{x_{i,\,j+1}-x_{i,\,j}}\right]-\frac{1}{2}\left[\left(\frac{K_x T}{\mu Z}\right)_{i,\,j,\,L}+\left(\frac{K_x T}{\mu Z}\right)_{i,\,j-1,\,L}\right]\left[\frac{P^2_{i,\,j,\,L}-P^2_{i,\,j-1,\,L}}{x_{i,\,j,\,L}-x_{i,\,j-1,\,L}}\right]\right\}\left\{\frac{1}{\frac{1}{2}(x_{i,\,j+1,\,L}-x_{i,\,j-1,\,L})}\right\}+\left\{\frac{1}{2}\left[\left(\frac{K_y T}{\mu Z}\right)_{i+1,\,j,\,L}+\left(\frac{K_y T}{\mu Z}\right)\right]\left[\frac{P^2_{i+1,\,j,\,L}-P^2_{i,\,j,\,L}}{Y_{i+1,\,j}-Y_{i,\,j}}\right]-\frac{1}{2}\left[\left(\frac{K_y T}{\mu Z}\right)_{i,\,j,\,L}+\left(\frac{K_y T}{\mu Z}\right)_{i-1,\,j,\,L}\right]\left[\frac{P^2_{i,\,j,\,L}-P^2_{i-1,\,j,\,L}}{Y_{i,\,j,\,L}-Y_{i-1,\,j,\,L}}\right]\right\}\left\{\frac{1}{\frac{1}{2}(Y_{i+1,\,j,\,L}-Y_{i-1,\,j,\,L})}\right\}=$$

$$-\phi_{i,\,j}T_{i,\,j}\frac{1}{(PZ)_{i,\,j,\,L}}\left[\frac{P^2_{i,\,j,\,L+1}-P^2_{i,\,j,\,L}}{t_{L+1}-t_L}\right] \qquad (24)$$

In forming equation (24), two apparently arbitrary choices of time level are used for the terms $\frac{KT}{\mu Z}$ and P's on the left hand side of the equation.

Since μ and Z normally do not change rapidly with pressure it usually does not make a great deal of difference which time level is used and the past one is much easier to handle. In the case of the P's on the left side of the equation, it has been found by Douglas, Peaceman and others that the choice of the future time step level, L+1, results in fewer computations in a machine of finite length numbers. This choice is not obvious but it is not the purpose of this paper to show the mathematical reasons for it.

Equation (24) is rearranged to give,

$$\left[\frac{\left(\frac{K_x T}{\mu Z}\right)_{i,\,j+1,\,L}+\left(\frac{K_x T}{\mu Z}\right)_{i,\,j,\,L}}{(x_{i,\,j+1}-x_{i,\,j})(x_{i,\,j+1}-x_{i,\,j-1})}\right]P^2_{i,\,j+1,\,L+1}-\left[\frac{\left(\frac{K_x T}{\mu Z}\right)_{i,\,j+1,\,L}+\left(\frac{K_x T}{\mu Z}\right)_{i,\,j,\,L}}{(x_{i,\,j+1}-x_{i,\,j})(x_{i,\,j+1}-x_{i,\,j-1})}+\frac{\left(\frac{K_x T}{\mu Z}\right)_{i,\,j,\,L}+\left(\frac{K_x T}{\mu Z}\right)_{i,\,j-1,\,L}}{(x_{i,\,j,\,L}-x_{i,\,j-1,\,L})(x_{i,\,j+1,\,L}-x_{i,\,j-1,\,L})}\right]P^2_{i,\,j,\,L+1}+\left[\frac{\left(\frac{K_x T}{\mu Z}\right)_{i,\,j,\,L}+\left(\frac{K_x T}{\mu Z}\right)_{i,\,j-1,\,L}}{(x_{i,\,j,\,L}-x_{i,\,j,\,L})(x_{i,\,j+1}-x_{i,\,j-1})}\right]P^2_{i,\,j-1,\,L+1}+\left[\frac{\left(\frac{K_y T}{\mu Z}\right)_{i+1,\,j,\,L}+\left(\frac{K_y T}{\mu Z}\right)_{i,\,j,\,L}}{(Y_{i+1,\,j}-Y_{i,\,j})(Y_{i+1,\,j}-Y_{i-1,\,j})}\right]P^2_{i+1,\,j,\,L+1}-\left[\frac{\left(\frac{K_y T}{\mu Z}\right)_{i+1,\,j,\,L}+\left(\frac{K_y T}{\mu Z}\right)_{i,\,j,\,L}}{(Y_{i+1,\,j}-Y_{i,\,j})(Y_{i+1,\,j}-Y_{i-1,\,j})}+\frac{\left(\frac{K_y T}{\mu Z}\right)_{i,\,j,\,L}+\left(\frac{K_y T}{\mu Z}\right)_{i-1,\,j,\,L}}{(Y_{i,\,j}-Y_{i-1,\,j})(Y_{i+1,\,j}-Y_{i-1,\,j})}\right]P^2_{i,\,j,\,L+1}+\left[\frac{\left(\frac{K_y T}{\mu Z}\right)_{i,\,j,\,L}+\left(\frac{K_y T}{\mu Z}\right)_{i-1,\,j,\,L}}{(Y_{i,\,j}-Y_{i-1,\,j})(Y_{i+1,\,j}-Y_{i-1,\,j})}\right]P^2_{i-1,\,j,\,L+1}=$$

$$\frac{\phi_{i,\,j}T_{i,\,j}}{(PZ)_{i,\,j,\,L}(t_{L+1}-t_L)}P^2_{i,\,j,\,L+1}-\frac{\phi_{i,\,j}T_{i,\,j}}{(PZ)_{i,\,j,\,L}(t_{L+1}-t_L)}P^2_{i,\,j,\,L} \qquad (25)$$

In addition to the system of equations, one for each grid point described by equation (25), it is necessary to have a set of equations for the grid boundary point equations which contain values outside of the grid. For example, when j=1, it is necessary to have values for j=0. The convenient boundary condition is one of no flow or relfected boundary values. This condition is obtained by the following equations:

$$P_{i,\,o,\,L}=P_{i,\,z,\,L} \qquad (26)$$

$$P_{o,\,j,\,L} = P_{z,\,j,\,L} \tag{27}$$

$$P_{i,\,n+1,\,L} = P_{i,\,n-1,\,L} \tag{28}$$

$$P_{m+1,\,j,\,L} = P_{m-1,\,j,\,L} \tag{29}$$

$$\left(\frac{K_x T}{\mu Z}\right)_{i,\,o,\,L} = \left(\frac{K_x T}{\mu Z}\right)_{i,\,2,\,L} \tag{30}$$

$$\left(\frac{K_x T}{\mu Z}\right)_{o,\,j,\,L} = \left(\frac{K_x T}{\mu Z}\right)_{2,\,j,\,L} \tag{31}$$

$$\left(\frac{K_x T}{\mu Z}\right)_{i,\,n+1,\,L} = \left(\frac{K_x T}{\mu Z}\right)_{i,\,n-1,\,L} \tag{32}$$

$$\left(\frac{K_x T}{\mu Z}\right)_{m+1,\,j,\,L} = \left(\frac{K_x T}{\mu Z}\right)_{m-1,\,j,\,L} \tag{33}$$

$$\left(\frac{K_y T}{\mu Z}\right)_{i,\,o,\,L} = \left(\frac{K_y T}{\mu Z}\right)_{i,\,2,\,L} \tag{34}$$

$$\left(\frac{K_y T}{\mu Z}\right)_{o,\,j,\,L} = \left(\frac{K_y T}{\mu Z}\right)_{2,\,j,\,L} \tag{35}$$

$$\left(\frac{K_y T}{\mu Z}\right)_{i,\,n+1,\,L} = \left(\frac{K_y T}{\mu Z}\right)_{i,\,n-1,\,L} \tag{36}$$

$$\left(\frac{K_y T}{\mu Z}\right)_{m+1,\,j,\,L} = \left(\frac{K_y T}{\mu Z}\right)_{m-1,\,j,\,L} \tag{37}$$

One further boundary condition is necessary to provide for wells to produce or inject gas at different grid points. This is accomplished by adding a sink term. The term to be added to the right hand side of equation (25) is

$$-\frac{Q P_s T_r}{\frac{1}{2}(x_{i,\,j+1} - x_{i,\,j-1})\,\frac{1}{2}(Y_{i+1,\,j} - Y_{i-1,\,j})\,T_s Z_s} \tag{38}$$

where Q = volume of production per unit time measured at surface conditions,

P_s = Pressure at the surface,

T_s = Temperature at the surface,

Z_s = Compressibility factor at surface conditions, and

T_r = Absolute temperature in reservoir.

This completes the conversion of the partial differential equation (13) into a set of algebraic equations for which there are a number of known solutions. The Peaceman alternating direction method is recommended; however, the discussion of this method is beyond the scope of this paper.

Each time the set of algebraic equations is solved, time is advanced and the process repeated. Thus these solutions show the changes in pressure at each grid point as a function of time.

The validity of these solutions has been tested in a number of situations. First, at some finite difference level of space and time, the solution should not vary with the size of these differences. Fortunately, the size of the differences may be large and yet satisfy this limitation. Second, the solutions have been compared in instances where there are known solutions. Here, the numerical solutions are close approximations.

An example of the results of one of these computations is shown in Figures 6, 7, 8, and 9. These figures are pressure contour maps of a three-well gas field at different times during production of the field. These maps were produced by a digital computer and in this instance the 100's digit of the computed pressure is printed if it is an even digit. Thus, the edges of the area form the contour lines.

A large number of these maps have been computed and printed at a series of small increasing time steps. These plates were then used with standard animation techniques to produce a movie showing a nine-year pressure history of the gas field.

For geologists viewing the computer movie (or Figures 6, 7, 8, and 9), I would like to have them use their imagination. Suppose the equations for elastic and plastic deformation had been solved by the above technique for a sedimentary basin, where large reefs were growing and causing subsidence. A situation similar to that shown in the movie would result. Thus the movie could be considered a gross simulation of geologic behavior. It is, however, my prediction that in the near future the mathematical equations describing geological processes will be solved by numerical techniques. These solutions will increase our understanding of the geology and lead to better predictions.

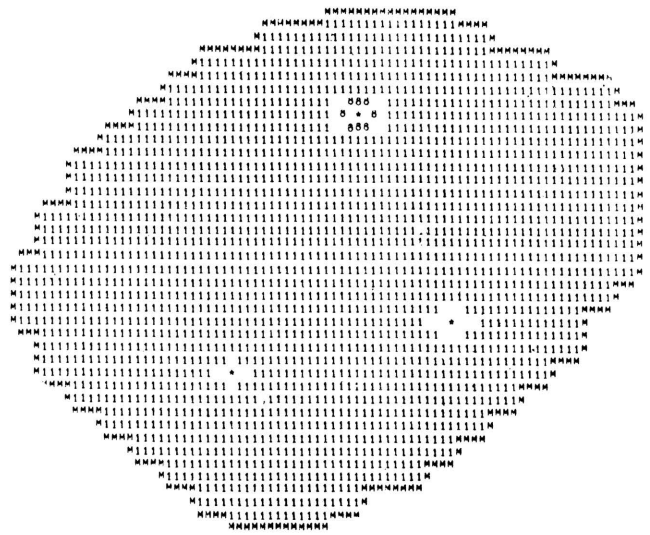

Figure 6.- Near initial reservoir conditions.

Figure 7.- About one-third of reserve produced.

Figure 8.- About two-thirds of reserve produced.

Figure 9.- Near reservoir abandonment.

COMPUTER CONTRIBUTIONS

Kansas Geological Survey
University of Kansas
Lawrence, Kansas

Computer Contribution

1. Mathematical simulation of marine sedimentation with IBM 7090/7094 computers, by J.W. Harbaugh, 1966 . . . . . .$1.00
2. A generalized two-dimensional regression procedure, by J.R. Dempsey, 1966 . . . .$0.50
3. FORTRAN IV and MAP program for computation and plotting of trend surfaces for degrees 1 through 6, by Mont O'Leary, R.H. Lippert, and O.T. Spitz, 1966 . . . . .$0.75
4. FORTRAN II program for multivariate discriminant analysis using an IBM 1620 computer, by J.C. Davis and R.J. Sampson, 1966 . . . . . .$0.50
5. FORTRAN IV program using double Fourier series for surface fitting of irregularly spaced data, by W.R. James, 1966 . . . . . .$0.75
6. FORTRAN IV program for estimation of cladistic relationships using the IBM 7040, by R.L. Bartcher, 1966 . . . . . .$1.00
7. Computer applications in the earth sciences: Colloquium on classification procedures, edited by D.F. Merriam, 1966 . . . . . .$1.00
8. Prediction of the performance of a solution gas drive reservoir by Muskat's Equation, by Apolonio Baca, 1967 . . . . . .$1.00
9. FORTRAN IV program for mathematical simulation of marine sedimentation with IBM 7040 or 7094 computers, by J.W. Harbaugh and W.J. Wahlstedt, 1967 . . . . . .$1.00
10. Three-dimensional response surface program in FORTRAN II for the IBM 1620 computer, by R.J. Sampson and J.C. Davis, 1967. . . . . .$0.75
11. FORTRAN IV program for vector trend analyses of directional data, by W.T. Fox, 1967 .$1.00
12. Computer applications in the earth sciences: Colloquium on trend analysis, edited by D.F. Merriam and N.C. Cocke, 1967 . . . . . .$1.00
13. FORTRAN IV computer programs for Markov chain experiments in geology, by W.C. Krumbein, 1967 . . . . . .$1.00
14. FORTRAN IV programs to determine surface roughness in topography for the CDC 3400 computer, by R.D. Hobson, 1967 . . . . . .$1.00
15. FORTRAN II program for progressive linear fit of surfaces on a quadratic base using an IBM 1620 computer, by A.J. Cole, C. Jordan, and D.F. Merriam, 1967. . . . . .$1.00
16. FORTRAN IV program for the GE 625 to compute the power spectrum of geological surfaces, by J.E. Esler and F.W. Preston, 1967 . . . . . .$0.75
17. FORTRAN IV program for Q-mode cluster analysis of nonquantitative data using IBM 7090/7094 computers, by G.F. Bonham-Carter, 1967 . . . . . .$1.00
18. Computer applications in the earth sciences: Colloquium on time-series analysis, D.F. Merriam, editor, 1967. . . . . .$1.00
19. FORTRAN II time-trend package for the IBM 1620 computer, by J.C. Davis and R.J. Sampson, 1967 . . . . . .$1.00
20. Computer programs for multivariate analysis in geology, D.F. Merriam, editor, 1968 . . .$1.00
21. FORTRAN IV program for computation and display of principal components, by W.J. Wahlstedt and J.C. Davis, 1968 . . . . . .$1.00
22. Computer applications in the earth sciences: Colloquium on simulation, edited by D.F. Merriam and N.C. Cocke, 1968 . . . . . .$1.00